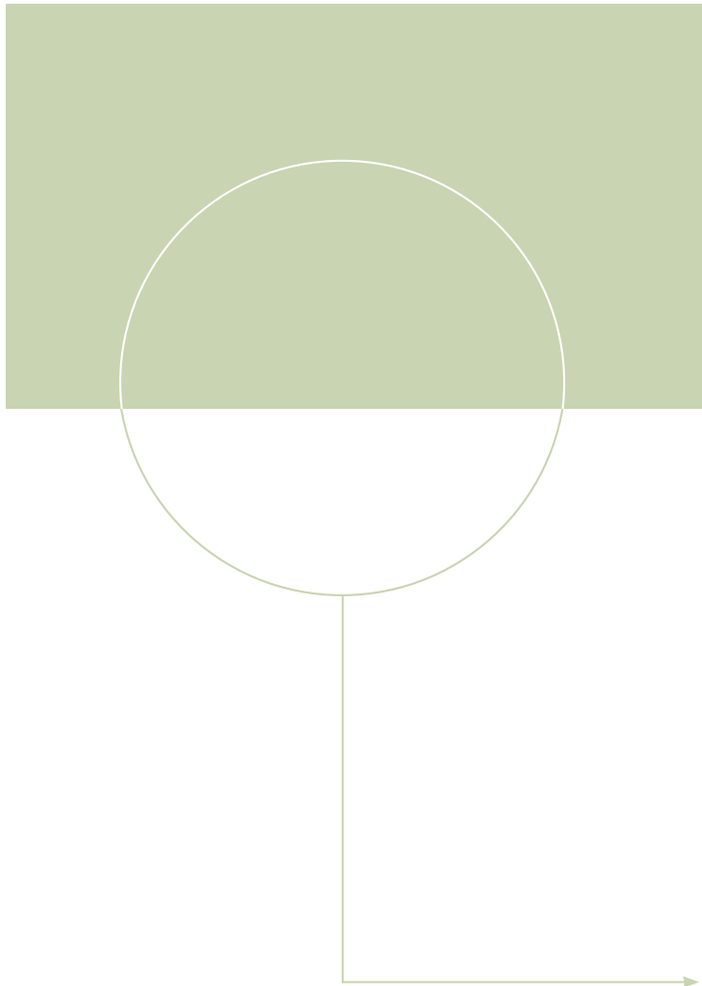

Master's thesis

2020

Per Øyvind Valen

NTNU
Norwegian University of
Science and Technology
Faculty of Engineering
Department of Energy and Process Engineering

Master's thesis

Per Øyvind Valen

Modelling and simulation of a trombe wall

Analysis for Nordic and Chinese climates

July 2020

NTNU
Norwegian University of
Science and Technology

NTNU
Norwegian University of
Science and Technology

NTNU
Norwegian University of
Science and Technology

Modelling and simulation of a trombe wall

Analysis for Nordic and Chinese climates

Per Øyvind Valen

MTPROD
Submission date: July 2020
Supervisor: Vojislav Novakovic, NTNU
Co-supervisor: Yanjun Dai, SJTU

Norwegian University of Science and Technology
Department of Energy and Process Engineering

Contents

List of Figures

List of Tables

Sammendrag

I denne oppgaven blir en ventilert solvarmevegg analysert ved bruk av simuleringsprogramvaren TRNSYS, og Matlab. Arbeidet ble utført i samarbeid med Shanghai Jiao Tong University i Kina, som en del av Joint Research Centre in Sustainable Energy på NTNU og SJTU. Kandidaten sitt opphold i Shanghai, samt eksperimenter utført på Green Energy Lab på SJTU ble avbrutt som følge av Corona-viruspandemien.

I følge the International Energy Association så representerer byggenæringen 36 prosent av all årlig energibruk i verden. Dette tallet er forventet å stige, som følge av at totalt antall utbygd areal i verden stiger og at tilgang til energi i utviklingsland stiger hurtig. I en tid med mye politisk fokus på hvert lands total utslipp er arbeidet med å senke utslippene sentrale. Da er en mer miljøvennlig byggenæring veldig viktig. En måte å redusere byggenæringens utslipp på, er å bruke fornybare energykilder på kostnadsbesparende, enkle og miljøvennlige måter. I denne oppgaven blir bruken av en enkel solvarmevegg presentert. Denne solvarmeveggen blir kalt trombevegg.

I oppgaven presenteres et litteraturstudium utført for å få dypere innsikt i dagens status i den norske og europeiske byggenæringen, energibruk i byggenæringen globalt, bruk av solenergi i bygg og studier utført på trombeveggliknende systemer. Det finnes mange studier på trombevegger, og det er tydelig at trombevegger har potensiale. IDA ICE, Polysun, TRNSYS og Matlab blir vurdert som mulig simuleringsprogramvare til prosjektet. Videre blir grunnleggende teori bak varmeoverføring gjennom stråling, konduksjon og konveksjon gjennomgått, samt det matematiske grunnlaget til komponentene brukt i simuleringen. Grunnleggende teori og kilder som legger grunnlaget for trombeveggsimuleringen blir gjennomgått. Basisen for Matlab-scriptet blir også gjennomgått. I kapittel 4, Method, presenteres arbeidet med å bygge opp simuleringen kronologisk. For å bedre finne feil og mangler i simuleringen underveis bygges simuleringen opp delvis. Det enkle kontrollsystemet blir også presentert. Enkel validering av simuleringen blir også gjennomført, ved brukt av eksperimenter funnet i litteratur.

En analyse av trombeveggens effekt i Kina og Norden blir gjennomført og presentert. Gøteborg i Sverige, Reykjavik på Island og Kashgar og Shanghai i Kina er valgt som lokasjoner. Dette er for å representere et varmt og et kaldt område fra både Kina og Norden. En årlig simulering, samt ukentlig sommer- og vintersimuleringer, blir gjennomført på alle fire lokasjoner. For å bedre hjelpe arbeidet med videreutvikling av trombevegger presenteres påvirkningen trombeveggens og luftåpningens tykkelse har på effekten av veggen, i Shanghai og Gøteborg. En drivhusgassanalyse blir gjennomført, og alle lokasjonene blir kalkulert som miljøvennlige. Til slutt blir simuleringens treffsikkerhet gjennomgått, og lærdommen fra resultatene presentert videre. Anbefalt videre arbeid med trombevegger presenteres til slutt.

Matlab-scriptet som legger grunnlaget for simuleringen legges ved i sin helhet.

Preface

This master thesis work was completed in a collaboration between the Norwegian University of Science and Technology in Norway and the Shanghai Jiao Tong University in China. I had planned to work at the Green Energy Laboratory (GEL) at SJTU's Minhang Campus in Shanghai, but these plans were ultimately cancelled due to the ongoing Coronavirus pandemic. This affected the project as no trombe wall experiments at GEL could be performed. The scope and focus of the thesis was changed accordingly, months after the start of the project. The supervisors for the project are Vojislav Novakovic from NTNU and Yanjun Dai from SJTU, and is meant to further understand the solutions to the need to lower the building stock's energy demand in Norway and in China.

Writing a thesis in this period of home office work has proven to be a challenge, and I would like to thank my friends and family for helping me with my motivation and spirit through this. I would also like to thank my supervisor Vojislav Novakovic, who quickly stepped up as my closest supervisor when my plans for exchange fell apart. His help and knowledge was very valuable when redefining my project and finding its new and changed course. Without his help, being able to deliver this project on schedule would have been an even bigger challenge.

1 Introduction

According to the International Energy Association, the building sector represents 36 percent of the yearly total final energy demand in the world(IEA 2019). This number is expected to continue to rise, as seen in figure 1, with the ever-increasing global building floor area and the rising demand for and access to energy in developing countries being two of the main reasons. And, in today's political landscape, with the growing global focus of lowering each country's total energy use, the benefits of a more energy-efficient building sector is evident. One way to reduce the energy need of a building, is to utilize some of the renewable energy sources in a cost-effective, realistic and environmentally friendly manner. In this assignment, the use of a simple solar power installation will be researched. The installation is called a trombe wall.

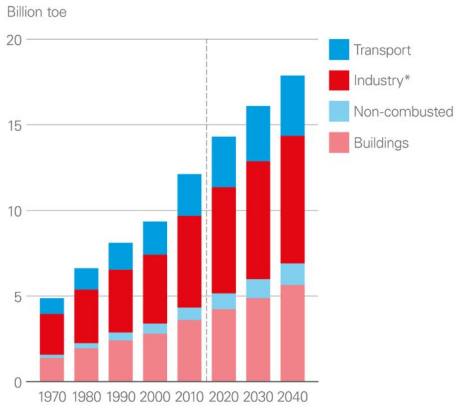

Figure 1: Annual energy demand by sector (Petroleum 2019). 1 toe = 11,630 kWh.

The work presented in this report consist of a literature review, a review of the relevant theory, the setup of a simulation, validation, calibration, and results from the simulation and an assessment of further work on this project. The literature review section begin by presenting the current status of the research and regulations on the energy demand of buildings. Subsequently the worldwide research into trombe wall, solar heating wall and solar chimney technology is presented, to clarify which aspects of the trombe wall that is firmly established in literature and which should be researched further by the author. At the end, different simulation software is presented, as choosing a fitting simulation software is crucial for the project. IDA ICE, Solar Plus and TRNSYS are found to be the three most relevant software.

In the theory section, basic physical mechanics and governing equations in the system is presented. Radiation, conduction and convection heat transfer modes is presented briefly. Then, some aspect of the simulation of building simulation are presented. It is presented generally, and specifically on how TRNSYS operates. The mathematical foundations of different components of the TRNSYS simulation are also presented. The framework for doing green house gas emission calculations is presented as well.

The control strategy for the simulation is presented as well. To validate the simulation, some recreation of experiments from literature is performed and presented in this section.

In the method section, the work with producing the simulation is presented chronologically. The simulation was defined step by step, with the purpose of testing and verifying the simulation by comparison to literature at each major step. This was to prevent large inaccuracies in vital components of the simulation, and to ease error detection when creating the simulation. Here, the viability of each simulation is discussed, and key parameters are measured against relevant numbers from sources presented in the literature review. A more thorough validation is performed as well, by replicating experiments found in litterature.

The result section details the results from the different simulation. Four different locations, two in China and two in the Nordic countries are simulated and presented. Summer and winter simulation for each of these locations, as well as simulations for different slit and wall sizes are presented as well. These results are discussed in this section. In the discussion section, sources of error in the simulation is presented. More broad results from the simulations is discussed as well, and further work is discussed.

2 Literature

A very important aspect of the energy use of a building is the building's envelope. The buildings envelope considers the properties of a buildings facade, foundations and roof, and directly impacts the heat losses in the building. This means that having a building sector that constructs high quality building envelopes leads to lower energy demand of the sector. One way to reach this goal is through government regulations that demand certain key properties of all new and refurbished buildings in a country.

2.1 Passive houses

This is partly why the Regulations on technical requirements for construction works (TEK-17)(bygningskvalitet 2020) in Norway has become more and more strict on building envelope demands. For an even stricter and more energy-efficient building, the passive house standards NS-3700(Norge 2013) and NS-3701(Norge 2012) can be used, for residential buildings and commercial buildings respectively. These documents presents strict rules on which buildings that will be determined to be a passive house. There are demands for documentation and calculation of the buildings energy use, with a heavy focus on the buildings envelope. Maximum U-values for windows and doors, as well as maximum values for infiltration rate, is set, while U-values for walls, roof and foundation is merely recommended. These values will indirectly be set by the maximum amount of heating energy allowed to be supplied to the building. Other than that, and some demands for the heat recovery unit and maximum cooling demand, the passive house house standard does not set too many rules for how a passive house building is supposed to be made. Active auxillary cooling and heating system are therefore not disapproved of, which is in direct opposition of the more used German definition of a passive house, which is very different(Anton and Vestergaard 2013).

In the German definition, the goal of a passive house is to rely only on heating or cooling the incoming ventilation air and heating through the internal gains, and to not use any other active heating or cooling systems(Institute 2020a). The German Passivhaus definition is not defined in German government regulations, but is a design strategy. The Norwegian passive house regulations got their name from this design strategy, and implemented a different strategy into regulations. With the Passivhaus definition, given that the incoming air of a correctly sized ventilation system has a limited heating and cooling potential, the aforementioned restriction therefore necessitates heavy use of passive heating and cooling techniques as well as on the design of the building envelope. These buildings are gaining a lot of traction, evident by the Passive House Institute's database boasting 4811 passive houses across the globe at the time of writing(Institute 2020b), and the UK Passivhaus Trust homepage claiming that 65,000 houses with the "passivhaus" standard and methodology has been built(Trust 2019).

The German definition also has the passive use of solar power as a main component in its definition, while the Norwegian standard does not(Anton and Vestergaard 2013). The Norwegian standard also has a net heating energy demand that is 5-10 kWh/m^{2}year higher than the German definition(Anton and Vestergaard 2013).

2.2 Zero emission buildings

Common for both NS-3700/3701 and passivhaus however, is that their focus is on the minimization of energy use, and not directly on the minimization of emissions. The reduction of energy use does, naturally, reduce the emissions indirectly, but one could technically fulfill the requirements of both these standards and still use environmentally straining materials. The use of environmentally-friendly materials, construction practises and operation practises are of course recommended, but there are no demands for calculations of these emissions. This is however, a very central part in the Norwegian definition of ZEB, the zero emission building, which is a design strategy not yet put into government regulations. In this Norwegian definition, a ZEB building is a building that produces enough renewable energy on site to compensate for all the emissions from all of its building components through its entire lifetime(Zero Emission Buildings n.d.). This is a very ambitious goal, and the amount of ZEBs in Norway is still zero, although some are quite close(Andresen

et al. 2019). To help differentiate the near ZEBs (nZEBs) and to create clear and concise goals for ambitious builders, The Research Centre on Zero Emission Buildings has defined some different nZEB goals(Zero Emission Buildings n.d.):

- ZEB-O. The building produces enough renewable onsite to compensate for the emissions stemming from the buildings operational time.
- ZEB-OM. The building also compensates for the emissions related to the manufacturing of all the materials in the building.
- ZEB-COM. The building additionally compensates for the emissions related to the construction of the building.
- ZEB-COMPLETE. The building additionally compensates for the emissions related to the demolition of the building, and the emissions from the resulting materials.
- ÷EQ. This is added if the building does not compensate for the emissions related to equipment.

The new Powerhouse Brattørkaia in Trondheim is a ZEB-COM-EQ, which, along with Powerhouse Kjørbo, is the second highest "grading" a building in Norway has attained as of yet(Andresen et al. 2019). Campus Evenstad in Gudbrandsdalen is currently the most environmentally friendly building in Norway with regards to the ZEB-scale, it being classified as ZEB-COM(Statsbygg 2019).

These Norwegian standards and definitions are precisely that, Norwegian. The Research Centre on Zero Emission Buildings is a Norwegian endeavour, as the building is constructed according to the centre's guidelines. This is evident when seeing how ZEB is usually defined, i.e. in Sartori et.al's article presenting a definitive framework on how ZEBs are defined globally(Sartori, Napolitano, and Voss 2012). Here the focus is on Zero *Energy* Buildings, which entails balancing out the produced energy by the building with the energy used by the building, as well as sometimes the energy used in manufacturing, construction and end-of-life. This definition is also used in the European Union, where they state, in a directive on the energy use in buildings that:

Nearly zero-energy building means a building that has a very high energy performance(...). The nearly zero or very low amount of energy required should be covered to a very significant extent by energy from renewable sources, including energy from renewable sources produced on-site or nearby(Union 2010).

This version of ZEB does naturally result in a somewhat different focus than with Zero Emission Buildings, where the environmental impact of the building in question is directly evident. The Norwegian definition of ZEB could spread globally. No matter the popularity of each definition of ZEB, the Norwegian definition of Zero Emission Buildings will be used in this paper, along with its supplementary nZEB definitions. This definition is more robust and concise, and when environmental-friendly buildings is the goal, this is the obvious choice.

As ZEB is such a high goal to reach, and some on-site energy generation is required, smart solutions are necessary. This project is focused on one of these simple solutions.

2.3 The solar chimney

The proposed simple solution is a type of thermal storage wall, called a trombe wall. It is a simple design, similar in design and working principle as the solar chimney(Hirunlabh et al. 1999). The principle of a solar chimney, whose only goal is ventilation and cooling, is to utilize the stack effect to draw hot air out of the building through a solar heated chimney or wall, as described and modelled by for example Bansal et.al in 1993(Bansal, R. Mathur, and Bhandari 1993). A simple representation of a solar chimney is shown in figure 2.

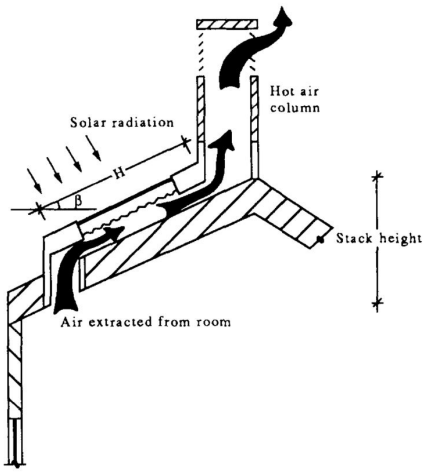

Figure 2: A simple sketch of a solar chimney(Bansal, R. Mathur, and Bhandari 1993)

As seen in figure 2, the solar radiation is allowed to pass through the glass cover and is absorbed by the high absorbance wall. This wall, in return, emits low wavelength light, which the glass cover does not transmit as easily, forcing the air inside the slit to heat up. As air is a compressible fluid, and expands in tandem with rising temperatures, the pressure in the slit increases. It is this pressure difference between the air inside the chimney and the ambient air that is the driving force in the classic solar chimney. This is also known as the stack effect. Bansal et.al found that a collector area of 2.25 m^2 resulted in an airflow of 100-350 m^3/h for horisontal solar radiation of 100-1000 W/m^2. It should be noted that this is just a calculated value, not based on experiments.

Research and simulations with experimental validations of this kind of setup is easily found. I.e Ong and Chow(K.S. Ong 2003), who successfully developed and validated a solar chimney wall in Malaysia in 2003. Their work rely a lot on experimental analysis by other authors in the same field to evaluate a lot of the empirically based equations in heat and mass transfer. By inspection of this article, the importance of cooperation in the scientific community is emphasized. Ong and Chow source different others for the value of γ, C_d, for sky temperature, and Incropera and Dewitts *Principles of heat and mass transfer*(Incropera et al. 2013) for a lot of the equations.

Ong and Chow further presents a sketch presenting the solar chimney in its simple design and fairly complex physics, as well as an accompanying thermal network, as seen in figure 3a and 3b.

2.4 Trombe Walls

However, although the solar chimney and the trombe wall does have similar working principle, they differ in regulatory strategy and overall goal. The solar chimney's goal, as discussed, is ventilation(Bansal, R. Mathur, and Bhandari 1993), while the trombe wall also wants to heats up the building in question(Wilson 1979). This is possible by having the exhaust air from the heated slit directed back into the room. With this setup, the heating effect caused by the sun is not just used to fuel the airflow through the slit, but also by heating up the air flowing into the room. The placement of the trombe wall is naturally more restricted than the placement of the solar chimney, but, in climates were space heating need coincides with a sufficient solar flux, the trombe wall is the best solution. Another issue with heating through solar power is that there often is an offset between when the solar flux is at its peak, and when the need for space heating is peaking, because of the higher ambient air temperature and passive solar heating during the daytime.

2.4.1 Thermal storage wall

To solve this issue, a thermal storage wall is used. This is a simple and easily implementable solution, because the wall can absorb, store and release its energy passively, with no active regulation required. The

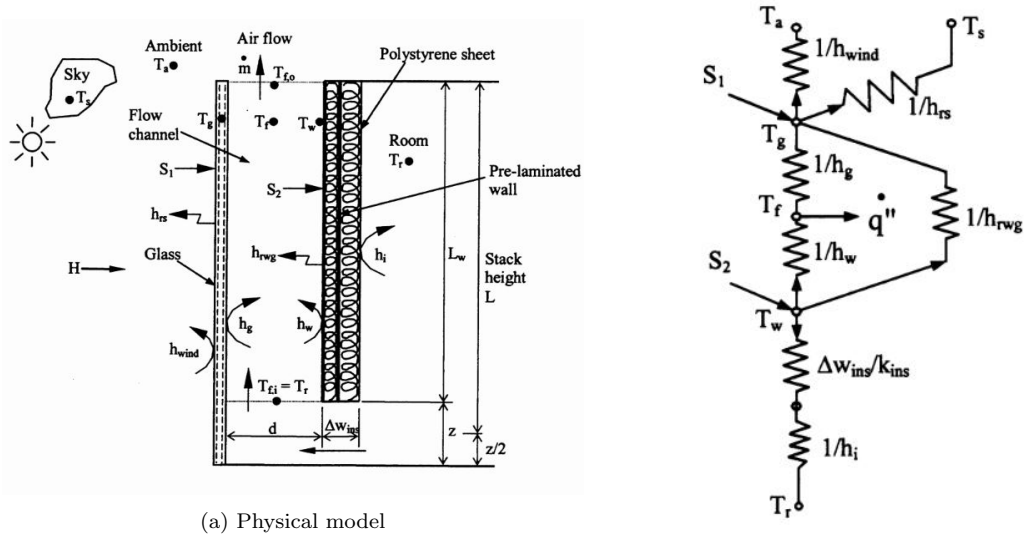

(a) Physical model

(b) Thermal Schematic

Figure 3: A representation of the heat and mass transfer of a solar chimney(K.S. Ong 2003)

.

inertia of the system, with high rate of solar absorption and low rate of convection between the wall and the air leads to a delayed response to the incoming solar flux. To decrease the delay, opening and closing of the vents between the trombe wall and the room can be performed, if installed. For a non-ventilated and non-insulated concrete trombe wall, each 10 cm of concrete releases its energy at a delay of 2-2.5 hours after the solar radiation first strikes and heats up the wall(Ram and Garg 1985), found through numerical analysis. This means that at 30 cm of concrete, and peak solar radiation at noon, the peak heating rate will be between 6 and 7:30 pm. This might be too early in the evening for some systems, leading Agra et.al to propose between 30-40 cm of concrete thickness as optimal thickness(Agrawal and Tiwari 2010), at least for Indian climates. A lag time simulation that does have some experimental validation is Zalewski et.al's study of different types of solar heating walls(Zalewski, Lassue, et al. 2002). They found that for a solar heating wall with a 15 cm thick massive wall, made of solid breeze-blocks with a heat conductivity of 0.82 W/mK, the delay is five hours. Dense concrete has a heat conductivity of 1.0-1.8 W/mK(Engineeringtoolbox.com

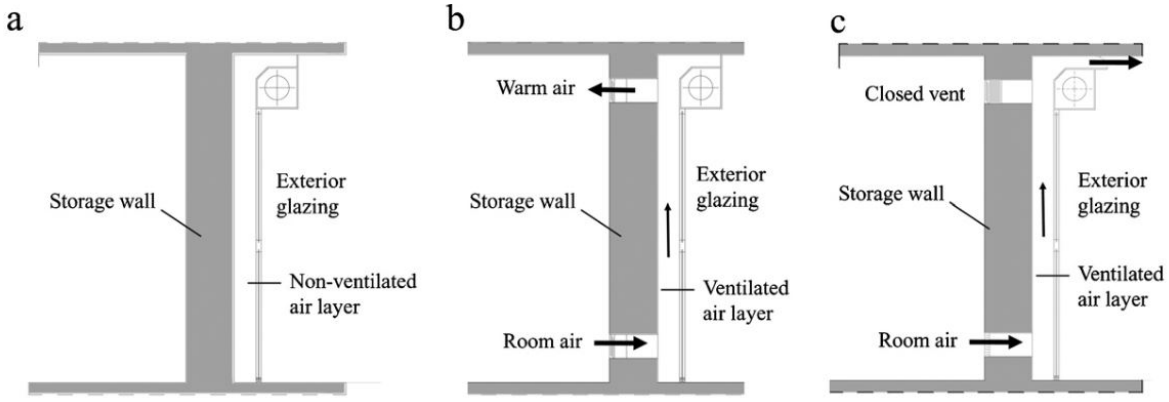

Figure 4: Different operating schemes, a:non-ventilated solar wall, b:Trombe wall in winter, c:Trombe wall in summer, with cross-flow(Stazi, Mastrucci, and Perna 2012a).

2020), which is a lot higher, explaining the differing lag times for the walls of Zalewski et.al(Zalewski, Lassue, et al. 2002) and Agrawal et.al(Agrawal and Tiwari 2010).

2.4.2 Overheating

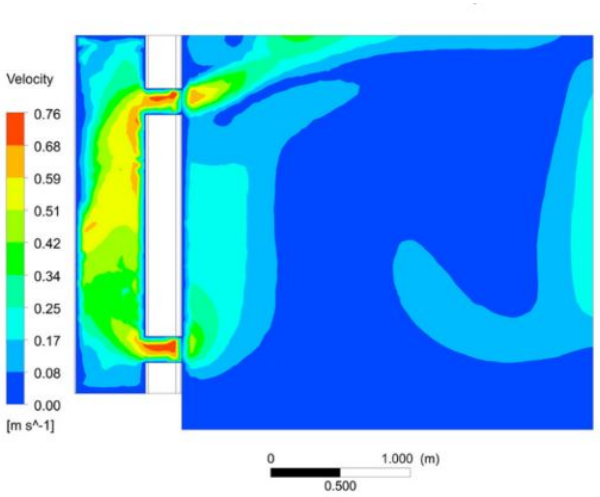

Figure 5: Velocity distribution in a double glass module at 1300 (February 26th), in Turkey(Koyunbaba and Yilmaz 2012).

Another common concern with the integration of solar thermal walls is the possibility of summer-time overheating, especially for highly insulated building envelopes(Stazi, Mastrucci, and Perna 2012a). This can be somewhat negated by the use of insulation between the collector and the interior(Matuska and Sourek 2006). Matuska et.al(Matuska and Sourek 2006) found that by increasing the insulation from a U-value of 1.0 to a value of 0.167 W/m^{2}K, the annual positive heat gain through the wall was reduced from 9.9 to 2.1 kWh/m^2, and the temperature gain for a hot summer day was below 1K. This was also confirmed by Zalewski et.al's experiments, showing that the insulated trombe wall has 2.6 times lower positive transmission during cooling periods than the uninsulated wall(Zalewski, Lassue, et al. 2002). In a study done by Kundakci et.al in Turkey in 2012, speeds of up to 0.76 m/s was found, in a trombe wall setup with double glazing(Koyunbaba and Yilmaz 2012). They performed a numerical analysis of the flow pattern in the slit, vents and room, showing the high variation of speeds inside the slit. This can be seen in figure 5.

This positive solar flux can also be negated by having an opening in the exterior glazing, allowing the trombe wall to act as a solar chimney during periods with cooling demand, by having cross flow in the wall, as seen in figure 4. It would then function as an exhaust fan allowing new, cooler ambient air to enter the building. This was demonstrated by Stazi et.al, who performed an experimental study of unvented solar walls in Italy in 2011. They found that by introducing cross-flow the solar wall went from being very detrimental to the indoor environment to having a slight cooling and good stabilizing effect on the indoor environment(Stazi, Mastrucci, and Perna 2012a). In a later and more thorough study, Stazi et.al found that cross flow ventilation reduced the yearly cooling need 15.1% compared to an unvented wall(Stazi, Mastrucci, and Perna 2012b). They also found that cross flow was the most effective in super-insulated buildings.

Another method of lowering the heating gain from the wall is solar shading. This will, of course, lower the solar radiation hitting the wall, lowering the wall's temperature. Stasi et.al found, by experimentation over three years and with multiple trombe walls, that solar shading results in a huge drop in annual cooling demand, in some cases as much as 70%(Stazi, Mastrucci, and Perna 2012b). It is however important to note that this was tested for non-insulated trombe walls only. An increase in ventilation behind the wall would probably lower the effect of solar shading by some amount.

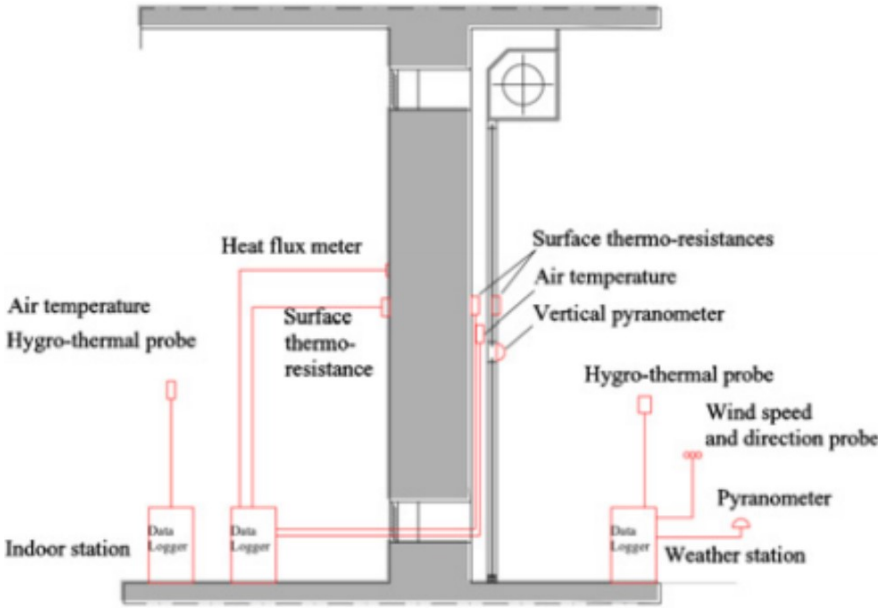

Figure 6: Experimental setup of Stazi et.al's trombe wall experiment(Stazi, Mastrucci, and Perna 2012a).

2.4.3 Experimental measurements

In this study, Stazi et.al also provide a detailed description of their logging method, which is claimed accordance with ISO7726:1998(Stazi, Mastrucci, and Perna 2012a). This can be seen in figure 6. An accurate method of logging experimental data is essential for any simulation or data verification, and that is why ISO7726:1998, or the Norwegian version NS-EN ISO7726:2001(Norge 2001) is important legislation. This standard stipulates a common practise for logging of the thermal environment, ensuring that under-measuring, leading to inaccurate values, or over-measuring, leading to loss of time and higher costs, is more easily avoided.

2.4.4 The exterior glazing

With the trombe wall, it is important for the exterior glazing to be air-tight. If the glazing is leaking, then cold ambient air will enter the air cavity, ruining the stack effect and also potentially cooling down the airflow enough to initiate reverse-flow and cooling of the interior. An insufficient air-tightness will also lead to a higher air leakage number, which could result in a failed criteria for achieving for example the Norwegian passive house standard(Norge 2012; Norge 2013).

The effect of low emitting materials on the exterior glazing is also worth to note. Zalewski et.al. used their validated numerical model to test the effect of changing different parameters of the trombe wall(Zalewski, Lassue, et al. 2002). They found that the use of low-emitting glazing almost doubles the amount of energy collected during the heating season. This applies for an unventilated trombe wall, a ventilated wall as well as a composite wall, at least in the north of France.

2.4.5 Material choices

The material choice of the trombe wall is an essential part of the wall design. It affects conduction, convection, heat storage, cost, life cycle GHG-emissions and solar radiation absorption(Saadatian et al. 2012). Concrete(Stazi, Mastrucci, and Perna 2012a), breeze-blocks(Zalewski, Lassue, et al. 2002), phase change materials(Zhou, Yu, and Zhang 2018) and water(Wilson 1979) are all examples of trombe wall materials that have been utilised in literature. Concrete is the most standard solution, as it is cheap and has a high

thermal capacity and a medium conductance, allowing a time delay in energy transfer from exterior to the interior. The breeze-blocks have similar properties to the concrete, but is easier to mount and has a lower density. The use of phase change materials has shown promise, which could result in a very positive mode of energy storage and release, as found in (Zhou, Yu, and Zhang 2018).

2.4.6 Trombe wall aesthetics

In most studies, the aesthetic aspect of a proposed trombe wall is often not mentioned(Gan 1998; Agrawal and Tiwari 2010; Wilson 1979; Stazi, Mastrucci, and Perna 2012a; Saadatian et al. 2012). It could be argued that the aesthetic of an energy saving measure should not be of great importance, as long as long term energy and environmental gains are present. But, if large-scale implementation of an energy measure is to be considered, then the aesthetics and its ability to fit the architect's vision is important. And with the exterior view of a large double glazed window with a large black wall right in front, and the interior view of a solid wall with no windows, it is perhaps not the easiest systems to design around.

In the world of photovoltaics, for example, "invisible" PV-panels are gaining traction, with even companies like Tesla launching its own brand of PV-panels that look like ordinary roofing(Tesla 2019). The focus and importance on design and looks in PV is evident, and the variety in PV aesthetics is large(Solar n.d.). A study performed by Probst and Roecker in Switzerland in 2007 showed that architects and engineers have some differing opinions of building integration of solar collectors, and that the technology at the time was not sufficient to achieve great building aesthetic integration across the board(Probst and Roecker 2007).

2.4.7 Vented vs unvented wall

The effectiveness of a vented versus an unvented trombe wall is contested, with some advocating the trombe uvented wall (Ellis 2003; Balcomb et al. 1980) and some advocating the vented trombe wall (Koyunbaba and Yilmaz 2012; Stazi, Mastrucci, and Perna 2012a; Stazi, Mastrucci, and Perna 2012b).

2.5 Simulation software

Multiple simulation software is relevant for this project, with Polysun, IDA ICE, TRNSYS and Matlab being the most relevant. IDA ICE is a simulation software that is focused on the energy use and indoor environment of an entire building. It has a easy to use interface, and building the simulation and viewing the results is intuitive. The software is considered quite user friendly. There is a possibility for the creation of custom components, however limited. Polysun is a simulation software with multiple capabilities, and has a graphic simulation environment, where the setup of the simulation is easily viewed, with piping and more being similar to a real world setup. As with IDA ICE, it is quite user friendly, but has limited support for the creation of custom components.

TRNSYS is a highly flexible simulation tool, with good support for the creation of custom components, and with a big library of components already built. There are few restrictions on the setup of the simulation, and complex and non-standard simulations is almost as simple to setup standard simulations. This high level of flexibility is the main reason for choosing TRNSYS, as the trombe wall is not a standard and well used component in simulation software. Therefore, easy implementation of a custom component written in Matlab or FORTRAN is considered the best option.

Creating the entire simulation from scratch in Matlab was considered, as it gives the user full flexibility. However, the gain in flexibility does not outweigh the massive loss of time that it will take to setup a simulation from scratch.

2.6 Previous master thesis work

Previous work has been done by students at NTNU, by Marte W. Nilsson in 2015 and Liv Mette Hamre in 2018. Nilsson worked on the Green Energy Lab at Shanghai Jiao Tong University, analysing a solar heating

wall installed in the GEL's building envelop(Nilsson 2015). The purpose of the project was to analyse the effect of facade integrated solar heating walls in Norwegian buildings. A parameter study was performed, with storage tank temperature, tank sizing, flow rate, control strategy and placement of the heat exchanger as parameters. To simulate this setup, as well as to perform the parameter analysis, TRNSYS was used. The project is similar to this project, both in location, scope, software and field of study. However, as this project deals with water at a high temperature, flowing through piping and heating the building domestic hot water, the similarities are limited to the surrounding system.

Liv Mette Hamre, as a master thesis student from NTNU, conducted an experiment on a serpentine flow photovoltaic and thermal system mounted on the roof of a Shanghai building(Hamre 2018). The project setup can be seen in figure 7a, and the symbiosis between the photovoltaic system and the thermal system can be seen. The photovoltaic system heats the airflow, and the bouyant flow in the air passage cools down the photovoltaic system, which helps with the PV performance. The system was modelled with a component written in Matlab, implemented into a TRNSYS simulation. This proved a satisfactory solution. Hamre found that the system covered the ventilation load the most during the transition seasons, because of the lower outdoor temperature, as seen in figure 7b. For reference, one month equals approximately 730 hours, and during the month of May around 17% of the ventilation is covered by the thermal system.

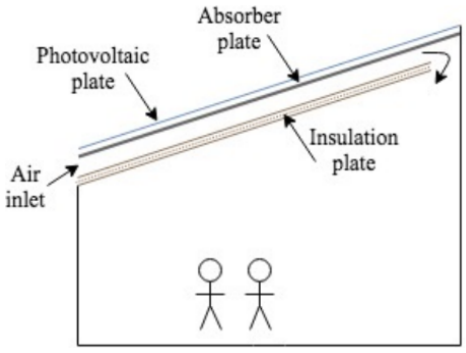

(a) Simple representation of Hamres setup

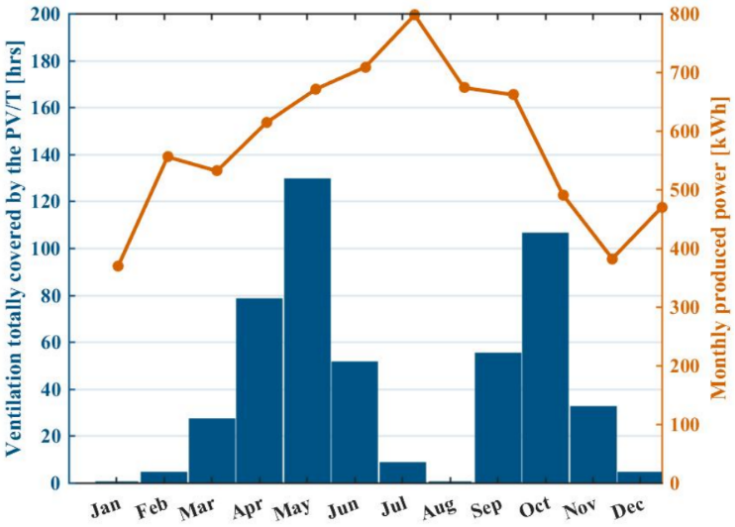

(b) The produced power and ventilation coverage of Hamres system.

Figure 7: LM Hamres setup and results(Hamre 2018)

.

2.7 Coding languages

The script for the trombe wall component needs to be coded by the author, as the trombe wall component is not of a high enough flexibility and accuracy. As TRNSYS has a high degree of flexibility, a component made to call other programs with code is standard in TRNSYS. In the most current version of TRNSYS (TRNSYS 18), the component can be coded in Fortran, Python, Matlab and C++. Python and C++ are both powerful languages that are very suited to be used with TRNSYS, and Python especially has a wide range of helps and guides online. This could be very useful for an author with medium experience with programming. However, in this project TRNSYS 17 will be used, and Python and C++ is not a possibility with this edition.

Matlab and Fortran are the two remaining candidates. With Fortran, a basis for creating a trombe wall

component is readily available, and one could by inspection see how a Fortran coded TRNSYS component could be created. This also has the added effect of not needing to call a separate programming language interpreter. The positives of Matlab are that the author has some knowledge of Matlab already, and that the program is used very extensively by the academic community. Troubleshooting and error-handling in Matlab is considered to be easier than in Fortran, due to Matlab's high amount of online communities. Matlab also has many helpful commands and a wide variety of built in mathematical commands.

3 Theory

In this section, the basic physical mechanics and governing equations in the system will be presented. If not otherwise stated, the equations and theory is based on the work of Incropera, Dewitt, Bergman and Lavine, in *Principles of Heat and Mass Transfer*, 7th edition(Incropera et al. 2013).

3.1 Heat and mass transfer

The three basic modes of heat transfer is radiation, conduction and convection. Heat is emitted, reflected, absorbed and transmitted through different materials in the trombe wall through radiation. Through the walls, and glazing, heat is conducted as a result of temperature difference between each side of the material. Conduction heat transfer is a result of temperature difference of a material and mass flow over the material.

3.2 Radiation

Radiation can be viewed as the loss or gain of energy as a result of net negative or net positive electromagnetic radiation exchange with the surroundings. The radiation flux from a surface is given by

$$q''_{rad} = \epsilon\sigma T_s^4 - \alpha G, \tag{1}$$

where q''_{rad} is the net radiation flux, ϵ is the emissisivity of the surface, σ is the Stephan-Bolzmann constant, T_s is the surface temperature, α is the absorbtivity and G is the incoming radiation.

Observing equation 1, the incoming radiation G needs to be defined. A simple definition of G can be made if the surface is a small surface contained inside larger isothermal walls, if the emission the surrounding walls is blackbody emission. We then get that

$$G = \sigma T_{sur}^4, \tag{2}$$

where T_{sur} is the temperature of the surroundings. Combined with equation 1, and if it is further assumed that $\alpha = \epsilon$ (a so called gray surface), we get

$$q''_{rad} = \epsilon\sigma(T_s^4 - T_{sur}^4), \tag{3}$$

which, as mentioned, describes the net radiation heat loss *from* the surface. In a solar heating application such as this, incoming radiation energy is also very much present and important. With solar radiation, a multitude of different sources of radiation heats up a non-shaded surface. The incoming radiation sources are

- Direct sunlight, striking the surface parallel to the solar zenith angle
- Diffuse radiation, stemming from the solar rays scattering in the atmosphere, in an amount in conjunction with the amount of sky coverage
- Reflected ground radiation, which is solar radiation reflected from the ground
- Sky radiation, which is heat emitted from the non-zero temperature air
- Ground radiation, which is heat emitted from the non-zero temperature ground

These radiation sources all hit the wall or the glass, and depending on what type of radiation energy it is, gets reflected and transmitted and absorbed. Glass, for example, has a high transmission value for solar radiation, but lower for radiated heat. This means that direct sunlight, diffuse radation and reflected ground radiation passes through the glazing more easily than sky and ground radiation.

3.2.1 Key properties

Emissisivity is the surface's ability to emit radiation energy as a result of heat, as evidenced by equation 3. A higher emissivity results in a higher net radiation flux, when there is a difference between the surroundings and the surface. If low heat losses is preferred, a low emissisivity is preferred.

Reflectance is the surface's ability to reflect incoming radiation energy. A high reflectance leads to a lower energy gain.

Absorptivity is the surface's ability to absorb incoming, not reflected, radiation energy. A high absorptivity leads to a higher energy gain.

3.3 Conduction

Conduction is the heat transfer through a material, as a result of a temperature difference inside the material. The simplest of the three modes of heat transfer, the conduction heat transfer rate is given by

$$q''_{cond} = k\frac{T_1 - T_2}{L}, \tag{4}$$

where q''_{conv} is the convection heat transfer, k is the thermal conductivity, T_1 and T_2 is the temperatures of the different sides of the material and L is the thickness of the material, parallel to the heat transfer. This definition is only helpful for an object of constant thermal conductivity, which is not always the case. To easily define the heat transfer rate through *composite walls*, thermal resistances are used. Thermal resistance is the inverse of the conductivity, noting the materials inherent ability to form steep temperature gradients. The conductivity of the composite wall, also called the U-value of the wall, is given by

$$k_{tot} = \frac{1}{\sum R'_i L_i}, \tag{5}$$

where k_{tot} is the total conductivity, R'_i is each section's thermal resistance, and L_i is each section's length.

3.3.1 Key properties

In most material databases, the given material property related to conduction heat transfer is the material's thermal resistance per meter. A higher thermal resistance gives a lower heat flux through the material, and a higher temperature difference between the sides of the material.

The heat capacity of a material, or its thermal mass, is the material's inherent ability to retain heat energy. The thermal mass is a measure of how much energy is needed to heat up the material a certain amount, as well as how much energy the material emits out when the material cools. A high thermal mass means a higher amount of energy is needed to heat the material up. If a stable temperature is wanted, a high thermal mass is preferred. If quick heating is wanted, then a low thermal mass is preferred.

3.4 Convection

Convection heat transfer is the heat transfer from a surface to a moving body of fluid. It is a very complex mode of heat transfer, with analytical solutions for complex systems mostly non-existant. Numerical solutions, and empirically validated equations with various dimensionless numbers and simplifications is the norm.

The simplest base equation for the convection heat transfer rate is

$$q''_{conv} = h(T_s - T_\infty), \tag{6}$$

where q''_{conv} is the heat transfer rate of convection, h is the convection heat transfer coefficient, and T_s and T_∞ are the temperatures on the surface and of the moving fluid, respectively. The unfortunate case with convection is the very high variance of the important convection heat transfer coefficient h. It varies in many orders of magnitude between different convection modes, fluid properties and temperatures. Fluid specific heat, density, viscosity, thermal conductivity, conditions of the flow and the surface geometry all impact the convection h.t. coefficient. To determine h, experimental validation is performed. There are many different experiments available in literature, and by finding a similar experiment setup the convection heat transfer coefficient can be found.

3.5 Building heat transfer simulation

To simulate the effects of each of these three modes of heat transfer, the simulation program calculates their loads for each timestep:

$$dQ_{node} = (q''_{rad} + q''_{cond} + q''_{conv})dt, \tag{7}$$

where dQ_{node} [kJ/kg] is the change in internal energy of the node and dt is the length of the timestep. Summing up all these step changes results in the total energy absorbed and released from the system.

The change in internal energy also results in a change in temperature, given by

$$dT_{node} = \frac{dQ_{node}\rho V}{c_{v,p}}, \tag{8}$$

where dT_{node} is the change in temperature, ρ is the density, V is the volume of the node and $c_{v,p}$ [kJ/K] is the heat capacity of the material.

On the next step, all calculations are repeated with the temperatures and values from the last step. A shorter timesteps leads for the most part to a more accurate solution, but it also extends the calculation time.

3.6 How TRNSYS operates

The components used in this simulation are free standing components, based on physical equations which can be found in the documentation(Solar Energy Laboratory 2012), and some table lookup for some values. Each component has its own internal calculation, and each component communicates through inputs and outputs. At each timestep, TRNSYS run through each component, trying to get the values to converge. Convergence is reached when the input and outputs of a found loop are similar, and equal. This operation, of iterating through every component until convergence is reached differs TRNSYS from other simulation programs, which often only calculate each component once for each step(Solar Energy Laboratory 2012). The result of this is a simulation that run somewhat slower, but also a simulation that will not produce results if the components do not communicate correctly. At least in this specific manner.

3.6.1 Weather data

The weather data used is Meteonorm weather data, with the measured data basis being monthly values. The hourly values that are used as inputs into the simulation are calculated through a stochastic model. I.e. the hourly values are found by a model with somewhat random, but realistic, results, based on the monthly values. The weather data used in the TRNSYS simulation is of Gothenburg, Reykjavik, Kashi and Shanghai.

Locations with Meteonorm weather data in is presented in figure 8 for Europe and figure 9 for Asia, where black dots are weather and solar radiation data, while white dots are locations lacking measured solar radiation data.

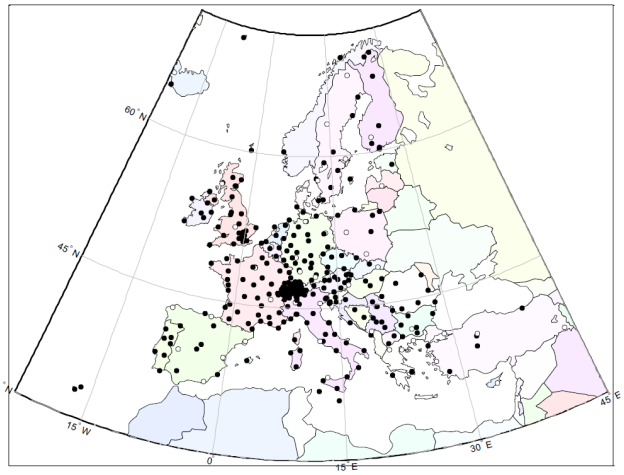

Figure 8: Meteonorm weather European data locations

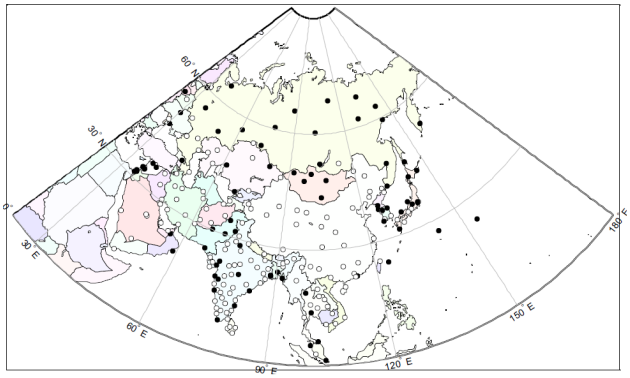

Figure 9: Meteonorm weather Asian data locations

To perform the initial simulations and validations of the building model and ventilation system, Gothenburg is used. This is to have a base case for the simulation and validation of the system.

3.6.2 Type 56 - building model

The building model component named *type 56* is models heat transfer through airnode calculations, through this energy balance:

$$\dot{Q}_{node} = \dot{Q}_{surf} + \dot{Q}_{inf} + \dot{Q}_{vent} + \dot{Q}_{int} + \dot{Q}_{bound} + \dot{Q}_{solar} + \dot{Q}_{shading}, \tag{9}$$

where $\dot{Q}_{node}$ is the heat transfer of the airnode, $\dot{Q}_{surf}$ is of the surfaces in the node, $\dot{Q}_{inf}$ is of the infiltration into the node, $\dot{Q}_{vent}$ is of the ventilation, $\dot{Q}_{int}$ is of the internal gains, $\dot{Q}_{bound}$ is of the airflow from connecting zones or boundary condition, $\dot{Q}_{solar}$ is of the direct solar gain and $\dot{Q}_{shading}$ is the solar gain from internal shading elements. There different elements of this balance can be found with varying levels of simplicity.

$$\dot{Q}_{surf} = \sum (T_{surf,i} - T_{node}) h_{ci}, \tag{10}$$

where h_c is the thermal convective coefficient of the surface.

$$\dot{Q}_{inf} = \dot{V}_{inf}\rho c_a ir(T_{amb} - T_{node}), \tag{11}$$

$$\dot{Q}_{vent} = \dot{V}_{vent}\rho c_a ir(T_{vent} - T_{node}), \tag{12}$$

$$\dot{Q}_{int} = \sum Q(\text{internal gains}), \tag{13}$$

$$\dot{Q}_{bound} = \dot{V}_{vent}\rho c_a ir(T_{bound} - T_{node}), \tag{14}$$

$$\dot{Q}_{solar} = f_{solar}(I_{trans,dif} - I_{trans,dir}), \tag{15}$$

where f_{solar} is the solar to air fraction, i.e. the fraction of incoming solar radiation that results in a direct convective heat gain for the airnode. $I_{trans,dif}$ and $I_{trans,dir}$ are the incoming transmitted diffuse and direct solar radiation, respectively.

$$\dot{Q}_{shading} = \sum \dot{Q}_{absorbed,i}. \tag{16}$$

Here, $Q_{absorbed,i}$ is found through

$$\dot{Q}_{absorbed,i} = \alpha Q_{solar}, \tag{17}$$

where α is the surface's absorptivity and Q_{solar} is the incoming radiation.

3.6.3 External walls

The external walls are modelled with a transfer function from (Mitalas and Arseneault 1972), based on a timebase specified by the user. The transfer functions define the internal heat flux to the outer, $\dot{q}_{s,o}$, and inner, $\dot{q}_{s,i}$, surface of the external wall, through

$$\dot{q}_{s,i} = \sum_{k=0}^{n_{b_s}} b_s^k T_{s,o}^k - \sum_{k=0}^{n_{c_s}} c_s^k T_{s,i}^k - \sum_{k=1}^{n_{d_s}} d_s^k \dot{q}_{s,i}^k \tag{18}$$

and

$$\dot{q}_{s,o} = \sum_{k=0}^{n_{a_s}} a_s^k T_{s,o}^k - \sum_{k=0}^{n_{b_s}} b_s^k T_{s,i}^k - \sum_{k=1}^{n_{d_s}} d_s^k \dot{q}_{s,o}^k. \tag{19}$$

a, b, c and d are computed through the procedure described in (Mitalas and Arseneault 1972). k is the timebase of the wall, with $k = 0$ being the current timestep, and $k = 1$ being the last timestep.

3.7 GHG-emission efficiency

The emission efficiency of the trombe wall is very important, if it is to be installed in ZEB structures. This means that a structure needs to have a positive effect on the building's total emissions over its life cycle. There are several ways to measure this efficiency, and two of the are through emission return factor, ERF, and the emission payback time, $EPBT$. The emission return factor is given by

$$ERF = \frac{m_m}{m_e}, \tag{20}$$

where m_i is the CO2 needed to manufacture and operate the device, and m_e is the CO2 that is gained through its entire operational years. This is a measure of the effectiveness of each component with regards to emissions of greenhouse gases. An ERF of more than one means that the component is GHG-negative, reducing total GHG-emissions of the building during its lifetime.

The payback time, $EPBT$ is amount of operational years it takes for the component to be environmentally friendly. This measure is good because it does not make any assumptions on the expected operational years of the component, it simply gives an indication of how long the component needs to be in use if its effect is to be positive. The emission payback time is defined by

$$EPBT = \frac{m_m}{m_{yearly}}, \tag{21}$$

where m_{yearly} is the yearly amount of CO2 gained by the use of this component.

3.8 Dimensionless numbers

3.8.1 Reynolds number

The Reynolds number of the flow, the ratio between inertial and viscous forces, is given by

$$Re = \frac{\rho_{air} D_h v}{\mu_{air}}, \tag{22}$$

where D_h, the hydraulic diameter, is given by

$$D_h = \frac{4A}{P}. \tag{23}$$

3.8.2 Grashofs number

The Grashofs number, the ratio between buoyant and viscous forces on the flow, is given by

$$Gr = \frac{g\rho_{air}\beta_{air}(\bar{T}_s - T_{room})h_w^3}{\mu_{air}}. \tag{24}$$

3.8.3 Rayleigh number

The Rayleigh number, which define if the boundary layer for natural convection heat transfer is laminar or turbulent, is the product of the Grashof and Prandtl number and given by

$$Ra = \frac{g\rho_{air}\beta_{air}(T_{w,s} - \bar{T}_s)h_w^3}{\mu_{air} a_{air}} = GrPr = [0, 10^6] \tag{25}$$

3.8.4 Richardson number

The Richards number determines if the heat transfer is dominated by forced or free convection, and is given by

$$Ri = \frac{Gr}{Re^2}. \tag{26}$$

3.8.5 Nusselt number

The Nusselt number determines the ratio of convective to conductive heat transfer in a fluids boundary and is given by

$$Nu = \frac{hL}{k}, \tag{27}$$

where h is either $h_{s,w}$ or $h_{s,g}$, which are both critical and hard to define numbers in this simulation.

It is also given by (Shen et al. 2007)

$$Nu_{open} = 0.107 Gr^{\frac{1}{3}} \tag{28}$$

If the vents are closed, the Nusselt number is given by (Shen et al. 2007)

$$Nu_{closed} = \text{Max}\{1, 0.288(\frac{d_s Ra}{H})^{0.25}, 0.039Ra^{0.33}\} \tag{29}$$

3.8.6 Radiative heat gain to slit from the exterior

The radiative heat gain of the air from the exterior is negligible, given by air's near zero absorbtivity. τ_{air} is therefore comparably equal to zero.

3.8.7 Radiative heat gain from glazing to wall

The radiative heat gain between the wall and the glazing is given by (Nwachukwu and Okonkwo 2008)

$$\dot{Q}_{w,s} = \frac{\epsilon_w \epsilon_g \sigma (T_w^4 - T_g^4)}{1 - R_w R_g} \tag{30}$$

This is a small radiation exchange, and it is in some literature coupled with the convective heat transfer rate in a total heat transfer coefficient (Nwachukwu and Okonkwo 2008).

3.8.8 Wind coefficient

The wind coefficient is given by the wind velocity, v_{wind}, (Shen et al. 2007)

$$h_{wind} = 5.7 + 3.8 v_{wind}. \tag{31}$$

The wind coefficient differs for in various studies, but this was ultimately chosen (Bassiouny and Koura 2008).

3.9 Simple trombe wall models

The trombe wall has been found to follow some simple models in some studies. It was found that for a solar chimney in Egypt, the average exit velocity of the solar wall was given by the average solar intensity by

$$\bar{v}_o = 0.013 \dot{I}^{0.4}, \tag{32}$$

which is a simplification, and was only found analytically.

3.9.1 The mass flow rate

The mass flow rate can be defined by (K.S. Ong 2003)

$$\dot{m} = C_d \frac{\rho_{f,o} A_o}{\sqrt{1 + \frac{A_o}{A_i}}} \sqrt{\frac{2gL(T_{mean} - T_{room})}{T_{room}}}. \tag{33}$$

or it can be defined by (J. Mathur et al. 2006)

$$\dot{m} = C_d \frac{\rho_{f,o} A_o}{\sqrt{1 + (\frac{A_o}{A_i})^2}} \sqrt{\frac{2gL(T_{mean} - T_{room})}{T_{room}}}. \tag{34}$$

With vents of similar size and area, it can be rewritten as

$$\dot{m} = C_d \rho_{f,o} A_o \sqrt{\frac{gL(T_{mean} - T_{room})}{T_{room}}}. \tag{35}$$

3.9.2 Non-interactivity

The glazing and wall can be modeled as to walls that are infinitely far apart, when considering convective heat gain (Zalewski, Chantant, et al. 1997). This means that each section can be considered separately when calculating their convective heat transfer coefficients.

3.9.3 L/d-ratio

The optimal L/d-ratio for a solar chimney was found to be 2.83, at a solar intensity of 700 W/m^2 (J. Mathur et al. 2006).

3.9.4 The convective heat transfer rate

The convective heat transfer rate between the wall and the slit air, the glazing and the slit air and the wall and the room are all central heat transfers in the vented trombe wall setup. There is also conduction heat transfer between the air and the wall, but this is considered under the joint convective heat transfer mode.

The heat transfer coefficient can be found through the Nusselt number by (Mehran Rabani, Kalantar, and Mehrdad Rabani 2017; Bassiouny and Koura 2008)

$$h_{conv} = \frac{\bar{Nu}k}{L}, \tag{36}$$

where $\bar{Nu}$ is given by

$$\bar{Nu} = 0.68 + \frac{0.67Ra^{\frac{1}{4}}}{(1 + (\frac{0.492}{Pr})^{\frac{9}{16}})^{\frac{4}{9}}}. \tag{37}$$

The heat transfer coefficient is also given by the heat transfer rate from a forced airflow over a vertical plate, (Akbarzadeh, Charters, and Lesslie 1982)

$$h_c = 5.68 * 4.1\bar{v}_s. \tag{38}$$

The internal convection coefficient rate can be found through equations from the ASHRAE handbook and are given by: (Shen et al. 2007)

if $10^4 < Gr_r < 10^8$

$$Nu_r = 0.516Ra_r^{\frac{1}{4}}, \tag{39}$$

and if $10^8 < Gr_r < 10^{12}$

$$Nu_r = 0.117Ra_r^{\frac{1}{3}}. \tag{40}$$

3.9.5 Sky temperature and long wave sky radiation

The sky temperature can be calculated to be (Bassiouny and Koura 2008; Bansal, J. Mathur, et al. 2005)

$$T_{sky} = 0.0552 T_{amb}^{1.5}. \tag{41}$$

The sky temperature can be calculated through (Martin and Berdahl 1984)

$$T_{sky} = T_{amb}(\epsilon_{sky} + 0.8(1 - \epsilon_{sky})C_{cover})^{0.25}, \tag{42}$$

where C_{cover} is the cloudiness factor, which can be read from the weather data file. ϵ_{sky}, the clear sky emittance, is found through

$$\epsilon_{sky} = 0.711 + 0.005 T_{sat} + 7.3 \times 10^{-5} T_{sat}^2 + 0.013 \cos(2\pi \frac{time}{24}) + 12 \times 10^{-}5(p_{atm} - p_0), \tag{43}$$

with *time* being the time of day. p_{atm} is found through

$$p_{atm} = p_0 e^{\frac{g \rho_0 h}{p_0}}, \tag{44}$$

where h is found through location data.

The long-wave radiation between the sky and the wall is found through

$$\dot{I}_{sky} = \frac{F_{w,sky} A_w \sigma (T_w^4 - T_{sky}^4)}{\frac{1}{\epsilon_{sky}} + \frac{1}{\epsilon_w} - 1}, \tag{45}$$

where $F_{w,sky}$ is the view factor from the wall to the sky. This factor is, for a vertical non-shaded surface with the ground modelled as an infinite horizontal surface equal to exactly 0.5 (Incropera et al. 2013, p.866).

The radiation and sky temperature heat rate exchange between the glazing and the environment can also be found through (Shen et al. 2007)

$$h_{g,rad} = \sigma \epsilon_g (T_{sky}^2 - T_g^2)(T_{sky} - T_g), \tag{46}$$

where the temperatures are in Kelvin.

3.9.6 Ground long-wave radiation

The very equivalent ground surface radiation is given by

$$\dot{I}_{ground} = \frac{F_{w,ground} A_w \sigma (T_w^4 - T_{ground}^4)}{\frac{1}{\epsilon_{ground}} + \frac{1}{\epsilon_w} - 1}, \tag{47}$$

where $F_{w,ground}$ is equal to 0.5, and the ground temperature is found through the weather data input.

3.10 Simulation

Setting up the simulation is a case of combining the knowledge of the theory and literature to set up the most efficient and usable simulation as possible. The simulation is set up with each glazing as its own part with its own temperature, as is the slit, room and nodes in the wall.

3.10.1 Heat flows in the system

The heat flows between the glazing, wall, room and ambient can be seen in table 1. The equations are based on the theory presented earlier, and the heat flows are evaluated at each timestep.

Table 1: Heat flow rate equations for the trombe wall system

#	**Heat flow**	**Equation**
Glazing heat transfer		
1	Internal energy change	$\Delta T_g c_g \rho_g d_g A_g$
2	Convective flow to ambient	$h_{wind}(T_{amb} - T_{g,ext})$
3	Convective flow to slit	$h_{g,s}(T_{g,s} - T_s) * A_s$
4	Radiative flow from wall	$\frac{A_g \sigma (T_{g,s}^4 - T_w^4)}{\frac{1}{\epsilon_g} + \frac{1}{\epsilon_w} - 1}$
5	Radiative flow from exterior	$\dot{I}_{total}(1 - R_g)(1 - \tau_g)$
6	Sky radiation loss	$h_{g,rad}(T_{sky} - T_{g,ext})$
Trombe wall slit heat transfer		
7	Energy flow to room	$\dot{m}_s c_{air}(T_o - T_i)$
8	Internal energy change	$\Delta T_s c_{air} \bar{\rho}_s A_s d_s$
Trombe solar wall heat transfer		
9	Convective flow from slit	$h_{w,s}(T_s - T_{w,s})$
10	Radiative flow from exterior	$\dot{I}_{total}(1 - R_g)\tau_g(1 - R_w)\alpha_w$
11	Radiative flow to room	$\epsilon_w \sigma (T_w^4 - T_r^4)$
12	Convective flow to room	$h_{w,r}(T_{w,r} - T_r)$
13	Top and bottom heat loss	$\frac{T_w - T_{ground}}{R_{w,ground}} + \frac{T_w - T_{ceiling}}{R_{w,ceiling}}$
14	Internal energy change	$\Delta T_w c_w \rho_w d_w A_w$

3.10.2 Transient conduction in the massive wall

A central heat transfer mechanic in the trombe wall is the transient conduction through the massive wall. Predicting accurate temperatures on the wall's interior and exterior surface is important to perform accurate heat transfer calculations from the slit air and to the room. The lumped capacitance method can not be used as this assumes infinite conduction in the solid. This is because in the trombe wall, the delay in heat transfer through the wall is an important design element and should be present in the simulation (Agrawal and Tiwari 2010). Because of this, the wall is considered through one dimensional transient conduction, with multiple nodal temperatures, $T_w(i)$, being evaluated at each timestep.

The temperature of the internal nodes $i = 2 : (N_{nodes} - 1)$ in the wall is calculated through (Incropera et al. 2013)

$$T_w(i) = F_o(T_{wp}(i+1) + T_{wp}(i-1)) + (1 - 2F_o)T_{wp}(i), \tag{48}$$

where $T_{wp}(i)$ is the nodal temperature at the previous timestep, and the Fourier number is given by

$$F_o = a_w \frac{dt}{dx^2}, \tag{49}$$

where dt is the timestep length, dx is the distance between each node and a [m/s^2] is the thermal diffusivity of the wall, given by

$$a_w = \frac{k_w}{\rho_w c p_w}. \tag{50}$$

k_w is the thermal conductivity, ρ_w is the density and cp_w is the specific thermal capacity.

The node closest to the slit, $i = 1$, is calculated through

$$T_w(1) = T_{wp}(1) + \frac{Q_{ws}dt}{cp_n} + 2F_o(T_{wp}(1) - T_{wp}(2)), \tag{51}$$

where Q_{ws} is the total heat transferred to the surface of the wall, see table 1 and cp_n is the heat capacity of each node. The latter is found through

$$cp_n = dxH_wW_wcp_w. \tag{52}$$

The node closest to the room is calculated through

$$T_w(N_{nodes}) = T_wp(N_{nodes}) - \frac{Q_{wr}dt}{cp_n} + 2F_o(T_{wp}(N_{nodes} - 1) - T_{wp}(N_{nodes})), \tag{53}$$

where Q_{wr} is the rate of heat transfer from the wall to the room, see table 1.

3.10.3 Glazing heat transfer simulation

Each pane in the glazing is considered separately, with unlimited conductivity on the glass panes. The only resistance between each pane is across the air layer. The model supports windows with multiple glazings. The absorbance of short wave solar radiation is very simplified, and the absorbance is split evenly between every pane.

The equation set for a triple pane window, with $i = 1$ for the outermost pane and $i = 3$ for the innermost pane is given as

$$T_g(1) = T_{gp}(1) + \frac{Q_{sky} + Q_{gamb} + \frac{Q_{solarg}}{N_g}}{cp_gn}dt + h_{glass}(T_{gp}(2) - T_{gp}(1)), \tag{54}$$

$$T_g(2) = \frac{Q_{solarg}}{N_gcp_{gn}}dt + h_{glass}(T_{gp}(3) + T_{gp}(1) - 2 * T_{gp}(2)) \tag{55}$$

and

$$T_g(3) = \frac{-Q_{gs} - Q_{wg} + \frac{Q_{solarg}}{N_g}}{cp_{gn}}dt + h_{glass}(T_{gp}(2) - T_{gp}(3)). \tag{56}$$

3.10.4 Skipping calculations on some timesteps

By allowing the Matlab script to skip calculating the air variables, dimensionless numbers and the convective heat transfer coefficients at every timestep, some efficiency is gained. Three simple if-sentences are defined, allowing calculation at every 100th timestep. At a timestep of 0.001 hr, the calculation time in the Matlab unit is reduced 9 %. The resulting calculated heating of the room is changed 0.3 %. The choice of every 100th timestep was based on inspection of the rate at which these variables changes values, weighed up against the possible time save in the calculation. Skipping every 1000th timestep, for example, would lead to the wall reacting too slow to a sudden shift in slit, wall or glazing temperature. Skipping less than 100 timesteps leads to a too small gain.

3.10.5 Errors and their impact

Errors of ±5°C from real case slit temperatures to simulated slit temperatures, the impact in total heat transfer will be negligible (Akbarzadeh, Charters, and Lesslie 1982).

3.10.6 Reverse flow

Reverse flow in the air slit can happen as a result of the wall or glazing temperatures being lower than the room temperature, resulting in a cooling effect and decrease in buoyancy in the slit, making the net air flow being downwards. This can also happen only on the glazing, with windows of a low U-value, especially in the morning hours (Akbarzadeh, Charters, and Lesslie 1982).

In periods of long absence of solar radiation, due to high cloud coverage, reverse thermal circulation can be experienced, but this can be prevented through the use of simple plastic films on the vents (Shen et al. 2007).

3.10.7 Transmission losses

Trombe wall transmission losses is an issue, where low wall temperatures due to low incoming solar radiation produces an unwanted negative heat flux from the interior to the exterior (Shen et al. 2007). This is one of the major drawbacks of using the classical trombe wall in high latitude areas, compared to the composite trombe wall, or *Trombe-Michel wall*, (Shen et al. 2007) and the insulated trombe wall (Saadatian et al. 2012).

3.10.8 The discharge coefficient

The discharge coefficient C_d is defined by

$$C_d = \frac{\dot{m}}{\rho \dot{V}} = \frac{\dot{m}}{A\sqrt{2\rho\Delta p}}, \tag{57}$$

(Akbarzadeh, Charters, and Lesslie 1982) found that

$$C_d = \frac{1}{\sqrt{2(1+\frac{1}{2})}} = 0.57, \tag{58}$$

Equation 57 can be rewritten for Δp to give

$$\Delta p = \frac{(\frac{\dot{m}}{C_d A})^2}{2\rho}. \tag{59}$$

3.10.9 Mass flow rate

The trombe wall mass flow rate is found, through simplifications (K.S. Ong 2003), to be

$$\dot{m} = C_d \frac{\rho_{f,o} A_o}{\sqrt{1+\frac{A_o}{A_i}}} \sqrt{\frac{2gL(T_{mean}-T_{room})}{T_{room}}}. \tag{60}$$

This is for a room with two openings and a uniform air temperature. This is based on the assumption that the airflow of both vents is of a high Reynolds number, and that the the airflow forms jets (Andersen 2003). However, this is far from the case in the trombe wall, where air flows are slow and through large vents.

The mass flow rate can also be written as (Hernández et al. 2006; Bansal, R. Mathur, and Bhandari 1993)

$$\dot{m}_s = \rho_e C_d A_v (gL\frac{T_e - T_r}{T_r})^{\frac{1}{2}} \tag{61}$$

3.10.10 The effective buoyant height, H_0

The effective height of the slit is an important aspect of the driving force of the slit, as can be seen in equations 61 and 60. This height is the distance that the pressure differences in the fluid drives the fluid through the flow. The effective height can be defined by

$$H_0 = \Delta H_{min} + 2C_H H_v, \tag{62}$$

where ΔH_{min} is the height between the top of the lower vent and the bottom of the upper vent, C_H is the effective height factor, often set to zero (Shen et al. 2007). Having a different C_H could be more correct, but it is set to zero in this simulation.

3.10.11 Slit average temperature

The average temperature $\bar{T}_s$ of the slit is given by

$$\bar{T}_s = C_s T_i + (1 - C_s) T_o, \tag{63}$$

where the slit average temperature coefficient C_s=0.74 (K.S. Ong 2003). Solved for T_o it becomes:

$$T_o = \frac{\bar{T}_s - C_s * T_i}{1 - C_s} \tag{64}$$

3.10.12 Air state variables

Some of the air state variables are temperature dependent, and are given by (Appendix A in Bansal, J. Mathur, et al. 2005)

$$\rho_{air} = 1.1614 - 0.00353(T - 300), \tag{65}$$

$$\mu_{air} = (1.846 + 0.00472(T - 300)) * 10^{-5}, \tag{66}$$

$$k_{air} = 0.0263 + 0.000074(T - 300) \tag{67}$$

$$c_{air} = (1.007 + 0.00004(T - 300)) * 10^3. \tag{68}$$

3.10.13 Steady state or transient system

The trombe wall system has a high thermal mass, and with the periodic solar loads and the slowly heating airflow, the trombe wall system should be considered as transient (Burek and Habeb 2007). This means that easy solutions like the lumped capacitance model cannot be used, as assuming instant heat transfer for a transient system with high inertia does not work.

3.10.14 Shading

Shading the trombe wall can be an effective and important measure to lower the trombe wall's summer overheating and winter transmission losses (Chen et al. 2006). A simple, low emittance shading can lower the winter night-time transmission losses by 20-40% (Chen et al. 2006).

In the summer, one must compare the beneficial heat losses from the solar chimney effect to the unwanted heat gains from the heated solar wall.

3.11 GHG-emission calculation

As stated in the literature review, the need for green house gas (GHG) emission calculation is present. This is to ensure that the emissions from the growing building stock is understood well, and to ensure that emissions from new buildings are low. To simplify the emission overview, CO2-equivalents are used, where each different emission is converted into CO2-equivalents by a set table. For this Trombe Wall GHG-emission calculation, only CO2-eq. will be used, as it is the by far most common measurement unit. Delving into the specifics of the basis of these CO2-equivalents is also grounds for its own separate project, due to its scale and complexity, so merely superficial review will be performed.

The CO2-emissions from the trombe wall installation is calculated through

$$m_{CO2} = \sum_{i=1}^{N} \rho_i V_i C_{CO2,i}, \tag{69}$$

where C_{CO2} is the emission factor, in kg emitted CO_2 per kg material, which is 0.15 for concrete (Winnipeg 2011). For the windows, it is estimated that a timber framed multiple-glazed window with argon releases 108 kg CO_2-eq per window unit, which is 1.3x1.65 m, with two units (Teenou 2012). This results in an emission factor of the window to be 50.4 kg/m^2 of triple glazed window.

The other side of this calculation is the GHG-emissions that are saved by the use of the trombe wall. These are simply calculated by summation of all the kWh of electricity saved, and combining this with the GHG-emissions per unit of electricity produced, through

$$m_{CO_2} = \Delta E C_{CO2,el}, \tag{70}$$

where ΔE is the energy saved, and $C_{CO2,el}$ is the GHG-emissions per unit of energy. In Europe, the emissions per unit of energy produced is 0.172 kg CO_2-eq per kWh, while in China it is 0.252 kg CO_2-eq per kWh (Assosiation 2020).

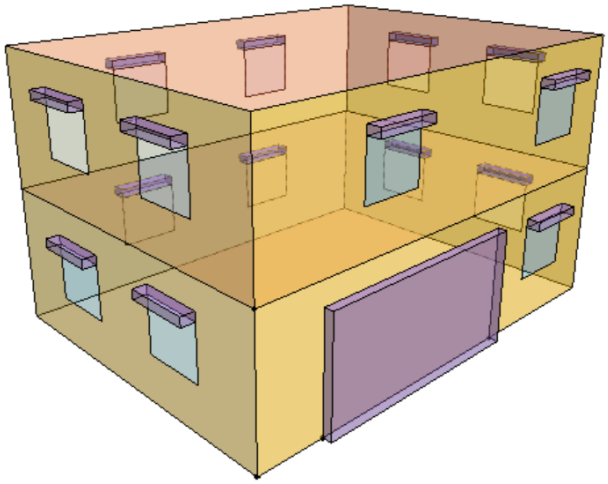

Figure 10: The Single Family Dwelling, as modelled in Sketchup 8 with the TRNSYS3D-plugin.

4 Method

The trombe wall is modelled in TRNSYS and Matlab. TRNSYS' standard models are used to simulate for the weather, ventilation and building loads. To model the solid trombe wall, the slit air and the trombe wall glazing, a freestanding Matlab model is created. The TRNSYS simulation studio calls the Matlab model multiple times each simulation step, until convergence for the timestep is reached.

The Matlab script in its entirety is attached in Appendix A, and is created in Matlab 2011b, for compatibility with TRNSYS 17. The script utilizes five functions, attached at the end of the appendix. The Matlab script is created following the equations of the Theory section.

4.1 The building

The building that is to be modelled is an ordinary two-story Norwegian single-family dwelling of 150 m^2, with each story being its own zone. It's 7.5x10 meters, with the biggest facade to the south and north, and a trombe Wall modeled as a shade object on the south side of the building, as can be seen in figure 10. The house has 15 identical windows, with a width of 1.4 m and a heigth of 1.2 m. Their placement is evident in the figure. A simple, flat, roof is also designed, as well as a simple floor with no basement.

4.1.1 Building envelope

Its walls, windows, roof and floor all confirm to the Norwegian passive house standard(Norge 2013). U-values in W/m^2K: wall = 0.109, roof = 0.084, floor = 0.083 and windows (glazing+frame) = 0.75. The infiltration rate is set to 0.04 air changes per hour, stemming from n_{50} = 0.6 h^{-1}(Hastings and Wall 2007). n_{50} of 0.6 h^{-1} is an attainable air change rate in nZEB-buildings(Andresen et al. 2019). To verify this model, a simple Excel calculation was performed to have a ground for comparison with the simulation data. Simplifications in this model are very much present, the most notable being the exclusion of solar gains, and simplifying the floor to be connected to the ambient air. These simplification will respectively increase and decrease the heating need of the building. This means that the simplifications have a smaller impact if they are to be verified in a period of low solar gains.

The building will also be defined as a medium heavy furnitured building with an added thermal capacity of 5 Wh/m^2K.

Gain type	Schedule	Heat gain [W/m^2]	Gain per floor [kJ/h×floor]
Lighting	07-23/7	1.95	526.5
People	24/7	1.50	405
Equipment	24/7	1.8	486

Table 2: The internal heat gains of the building

4.1.2 Internal Loads

The schedule for the building will follow the recommendations of SN/TS 3031(Norge 2016), with a set point heating temperature schedule of 22 degrees Celsius from 07-23, and 20 degrees from 23-07. The cooling set point is 24 degrees C throughout the day. These schedules are the same all year and through all weekends. The values and type of each internal load can be seen in table 2.

4.1.3 Ventilation system

To more accurately provide an assessment of the buildings heating and cooling needs, a simple ventilation system will also be defined. In passive houses in cold climates, heat recovery units need to be used, which requires a balanced ventilation system. Given that TS/EN 3031 demands that the ventilation system is activated at all times for a small residential ventilation system, a CAV-system will be used.

For these simple initial calculations, the given lowest value for the ventilation system in SN/TS 3031 table A.12(Norge 2016), is used. For a residential building with a heated floor area larger than 110 m^2, the lowest flow rate is 1.2 m^3/hm^2. For each floor, this results in a ventilation air flow of 90 m^3/h, or 109 kg/h. This value is probably too low, and could result in a higher cooling load and a lower heating load than using a more correct value. But, the impact is probably not high enough to necessitate further calculations of the ventilation load.

The heat recovery unit (HRU) also needs to be defined. The lowest acceptable annual average temperature efficiency of a HRU in a passive house in Norway is 80%(Norge 2013), and this will be the constant temperature efficiency of the unit in the simulation. Given that this house is a mere 150 m^2, and with such low ventilation rates, having a HRU of higher efficiency than this would most likely lead to a too high investment cost, compared to the gain. The temperature efficiency of a HRU is given by

$$\eta_t = \frac{\theta_2 - \theta_1}{\theta_3 - \theta_1} \tag{71}$$

where η_t is the temperature efficiency, θ_1 is supply air temperature before the HRU, θ_2 is supply air temperature after the HRU and θ_3 is exhaust air temperature before the HRU. The HRU is implemented in TRNSYS as a simple equation solver, driven by equation 71, and with inputs from weather data and the building simulation. The HRU will only be active when there is a heating need.

4.1.4 Type 56 - Multizone building model

Next to the trombe wall, type 56 is the most vital component in the simulation. It is a multizone building model, built up of different zones with a set number of airnodes inside. Each airnode has, at each timestep, a temperature calculated from the various inputs to the zone, through equation 9. In this simulation, each zone/floor has a single airnode. This is because the temperature variance inside each floor is not large enough to necessitate the slower calculation and higher complexity of multiple airnodes. The complexity is still high. The airnode is impacted by house geometry, shading geometry, solar zenith and azimuth, convection and radiation from interior walls and windows, infiltration through the envelope, ground heat loss, ventilation, auxillary heating, people, equipment and lighting loads and thermal mass of the building.

Type 56 is a vital part of the simulation, if a real case trombe wall is to be simulated. Without it, the loads and temperatures on the trombe wall would be wrong. One could argue that a simple weather, indoor temperature and heating/cooling load data set covering the year would be sufficient and a lot less time consuming, but finding an accurate and recent data set proved impossible. But, if one wants to see if a trombe wall should be implemented into an existing building, the data can be logged and fairly easily be implemented into TRNSYS.

4.1.5 Ventilation system components

The ventilation system consists of several different components, and is defined as simply as possible. The loop that feed the multizone building is comprised of:

- Heat recovery unit - implemented through a simple equation solver (section 4.1.3)
- Ideal pump - $\dot{V}_air = 218$ kg/hr
- Two pipes
- Ideal heater - $P_{max} = 21{,}000$ kJ/hr
- Ideal cooler - $P_{max} = 10{,}000$ kJ/hr
- Tee piece - connects heating/cooling with the trombe wall air
- Controlled flow diverter - controls ratio of flow between the floors

The governing equations for most of these units are modelled fairly standard and will not be discussed further. The equations governing the HRU is discussed in 4.1.3.

4.2 Automatic control

To obtain a working simulation, most parts of the simulation needs to be controlled to a varying degree and complexity.

4.2.1 Flow diverter

The flow diverter that split the ventilation system air flow into the 1st and 2nd floor is controlled by a feed-forward control scheme, where the temperatures exiting the house are the basis of control. The ratio between the sizes of each floors deviation from the goal temperature controls the diverter, through this equation:

$$FlowD_{control} = \frac{|T_{1st} - T_{set}|}{|T_{1st} - T_{set}| \times |T_{2nd} - T_{set}|}, \tag{72}$$

where $FlowD_{control} = 1$ results in all the flow going to the 1st floor, $= 0.5$ means its evenly split and $= 0$ means it all goes to the 2nd floor. T_{set}, T_{1st} and T_{2nd} are the temperature set point, at the 1st floor and at the 2nd floor, respectively.

4.2.2 Heat recovery unit

The heat recovery unit is partly a slave to the heating and cooling coil, never being activated if the cooling coil as active and always being activated if the heating coil is active. And, when the outside air is below 16 degrees C, and there is a cooling need, the HRU is used to heat the outside air to no more than 16 degrees C. This allows us to not use the heating coil to heat up outside air used for cooling, to avoid cooling with too cold air.

4.2.3 Heating and cooling coils

The heating and cooling coils are controlled by a thermostat, that is in itself controlled by a forcing function generating the scheduled temperature requirements for heating, from SN/TS 3031(Norge 2016), as discussed in 4.1.2.

4.2.4 Trombe wall control

The trombe wall is controlled by the thermostat as well as by an equation solver. First, the thermostat indicates weather there is a heating need or a cooling need in the building. Then, the solver checks if there is a possibility of heating or cooling using the trombe wall. For heating, it checks if the wall slit temperature is higher than the room temperature. For cooling, it checks if the room temperature is higher than the ambient temperature. If the condition is met, the trombe wall is activated for that timestep.

A check to see how long time it is since the trombe wall switched modes has not been implemented. The wall can therefore end up in situations where it switches modes very fast, somewhat simulating an electronically controlled wall.

4.3 Glazing validation

A triple glazed window filled with argon has a U-value of 0.65 W/m^{2}K (Weir and Muneer 1998), and this is the value used to validate the glazing simulation. This is the most important parameter of the window simulation, next to transmissivity, reflectivity and emissivity. These solar radiation related values, however, are defined as a simple input into the heat transfer equations and are easier to check and correct. The result U-value of the window is a result of many factors; the exterior and interior heat transfer coefficient, the conductivity of the glass, the internal heat transfer coefficients between each sheet and how each panes temperatures interact with one another from timestep to timestep. Therefore it was deemed necessary to verify that this part of the simulation ran as intended, and with the right results.

Setting the solar gain to zero, and the slit, wall and ambient temperature to a constant, the correct values for the internal heat transfer coefficient between each sheet, h_{glass} will be found. The U-value is also dependent on the exterior and interior heat transfer coefficients, but this method assumes that these heat transfer coefficients are near correct. The wind speed is set to 0 m/s. Then, the simulation is run until steady state is reached and the current U-value can be read by inspection of the heat flows from the ambient to the outer pane, and from the inner pane to the interior. The correction factor is adjusted while the simulation is running and found by trial and error. The correction factor is set to 0.85, resulting in an internal heat transfer coeffiecient in the glazing of

$$h_{glass} = C_g k_{air} \frac{A_g}{d_{g,air}} = 8.16\text{W/K}. \tag{73}$$

This results in a U-value of 0.65 W/m^{2}K with no wind, and steady 25 C temperature difference between the ambient and the entire interior.

4.4 Other validations

As the author was not able to conduct any experiments due to lockdowns caused by the COVID-19 pandemic, another solution was found. Using various sources from the literature, the simulation can be validated section by section. The scope of the validations was constrained by the available literature, and by each sources openly available data. This is not as effective and controllable as an experiment done by the author, as there are many unknowns that must be assumed.

4.5 Yearly simulations

To inspect the effect of the trombe wall in various climates, year long simulations will be performed. The trombe wall is a constant component, and its performance on the building's energy demand and emissions must be understood for the entire year. A component only functionable in the winter-time and not in the summer-time is not a functionable component. To do these simulations, for ease of comparision, the same building model, gains and set point temperatures will be used. This is in spite of different countries having different demands for which gains are defined, what the new building models look like and what the set point temperatures throughout the year are. As this is a master thesis in cooperation with the Shanghai Jiao Tong University of China, two of the locations are in China, namely the coastal city of Shanghai, and the inland city of Kashi. These are two cities of very different climates, making the difference in trombe wall use possibly very apparent. Shanghai is located in the "hot summer, cold winter" region in China, has warm summers and moderately cold winters, while Kashi is between the "cold" and "severe cold" climate regions, and has cold winters and moderately warm summers**??**. As will be obvious when observing the yearly average temperatures later, the term "cold" is relative. Kashi is also at an elevation of over 1200 metres, making the solar radiation even higher than Shanghai, even though they are at similar latitudes. This could result in the trombe wall having higher loads in Kashi.

The other two areas of research will be Gothenburg, Sweden, and Reykjavik of Iceland. These are of similar climates to locations in Norway, which the author would like to use, but the Meteonorm data for these locations seemed to be corrupted. Gothenburg is of somewhat similar climate to Oslo, while Reykjavik is similar to the northern parts of Norway.

The interesting parameters of these simulations are the unwanted heating and cooling gain from the trombe wall in the summer and winter respectively, the effects of the trombe wall slit air circulation and the trombe solid wall heating.

5 Validation of the Matlab model

To validate and calibrate the TRNSYS and Matlab simulation, experiments need to be performed. As mentioned in the preamble, the well known Corona virus pandemic has shut down labs worldwide. Calibration and validation, however, is still an important step that needs to be performed. Luckily, the trombe wall is a heavily researched piece of equipment, resulting in many experiments readily available for the author. The exact conditions in each physical experiment is replicated in the simulation parameters, and the results can be directly compared. The validity of this comparison will then be based upon the accuracy of the replication.

The downside is, however, that raw data from most experiments is not uploaded to open-access, often only presented in graphs. Many of the important simulation parameters must also be assumed by the author. Both of these issues lower the accuracy of the replication.

5.1 Simple building model validation

A simple test to analyze the performance of the Type 56 multi-zone model is performed. By setting the ambient temperature to a constant -20 degrees Celsius, and the indoor set temperature for heating to 21 degrees Celsius, an average value of 9900 kJ/h in sensible heating demand is attained. Compared to the simple calculations in the Method section, a difference of 15 percent is found. The heating demand of the simulation is higher, something that can be explained by the simplification of the floor transmission losses. These values are therefore deemed close enough to warrant further study using this component.

To further see if the Type 56 model functions according to the Norwegian passive house standard, another simple test was conducted. With the scheduled temperatures and internal loads as defined in Method section 4.1. This results in a total heating demand of 21.16 kWh/m^{2}year, which is somewhat lower than the calculated highest acceptable heating demand of NS3700(Norge 2013), which is 23.07 kWh/m^{2}year. And, having a lower heating demand is natural, given by the fact that there are no ventilation losses in the system at this time. When a ventilation system is defined there will be a higher heat losses when the ambient temperature is low, given by the fact that the heat recovery unit does not have an efficiency of 100 percent.

The cooling need introduced in this stage of the simulation is 12.01 kWh/m^{2}year, which is too high. But this is also a lot higher as a result of the lack of a ventilation system. There is no passive cooling through the use of ambient air in the ventilation with this setup. The ambient air temperature is lower than the indoor temperature for most of the cooling period. The model for the house could therefore still be accurate, and further use of this model is warranted.

5.2 Ventilation system integration

As previously stated, to make the system connectable to the trombe wall, a ventilation system and heating regime needs to be defined outside of the type 56 component. This also necessitates that some sort of control is implemented, to ensure that the heating and cooling energy comes from the correct sources. In the initial setup, without the trombe wall being integrated, the interaction between the radiator and the heating coil is examined. The goal is that the radiator is never on when the heating coil is running below maximum power. The radiator is therefore at full power when the heating coil is at full power, and off if not. This control scheme is a simplification.

Furthermore, the introduction of the HRU into the simulation will lower the heating load considerably. The cooling load will also be lower, because the ambient air can be used to cool the building, when the temperature is low enough.

The heating demand of the building was 37.03 kWh/m^{2}year and the cooling demand 1.83 kWh/m^{2}year. This is considerably higher than the lowest allowed heating demand discussed in the previous section. It seems that the introduction of ambient air into the building through the ventilation system is of a high

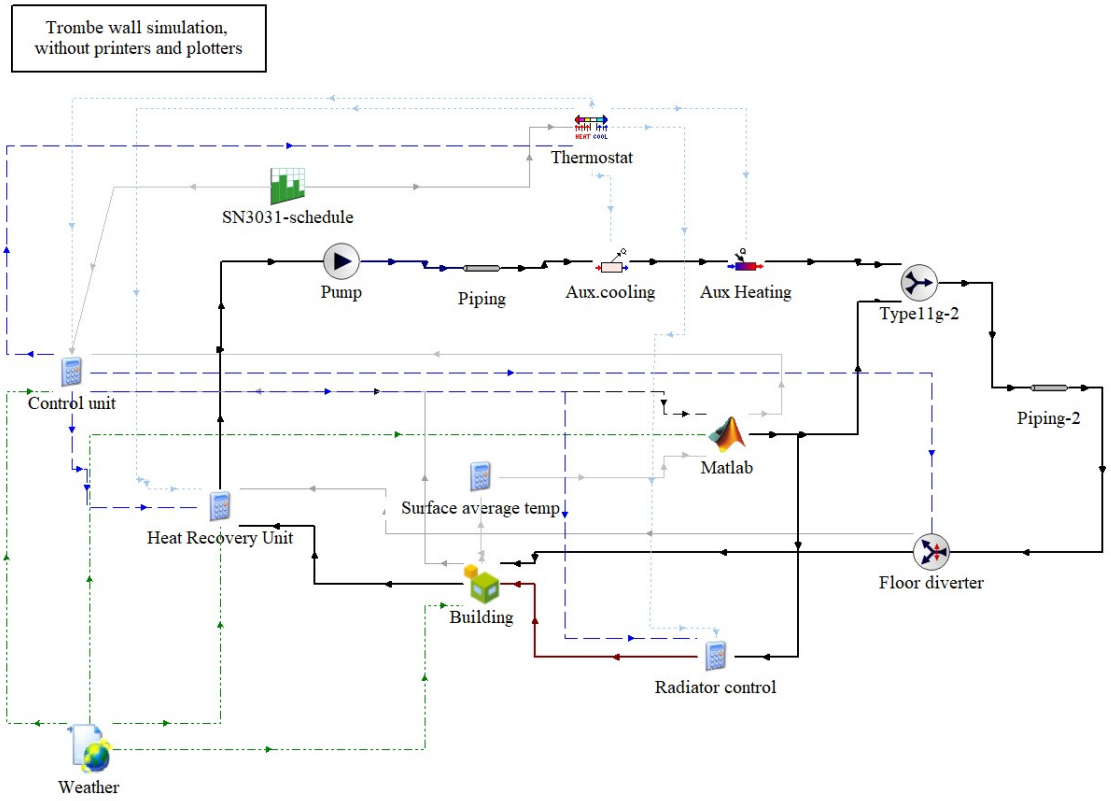

Figure 11: The setup of the simulation in TRNSYS 17.

enough degree to affect the system to a problematic extent. The HRU seems to be of a too low effect to negate this.

All this considered, the results of the simulation are realistic, and further use of the ventilation setup is warranted. The complete setup, with the trombe wall Matlab model incorporated, can be seen in figure 11

5.3 Replication of experiments by Abbassi et.al

Abbassi et.al performed a trombe wall experiment with different configurations, in Tunisia in 2014(Abbassi, Dimassi, and Dehmani 2014). The setup was a ventilated trombe wall, installed in a simple test room with one window and no additional ventilation.

Height: 1.86m, width/length:1.52m. Walls: 0.02m wood, assumed TRNSYS and 0.04m polystyrene. Trombe wall: 0.10m thick concrete brick storage wall, painted matt black, and assumed to have a size of 1.4x1.1 metres. The vents are given as 0.25x0.15 m with an air gap of 0.12 m. The glazing is assumed as a single glazing. The test room is on wheels, and the air temperature under the floor is considered to be equal to the ambient.

The room is simple, and is modeled in TRNSYS, through the TRNBUILD/Sketchup program extension. A high infiltration ACH of 1 $h^{-}1$ is assumed, as the test cell seems to be closely linked with the ambient temperature, even though it is somewhat isolated. The wall is assumed to have a density of 1900 kg/m3 and a conductivity of 1.2 W/mK. The density is for on the lighter end for concrete, and the conductivity is on the higher end of the scale. This was chosen as a result of observing the relatively short delay between the peak incident solar flux and the peak room heating flux.

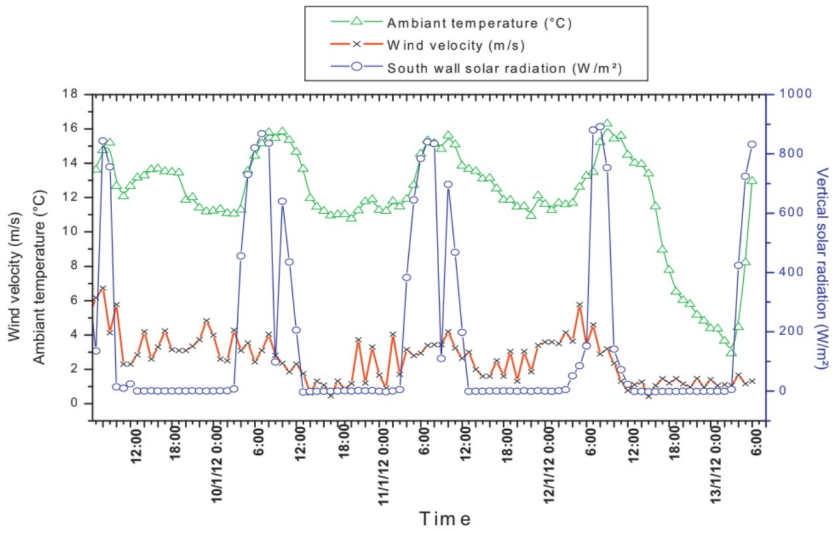

Figure 12: Meteorological data from the experiment (Abbassi, Dimassi, and Dehmani 2014)

.

The solar radiation and ambient temperature is essential to the trombe wall performance, and to simulate the correct weather, the solar radiation and temperature is inputted manually. The data is found by reading of a graph in the article seen in figure 12, and is only based on the first day of the experiment. The thermal absorptivity of the white walls of the building is assumed to be 0.5. This error could be avoided by shielding the walls from the solar radiation in the experiment. If this would have been done, all the temperature gains in the room could be attributed to the trombe wall, but now solar gain through the walls is a major factor as well.

By inspection of the test cell's response to trombe wall system and the ambient temperature, a drop of approximately 2.5 K/hr at night time can be seen. This is very high for such a small room with a hot trombe wall thermal mass. These measured quick drops in temperature further cements the need for a high ACH, low density of the trombe wall and thin walls. There is also the effects of top and bottom losses in the wall, which is introduced in the simulation. A simple top and bottom loss calculation is used, with top and bottom wall R-value of 4 K/W.

The system losses can also be attributed to a high U-value in the walls, due to high ACH or thermal bridging. This is deemed the most likely cause, and the simulated thickness of the polystyrene is reduced from 4 cm to 2 cm, to simulate the result of high thermal bridging.

The results show a very good match between the experimental data and the simulation. The deviation is its highest in the morning, when the room is heating up, where it peaks at an 8 % deviation. The average deviation is 5 %. This is very close to the experimental results, and shows that the simulation's response to solar radiation and the losses in the system are realistic. It seems that there is a bit too high inertia in the system, but the causes to that could be several. The wall could have a lower density, higher conduction rate, size or the heat flow through the natural ventilation could be higher then simulated.

It should be noted that major assumptions in this experiment replication are present. The solar absorption factor of the test cells walls, the U-value and infiltration rates, the losses in the wall and the wall's solar absorption factor are key properties that the author needed to assume. Considering the high amounts of assumed values in this experiment, however, such a good match could be the result of wrong assumptions of the experiment setup that actually decrease the error.

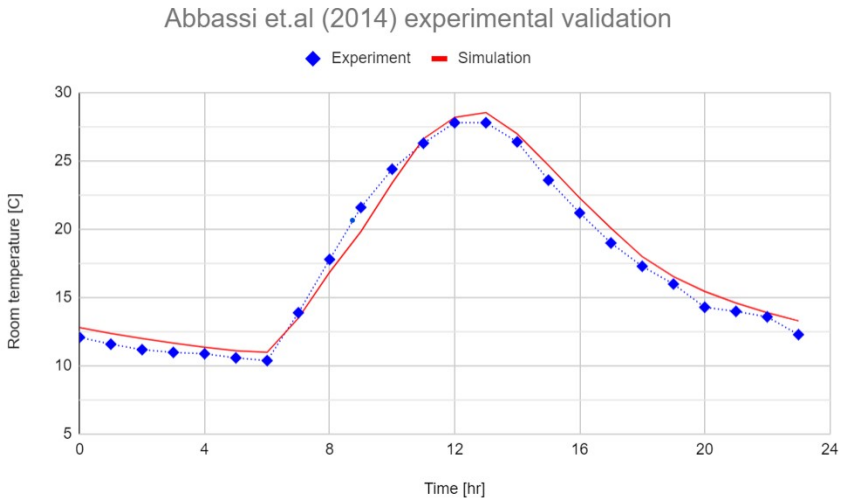

Figure 13: Comparison between experimental results (Abbassi, Dimassi, and Dehmani 2014) and the simulated results from the author's simulation.

Abbassi et. al also performed a more complicated experiment, but due to a lack of documentation available to the author, this experiment will not be replicated. It is apparent that this approach to experimental validation necessitates simple setup or at least very good documentation.

5.4 Replication of experiments by Mathur et.al

Mathur et.al performed a solar chimney experiment in India in 2004 (J. Mathur et al. 2006). A simple, variable setup was created, allowing for variations in the absorber wall height, slit thickness and solar radiation. The article lacks some experimental setup information, and multiple values needs to be assumed.

The test room is 1x1x1 m, from glazing to the end of the room. The absorber plate can be adjusted in position and height and the room has a big opening in the back end, to allow suction of ambient air. An aluminium plate is placed on the absorber and painted matte black, and it is isolated on the back side with 5 cm of "insulation". Because of the high ambient temperatures, between 294 and 306 K (21-33 C), losses to the ambience through the top and bottom of the trombe wall, as well as through the walls of the room is negated. The ambient temperature is set to a constant 300 K for the entire simulation. The walls of the room are set to a constant 300 K as well. An added benefit of this is that the author lowers the levels of complexity on the uncertainties, as the wall composition and weather data is not available.

The glazing is assumed to be double. To simulate the effects of the insulation behind the absorber, the wall is given an overall conductivity of 0.05 W/mK. This is a bit higher than a manufacturer's claim for the EPS sheet, which often has a conductivity of below 0.04 W/mK (EPS-Group 2020). This leads to a slightly conservative calculation, as the loss through the back of the wall could be lower than simulated. But it is chosen because the simulation simulates the entire wall with this conductivity.

The simulation is run with a 24-hour ambient temperature and solar radiation input on a loop until stability is reached, and each 24-hour day has the same simulation results. The results presented are one of these 24-hour days after stabilization.

For a 0.9 m high absorber, slit width of 0.3 m and 700 W/m^2 incident radiation, the experimental result is 2.93 ACH, and the simulation results in an ACH of 3.04, which is a 3.75 % difference. Lowering the radiation to 500 W/m^2 gives the experiment an ACH of 2.66, while the simulation has an ACH of 2.74, a 3.01 % difference. The lowest experiment solar radiation is 300 W/m^2, with an ACH of 2.4 for the experiment and 2.46 for the simulation. A 2.5 % deviation.

These results are very close to the experiment, considering all the uncertainties.

6 Results

6.1 Building and trombe wall simulation

The results of the year long simulations of the four different locations are presented below. Each location is presented with two graphs. One is a year long overview of the trombe wall's performance, viewed as weekly averages of the various parameters instantaneous power. Trombe solid wall, trombe natural ventilation (heating and cooling), as well as horisontal solar radiation on 2 m^2 is graphed on the left axis. Ambient temperature is graphed on the right axis. The other graph is a load diagram, graphing each parameter from its highest load to its lowest load, for the yearly simulation. Auxillary cooling and heating, as well as trombe wall natural ventilation and wall conductive heating is presented.

One note to understand the relationship between auxillary cooling and the trombe ventilation cooling, is that the auxillary cooling load is the total energy needed to cool the outside air to an acceptable indoor air level. Meanwhile the trombe natural ventilation cooling load is the total energy difference between the expelled room air and the incoming air. The result of this is that the cooling load of the trombe wall is not one to one transferrable to the cooling load of the auxillary cooling.

In table 3 some key results from the yearly trombe wall simulations can be seen. The average ambient temperature of the locations are a good indicator of what the main mode of ventilation for the building is. With the high ambient temperatures of Shanghai and Kashi, a need for high cooling loads and low solar gains in the summer is most likely present. Opposite to this, the low ambient temperature of Reykjavik and Gothenburg should necessitate higher need for heating.

As the main source of energy in the trombe wall system the levels of incident solar radiation is essential to get high effectiveness from the wall. This means that levels of high solar radiation is good for trombe wall efficiency, i.e. first and foremost, Kashi, but also Shanghai. It could also mean higher levels of overheating during periods of cooling need, which is evident through inspection of "Unwanted wall heat gain". Kashi and Shanghai has very high unwanted wall heat gain during the summer time. On the opposite side of this, Reykjavik has some unwanted wall heat loss in the winter-time, and by far the lowest cooling loads of the four locations.

Table 3: Yearly simulations key results

Location	**Gothenburg**	**Reykjavik**	**Shanghai**	**Kashi**
Average ambient temperature (C)	6.47	4.33	15.77	11.78
Average daily horizontal radiation (kWh/m2day)	5.09	4.27	7.18	9.72
Aux heating (kWh/m2)	29.43	34.69	7.86	17.76
Aux cooling (kWh/m2)	2.00	0.05	15.84	13.47
Trombe slit and wall heating (kWh/m2)	8.41	13.22	7.06	13.46
Trombe slit cooling (kWh/m2)	-10.22	-2.35	-11.62	-15.57
Unwanted wall heat gain (kWh/m2)	5.76	1.19	9.06	12.73
Unwanted wall cooling (kWh/m2)	-0.03	-0.17	0.00	0.00

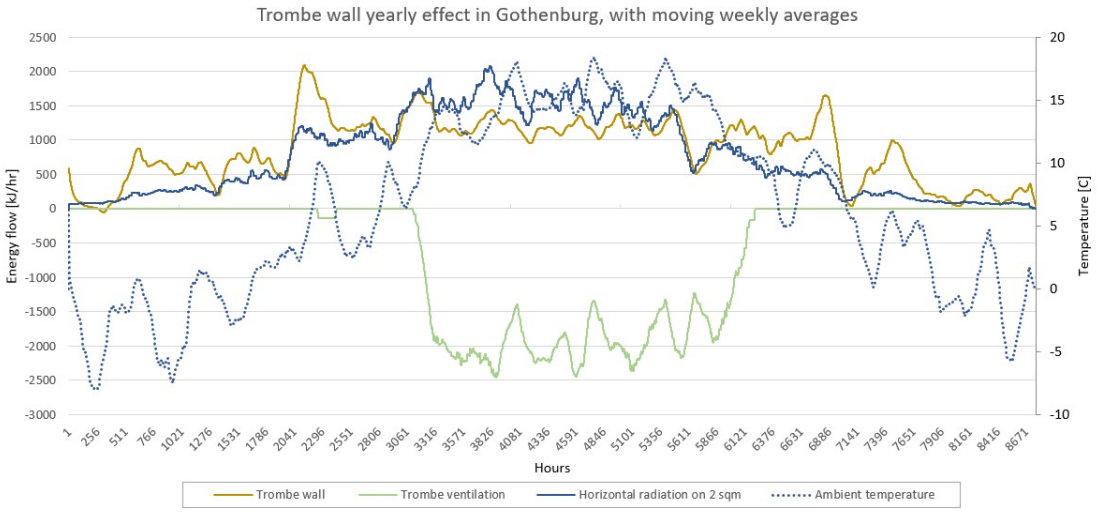

Figure 14: Moving weekly averages throughout the year, in Gothenburg, Sweden.

6.1.1 Gothenburg, Sweden

The first location to be analyzed is Gothenburg in Sweden. By inspection of figure 14, one can see the yearly effect of the wall. The solid wall represent for most of the year a positive heat flux to the room, and this effect is positive for more than half of the year. In the summer time, cooling is present and effective, outweighing the heat gains from the wall. The trombe wall heat gain is lower during times of trombe ventilation cooling, as the airflow in the slit cools down the wall. During the wintertime there is no heat flow of note through the slit in the wall. There are small heat gains from the slit to the room in the winter, but these are too small to be viewed on the graph, and are small enough to be negligible.

In the winter, the trombe wall has a negative heat flux into the room, losing some heat in the heating season. This can also be seen on figure 15, where the load diagram graph for the trombe wall is negative for some hours. This small transmission loss is, however, very small. The graphs for the auxillary heating and cooling system also shows that there are very low cooling and heating loads in the building. The heating loads are low and short, even though the ambient temperature is sub-zero for a larger portion of the year. Not needing auxillary heating for sub-zero temperatures is a testament to the trombe wall's positive effect.

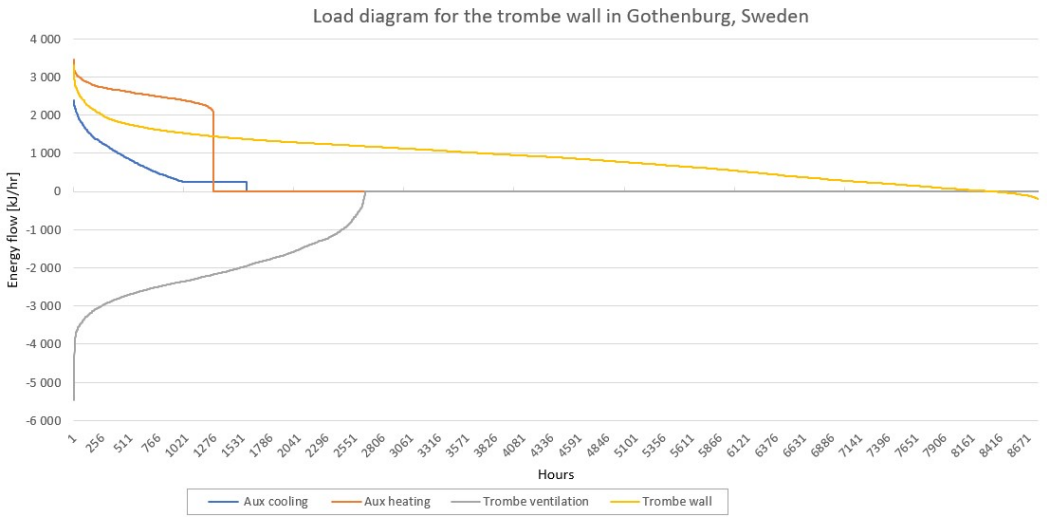

Figure 15: Load diagram of the heating and cooling throughout the year, in Gothenburg, Sweden.

6.1.2 Reykjavik, Iceland

In figure 16 the yearly effect of the trombe wall in the capitol of Iceland, Reykjavik, can be seen. Reykjavik is located on a high latitude, and has low average temperature and low solar radiation. The ventilation cooling loads of the system can be seen to be for quite a short period of the year. There are, however, cooling needs present even if the outside temperature is below 12 C. This is because the house is of the passive house standard and has low U-value walls, floor and windows. The infiltration is low as well, resulting in little losses through the building envelope. In the summer the interior gains from people, lighting and equipment coupled with the solar gains are high enough to outweigh the losses through the envelope, and cooling is needed. Observing figure 17, the auxillary cooling needs are very low, and are off for the most part of the year.

The trombe wall does, however, also introduce a transmission loss to the system in its coldest winter periods. The loss is small, but present. It should be noted that the initial values of the wall and house seems to be too high, and that there should realistically be some transmission losses in the start of the year as well. The earliest hours of the simulations has a large drop in the trombe wall heating values. The trombe solid wall heating is at its most effective during the spring and fall, when there is medium solar radiation and a heating need, and it drops down somewhat during the cooling period, when the slit air circulation cools down the wall.

Looking at figure 17, the load diagram for Reykjavik can be seen. It is clear that the introduction of the trombe wall in Reykjavik helps with the heating of the building during the spring and autumn, as the load graph is positive for most of the year. The cooling needs for the building is low, and the cooling gains from the trombe ventilation is also fairly low. The highest trombe wall gains are from the spring and autumn period.

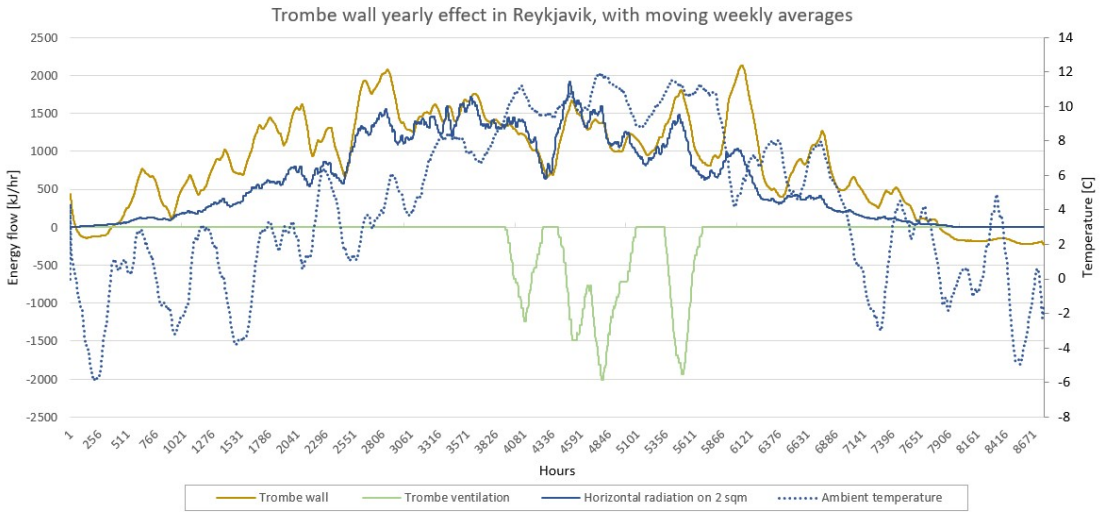

Figure 16: Moving weekly averages throughout the year, in Reykjavik, Iceland.

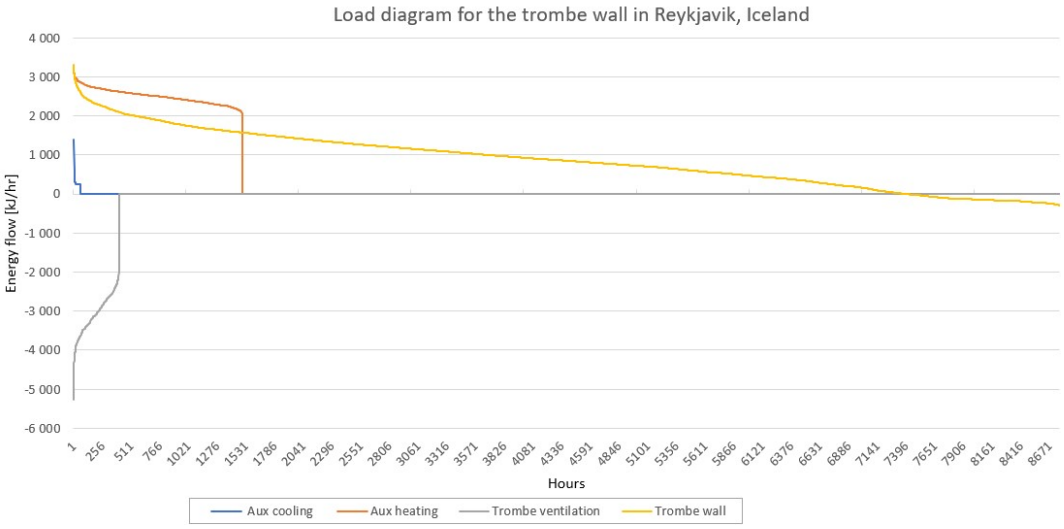

Figure 17: Load diagram of the heating and cooling throughout the year, in Reykjavik, Iceland.

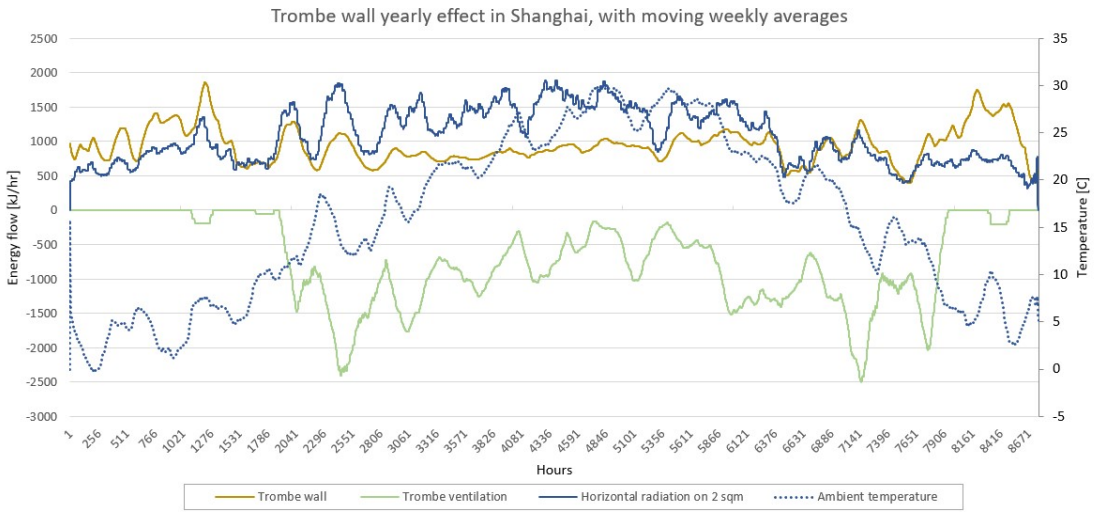

Figure 18: Moving weekly averages throughout the year, in Shanghai, China.

6.1.3 Shanghai, China

In figure 18, an entirerly different cooling load and heating need can be seen. The cooling season is very long, lasting for most of the year. The trombe wall helps with cooling for the most of the summer. However, due to an overheating issue in the building during the summer, the cooling loads of the natural ventilation is overstated. This leads to the natural ventilation of the trombe wall still being counted as effective even though the ambient temperature rises above 25 degrees. By observation of figure 18, this is seen. In the middle of the summer and under acceptable indoor temperature levels, there is no cooling load from the trombe wall. This is because the trombe wall utilizes natural ventilation, and necessitates a temperature difference between the interior and exterior.

There is also zero transmission losses from the trombe wall in the winter. During the entire winter, a high heating rate is achieved for the trombe solid wall, but there is no heating through circulation of air in the slit. The cooling effect through the slit is high in the fall and spring, and has dampening effect on the unwanted heat gains from the wall, as the heat gain from the wall is lower during periods of cooling. And, even though the exterior temperatures drop blow zero degrees, there is always a high positive heat flux through the wall.

Observing figure 19, the load diagram for the Shanghai-located trombe wall is seen. As this graph shows, there is never any need for the auxillary heating system, but there is a high need for an auxillary cooling system. The trombe wall ventilation cooling is far to small to address the house's entire cooling need. It is, however, quite large. The solid wall has a continuous positive transmission throughout the year.

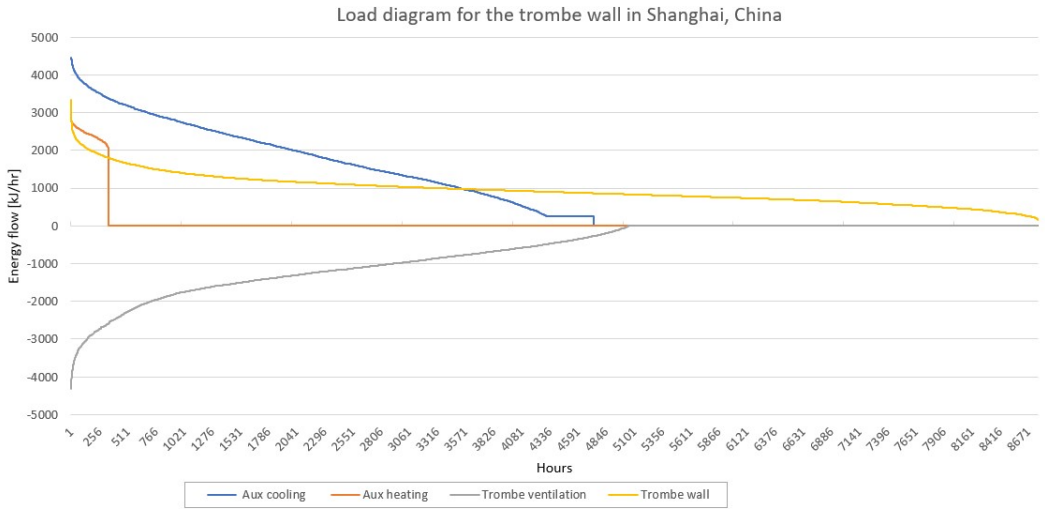

Figure 19: Load diagram of the heating and cooling throughout the year, in Shanghai, China.

6.1.4 Kashi, China

Kashi is an inland city with warm summers and cold winters, this can be seen in figure 20, where the ambient temperature ranges from -10 to almost 30 degrees during the year. The incident solar radiation is also high, due to its high altitude and its latitude. The heating from the solid trombe wall is very high in the late fall, and late winter, just after and before there are cooling needs in the building.

The cooling from the trombe ventilation is active for a large part of the year, and the heating season is short. There are therefore high unwanted heat gains in the wall during the year. These are lowered by the cooling effect of the slit air circulation, as can be seen in figure 20.

In figure 21, the high auxillary cooling load for Kashi can be seen. There are auxillary cooling needs for half of the year, while the trombe solid wall has a constant heat flux into the room. The auxillary heating load graph is high for a period of the year. There are high heating needs for this mountainous inland city, which makes the trombe wall heat gain in the winter needed.

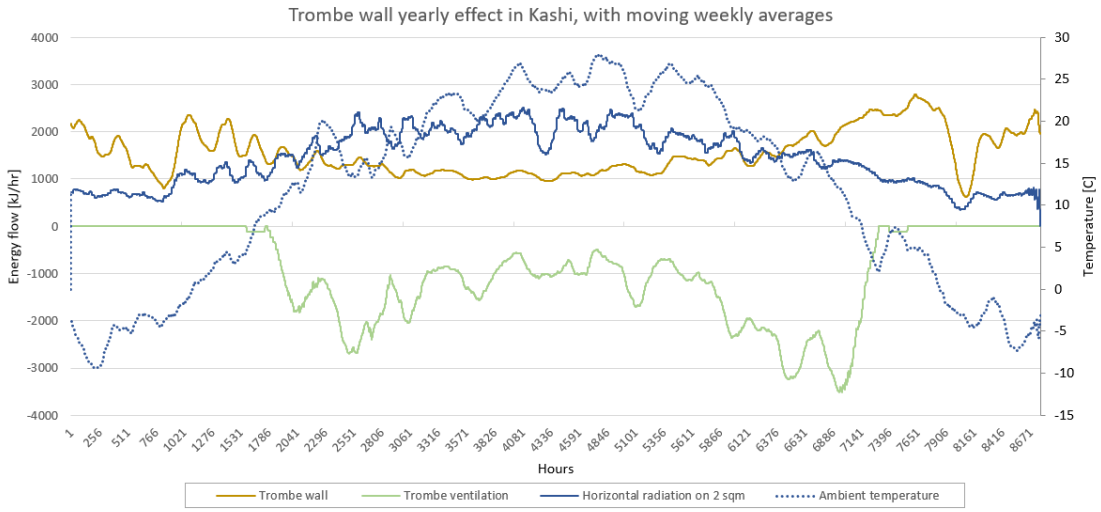

Figure 20: Moving weekly averages throughout the year, in Kashi, China.

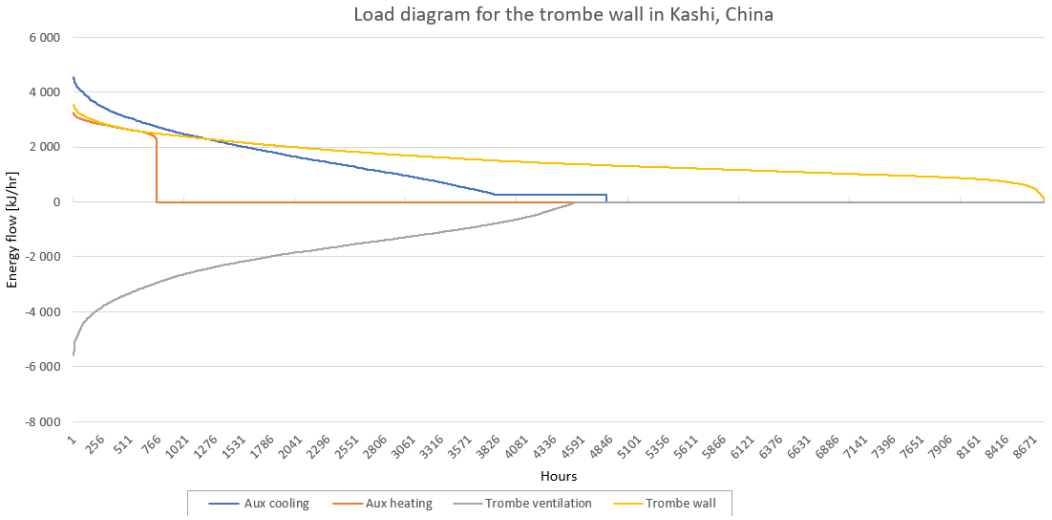

Figure 21: Load diagram of the heating and cooling throughout the year, in Kashi, China.

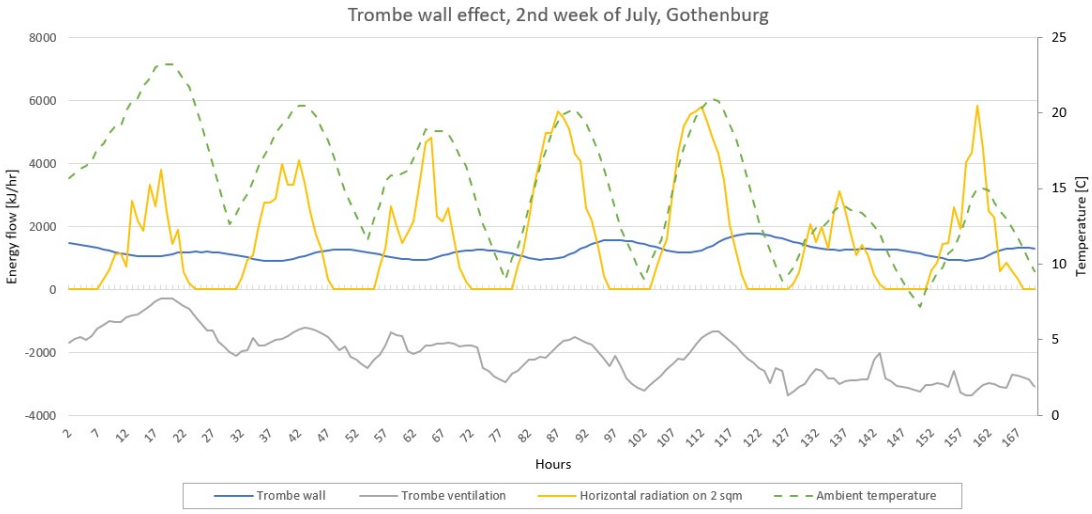

Figure 22: Trombe wall effect, 2nd week of July, Gothenburg

6.2 Summer loads

To gain more insight into the effect the trombe wall has on these four different locations, a study into a typical summer week was performed. The setup is the same as for the yearly simulations, in all locations.

Figure 22 shows how the trombe wall operates in summer conditions. The Gothenburg climate is moderately hot in this week, reaching temperatures of over 20 degrees. The trombe solid wall has a constant higher temperature than the interior, leading to radiation and convection heat gain with the interior from the surface of the solid wall. However, this effect is neutralized by the effect of the natural cooling, if the exterior temperature is low enough. For temperatures below 20 degrees C, the effect is negated. The cooling is also the most effective at nighttime, when the ambient temperature is the lowest, even though there is no solar radiation at night. This is possible because of the high thermal inertia of the wall, maintaining its higher temperature through the night, even if there is circulation through the slit.

In this graph, it is also obvious that the cooling in the wall is much closer linked to the solar radiation level than the wall. This is because the slit utilizes the temperature difference from the exterior facing side of the wall, while the conduction load is from the interior facing side of the wall. The unwanted heat gain from the wall peaks as the cooling load is on the rise, letting the cooling load of the wall negate the wall somewhat.

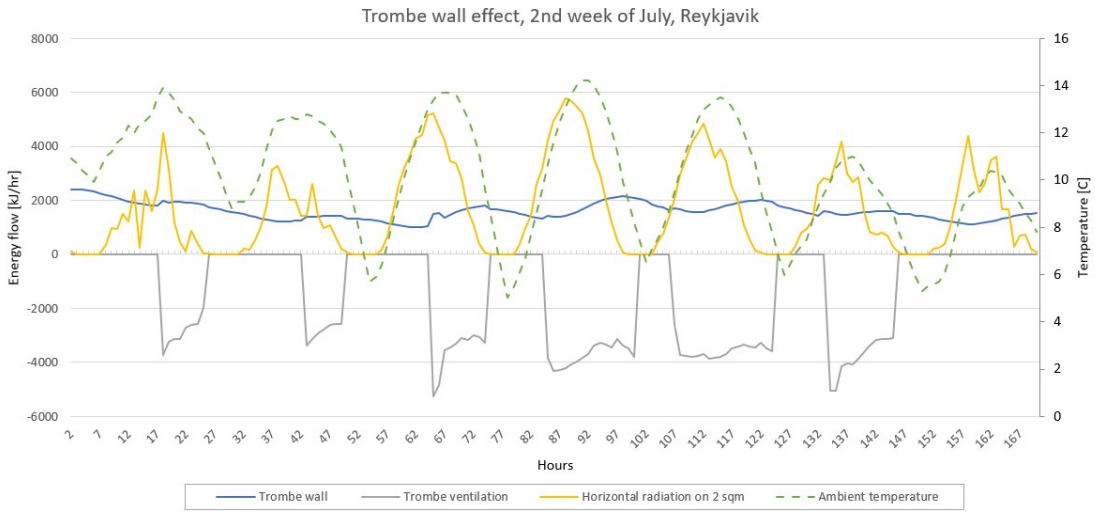

Figure 23: Trombe wall effect, 2nd week of July, Reykjavik

In figure 23, a very different trombe wall response can be seen. This system has higher heat gain, but also higher cooling load peaks, as a result of lower ambient temperature and less cooling need. The result of the low ambient temperature is that the natural ventilation cooling is more effective. It also ensures that the building itself has a lower need for cooling, allowing the trombe wall slits to be closed for large portions of the night. Closed slits leads to a higher slit air temperature, which again leads to a higher heat gain through the wall. However, this heat gain is not too damaging, as Reykjavik has a low cooling need. This was seen in figure 17.

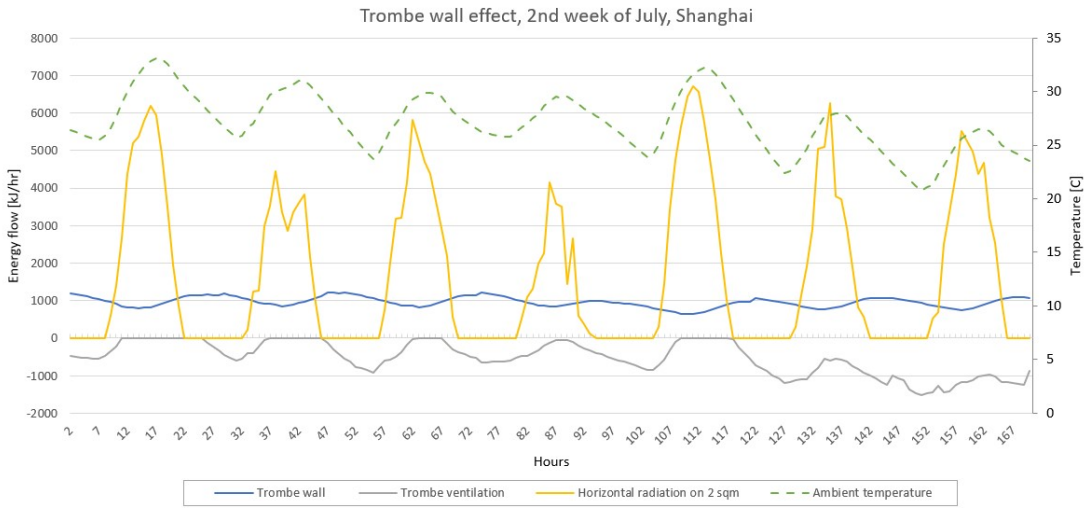

Figure 24: Trombe wall effect, 2nd week of July, Shanghai

Leaving the relatively cold summers of the Nordic countries to the Chinese cities of Shanghai and Kashi results in very different results. In figure 24, the trombe wall response to the Shanghai climate is seen. The high outdoor temperatures and high solar radiation results in unfavorable conditions for the wall. The unwanted heat gain is high, and the cooling from the slit ventilation is low. For a building with a high cooling load, the introduction of the ventilated, unshaded trombe wall is merely an additional heat load. The trombe wall is obviously not functioning with a cooling effect.

It should also be noted that the building has overheating issues in this period, averaging 28 degrees on both floors. This leads to a lower heat gain and a higher cooling load in the building than what it would have if the building was properly cooled.

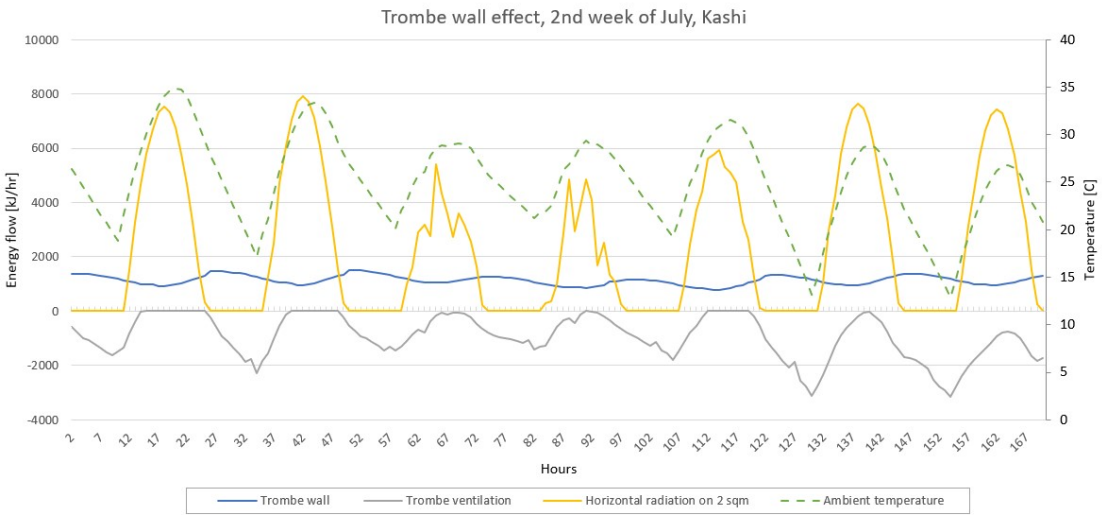

Figure 25: Trombe wall effect, 2nd week of July, Kashi

The same overheating issue was present in Kashi, as seen on figure 25. Here, the trombe wall has high unwanted heat gain and moderate cooling loads, which should be even higher and even lower, respectively. The floors averaged 28 degrees here as well. The trombe wall has a slighty less unfavorable performance in Kashi than in Shanghai, given Kashi's low nighttime temperatures. An ambient temperature of close to 15 degrees allows the airflow through the slit to aid in cooling the building at night. The heat gain from the solid trombe wall is, however, quite high, negating the effects of the cooling for the hotter nights of the week. As a cooling element in the summertime, the vented trombe wall without interior isolation seems to be a low efficiency device.

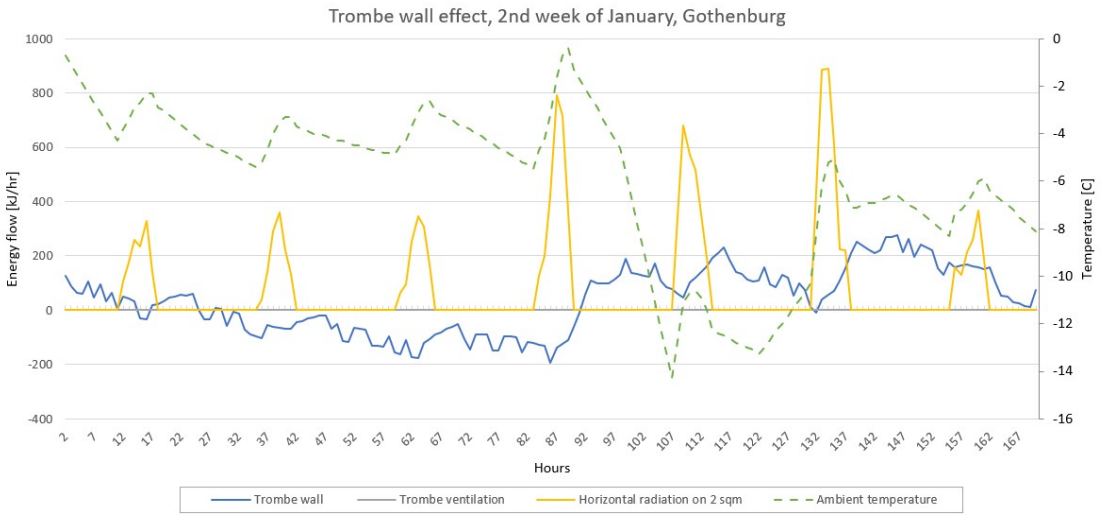

Figure 26: Trombe wall effect, 2nd week of January, Gothenburg

6.3 Winter loads

To gain even more insight into the effect the trombe wall has on these four locations an additional study into a typical winter week was performed. The performance and efficiency of the trombe wall in these conditions are very different from the summer, and warrant a closer look. The lower solar radiation levels, lower ambient temperature and the shift from a cooling to a heating need drastically change which trombe wall characteristics are deemed positive and which are deemed negative.

In figure 26, the trombe wall response to the Gothenburg January climate can be seen. The lowered amount of solar radiation and lower ambient temperature affects the trombe wall enough to make the trombe wall have a net cooling effect on the building. This cooling effect is only raised when the solar radiation is higher. Coincidentally, the ambient temperature drops at the same time as the solar radiation intensifies. This shows that the solar radiation is a major influence, more major than the ambient temperature. A large portion of this effect stems from having low value triple glazed windows. Over the entire course of the week, the trombe wall has a slightly positive heating effect on the room, but this effect is minor. Higher solar radiation levels seems to be necessary for trombe wall mid winter heating to work effectively.

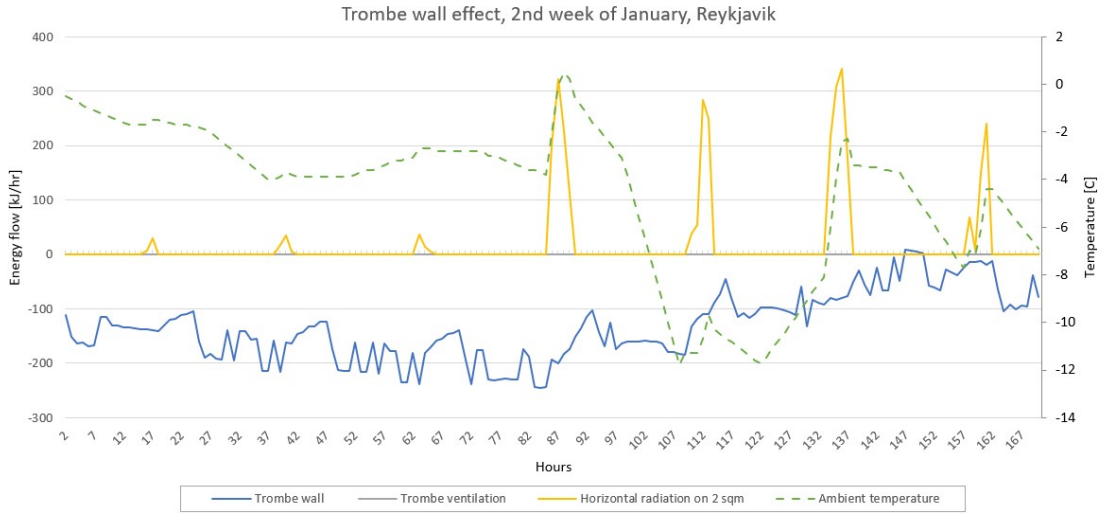

Figure 27: Trombe wall effect, 2nd week of January, Reykjavik

In Reykjavik, figure 27, the situation is worse than in Gothenburg. The solar radiation levels are lower, and the trombe wall has a constant cooling effect on the room in a week with heating need. The cooling load is not massive, but it is present. There are no positive results from having a trombe wall installed in the building for this particular week in Reykjavik.

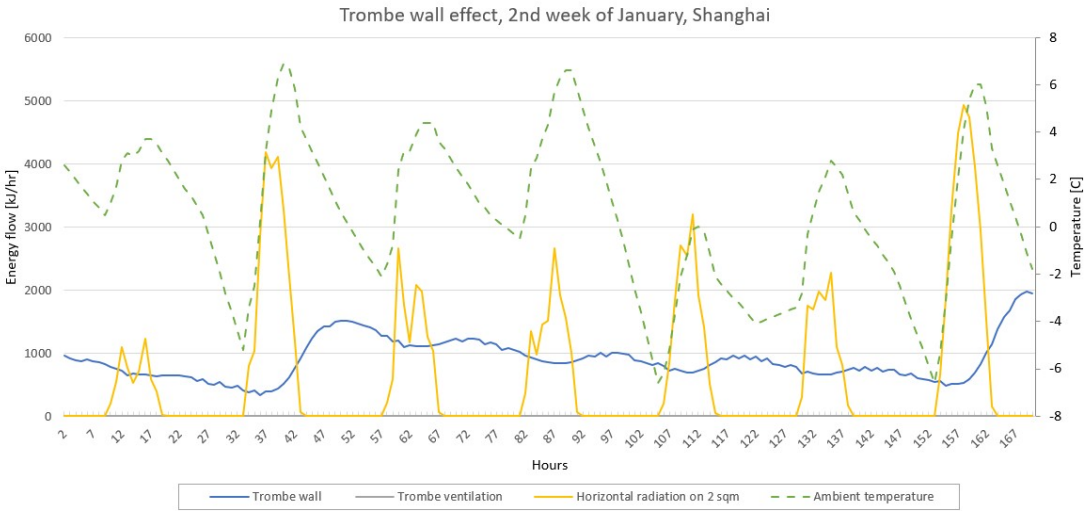

Figure 28: Trombe wall effect, 2nd week of January, Shanghai

In the sunnier latitudes of China, the situation is quite different. Having a trombe wall installed in Shanghai leads to positive results in the 2nd week of January, as seen in figure 28. The solar radiation is high, and even though the temperatures range between 6 and -6 degrees, the wall maintains a moderately high net heating rate to the building. This heating is fairly stable throughout the day, with a peak several hours after the solar radiation peak. A high solar radiation level is, however, key to its performance. A cloudy day affects the trombe wall massively, but a cold day does not affect it very much.

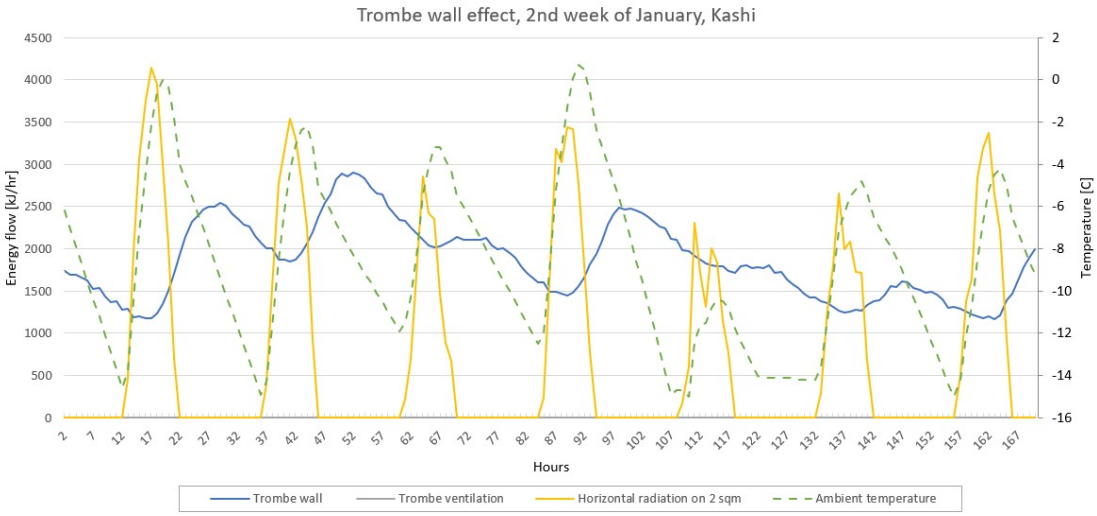

Figure 29: Trombe wall effect, 2nd week of January, Kashi

In Kashi, the trombe wall seem to excel during the winter period. High solar radiation levels, coupled with high heating needs, results in large favorable heating gains from the trombe wall. The peak heating gains are very high, as it was also shown in figure 21. Studying figure 29, the positive effects of the trombe wall in winter time in Kashi is apparent.

In all of the above graphs of the winter-time use of the trombe wall system, there was no heating gain through circulation of the air in the trombe wall slit. This could be a result of the air in the slit not being heated high enough to allow the slits to open, or some control issue with the simulation.

6.4 The effects of the wall width

The size of the trombe wall is an essential part of the trombe wall sizing, and the effect of different wall widths are studied. Trombe wall width most important impacts are the thermal storage capacity of the wall, the delay from peak solar radiation to peak room heating, and the cost/GHG-emissions of the wall. As the different locations has different trombe wall characteristics, both Shanghai and Gothenburg is chosen for review. These locations are very different to each other, but similar enough to Kashi and Reykjavik, respectively, to allow the review of just these two locations. Both winter and summer trombe wall heating/cooling loads are presented, and the 2nd week of January and 2nd week of July is used. These results are based on the same weather data as the summer and winter simulations performed in previous subsections. The 30 cm wall of these simulations has the exact same characteristics as these previous week-long summer and winter simulations.

The wall sizes used are 40, 30, 20 and 10 cm of width and are for a wall of length 2.7 metres and 2.0 metres of height. These values are chosen because somewhere between 20 and 30 cm are the usual thickness found in litterature, and because walls outside of this range will either be unwieldy, or have almost no thermal capacity. The effects of even thinner and even thicker walls can also be inferred by graph inspection.

Figure 30 shows the trombe wall heating/cooling load in response to the Gothenburg summer climate. Figure 31 shows the same graph for the Shanghai summer climate. As can be seen in these two figures, the wall width does have a major impact on the trombe wall summer cooling potential. In Shanghai, it determines the unwanted heat gain from the wall into the room, and in Gothenburg it also determines the cooling load from the slit air cooling.

The thinnest of the Gothenburg trombe wall has very high relative heat gain during the daytime, as the interior side of the wall heats up quickly. This leads to high heat gains during the daytime. The 20 cm wall also suffers from this, but to a lesser extent. The 10 cm wall also suffers from its low thermal storage capacity, as can be seen on the last night of the simulation. Having lost heat through the nighttime cooling, the wall does not have enough heat to maintain a positive cooling load in the morning hours. The curve only plunges downward after the morning sun has hit the wall, and the slit air is being heated enough to let the stack effect carry it from the hot room to the cool ambient. Having a larger wall removes this issues, as the thicker Gothenburg walls are able to maintain higher cooling loads than its thinner counterparts. The effect of having a thicker wall does plateu a bit, as the difference between the 30 cm and 40 cm wall is smaller than between the 10 cm and 20 cm wall.

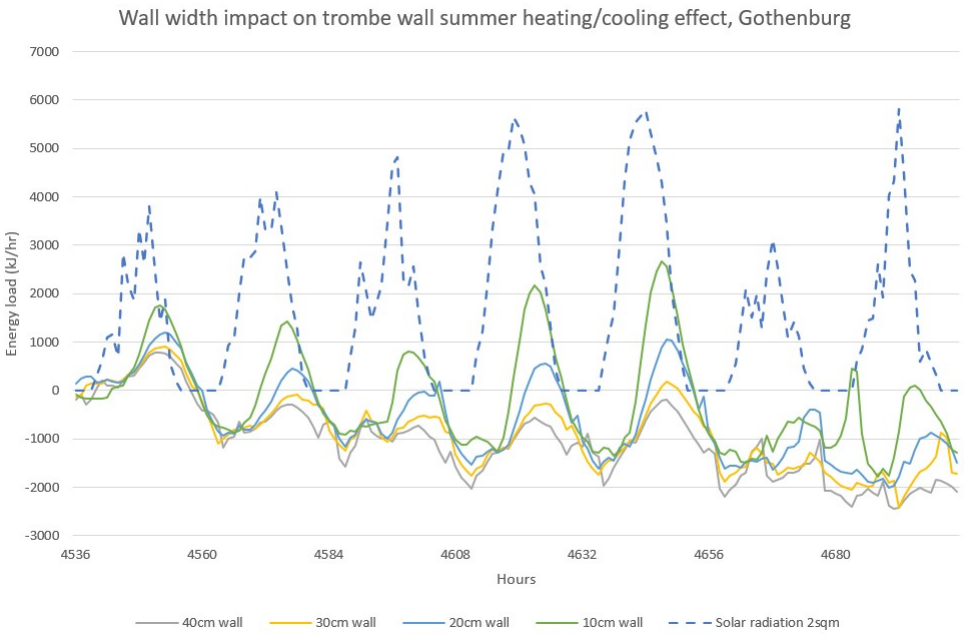

Figure 30: Wall width impact on trombe wall summer heating/cooling, Gothenburg.

In Shanghai and figure 31 much of the same effects can be seen. The thinner walls have a higher fluctuation of heat flux into the room, while the thicker walls are more stable. 10 cm thick walls also have a higher total heat gain than the thicker walls. These results does however present the need for shading on the trombe wall regardless of wall size, in the hot summers of Shanghai. Shading will reduce the heat gain in the wall.

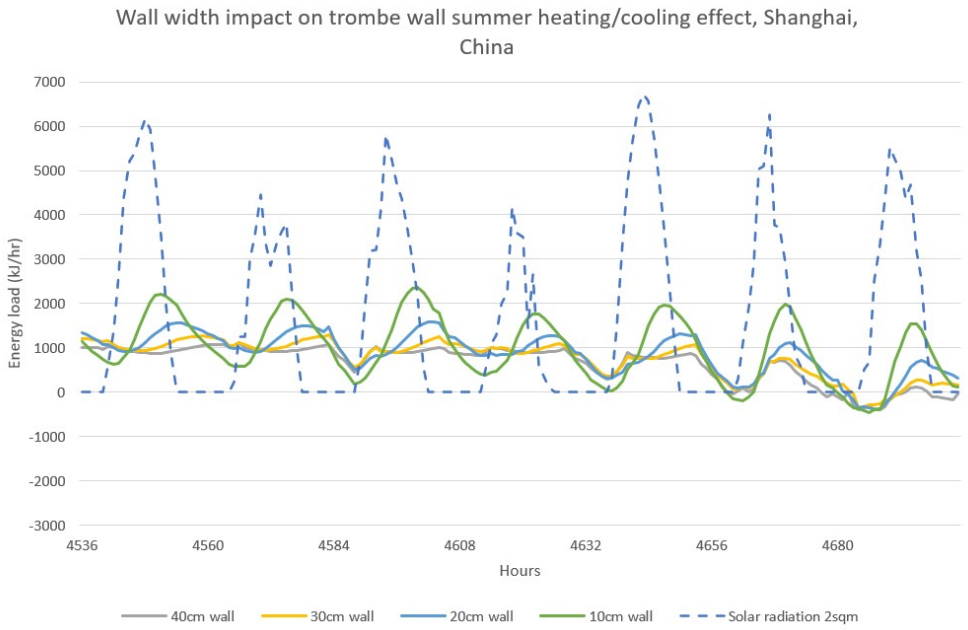

Figure 31: Wall width impact on trombe wall summer heating/cooling, Shanghai.

In the winter season, the characteristics are different. The wall is needed for heating only, and it is important to avoid that the wall becomes a cooling element. Figure 32, the trombe wall response to the winter climate in Gothenburg is presented. As with the summer simulations, the thinnest wall represents the highest fluctuations in heat gain. The thin wall also has the lowest delay between peak solar radiation and peak heat gain, which often is a downside, as peak heating demand often comes in the evening or at night. Even though the peaks are high for the wall, the thin wall plunges quickly down to heat loss when the solar gains are low. The bigger walls with their higher thermal inertia takes longer to fall from heating to cooling, which is very positive. During the winter, the thicker walls seem to be of very little effect in Gothenburg, varying between low heating values and low cooling values.

This results in the heating value being controlled a lot by the temperature of the other interior walls, which leads to this fluctuating heating load. The fluctuations are caused by the fact that the time base for the wall heat transfer calculations in the building model is 1 hour. Therefore, every hour the interior surface temperature changes, and the heat transfer loads through radiation with the interior surfaces suddenly changes as well.

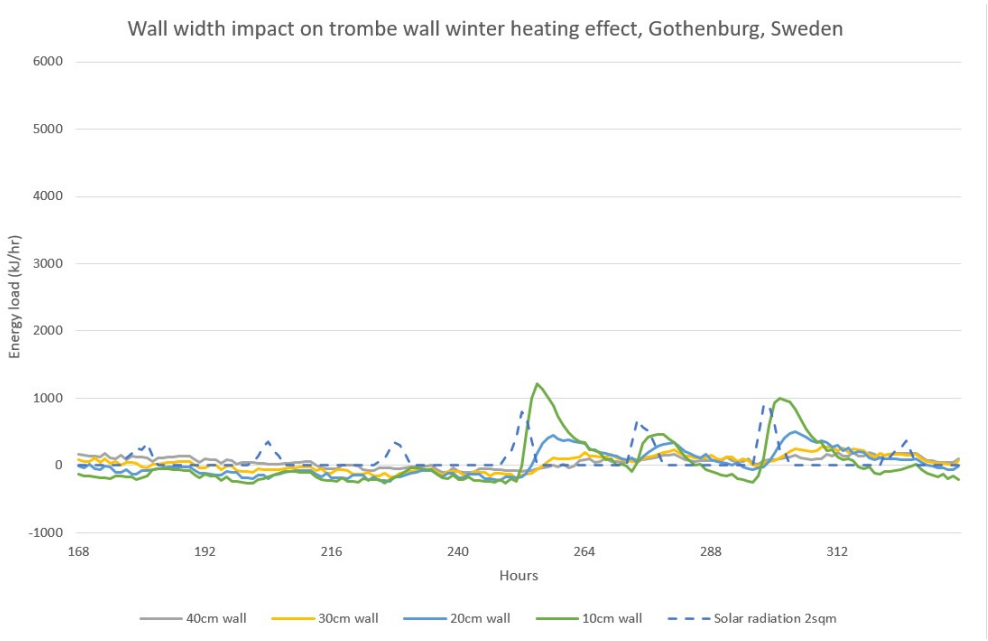

Figure 32: Wall width impact on trombe wall winter heating, Gothenburg.

Shanghai boasts much higher solar radiation levels, and higher winter heat gain through the wall. It is worth noting that Shanghai's lowest daily solar radiation level is the almost the same as Gothenburg's peak solar radiation level. In Shanghai, the thin walls have much higher fluctuations, and earlier peaks here as well. It is also close to negative flux through the wall in periods of low exterior radiation. The thinner walls does have a higher total weekly heat gain through the wall, but the peak heating load may come at a less than optimal time of the day. If this is of note or not depends a lot on the nature of the buildings load and heating needs. More often than not, however, a stable source of heating that keeps on during the nighttime is better.

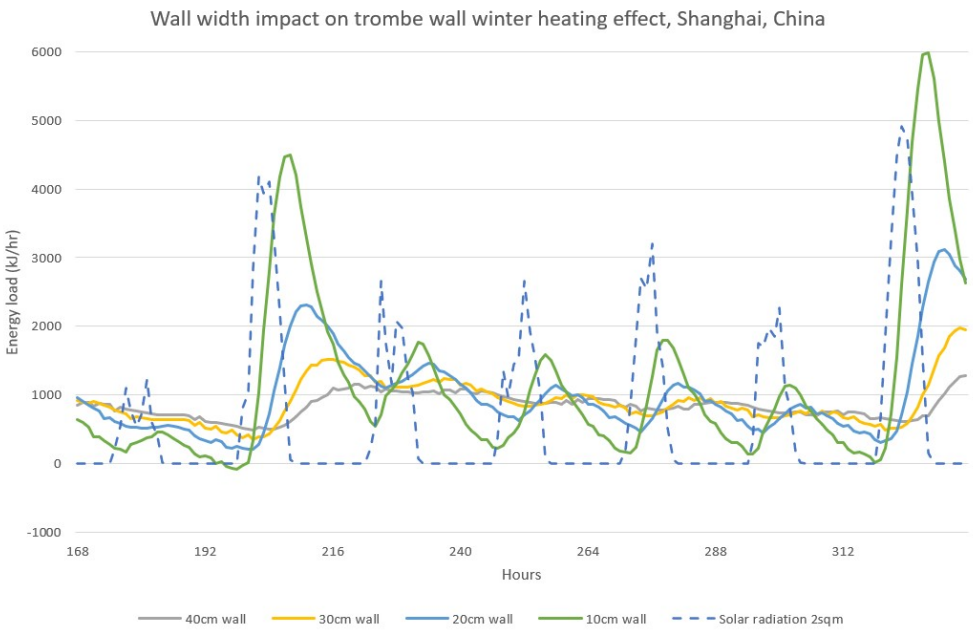

Figure 33: Wall width impact on trombe wall winter heating, Shanghai.

6.5 The effects of the slit size

The size of the slit in the Trombe wall is an important parameter as it is often found to impact the flow of air through the slit. To see the effects of the slit size in this simulation, a similar review as with the wall size was performed. The same locations, weeks and data was used as a basis. The trombe wall width was 30 cm for all calculations.

The slit sizes used are 40, 30, 20 and 10 cm of width and are for a slit of length 2.7 metres and 2.0 metres of height. These values are chosen because around 30 cm is the usual thickness found in literature, and the effects of thicker slit width can be inferred by inspection of the graphs. By inspection and understanding of the governing equations behind the heat transfer equations, the results of widening the slit even more would be negligible, and produce additional errors. If the slit size is too large, then the effects of the sides, bottom and the top of the slit should not be neglected anymore. They would interfere with radiation heat transfer and add to the convection heat transfer in the slit as well. As none of these effects are present in the simulation, large slit sizes are not simulated.

Similar issues are present when lowering the slit size as well, as the glazing and wall convection coefficients are considered independently of one another. If the slit is very thin, then this assumption is no longer viable, as more complex flow patterns would emerge. Therefore, lower slit sizes than 10 cm are not used in the simulation.

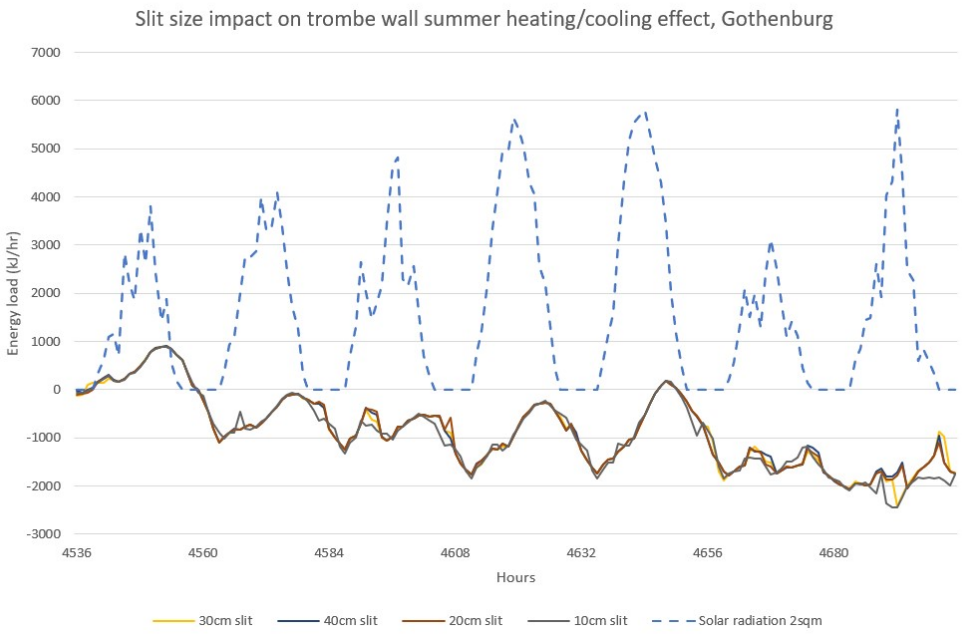

Figure 34: Slit size impact on trombe wall summer heating/cooling, Gothenburg.

The graphs are presented in the same order as with the wall with comparisons. In figures 34, 35, 36 and 37, the results of a varying slit size can be seen. Across all four simulations, extremely small differences between the varying slit sizes are seen. In Shanghai, it seems like the slit sizes have no effect on the trombe wall performance.

Observing figure 34, some positives of using a 10 cm slit can be seen in the last day of the simulation. The effect is small, but present. The reason behind this could be that the low thermal inertia of the small slit affects the performance positively, allowing higher output temperatures.

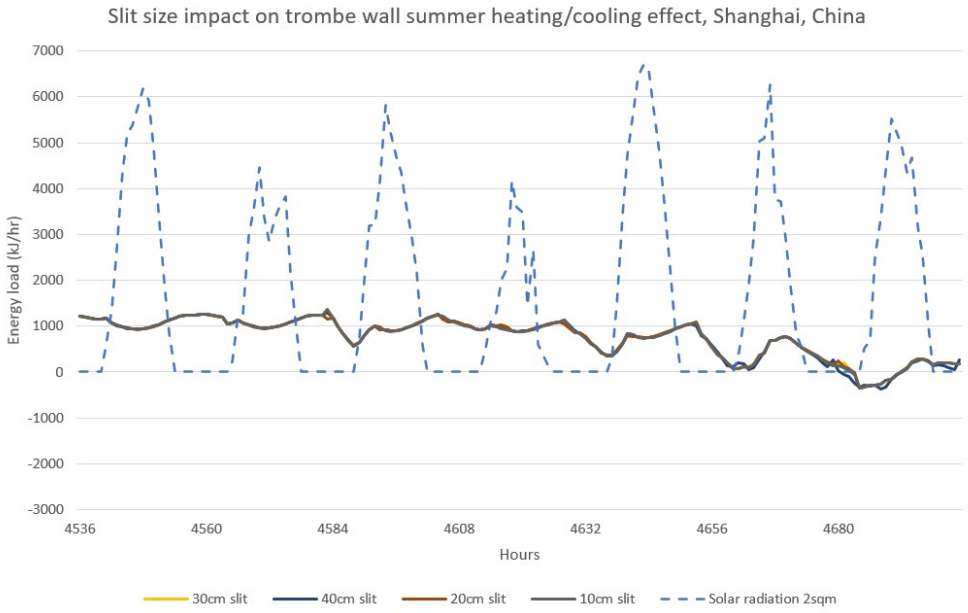

Figure 35: Slit size impact on trombe wall summer heating/cooling, Shanghai.

In the winter, there are no discernible difference between the slit sizes, as well as for Shanghai in the summer.

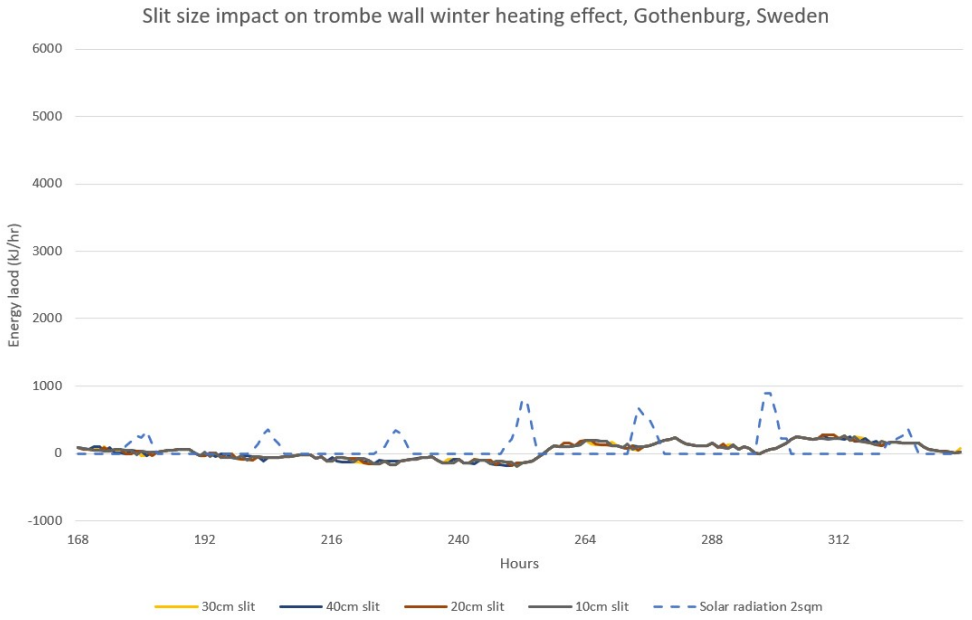

Figure 36: Slit size impact on trombe wall winter heating, Gothenburg.

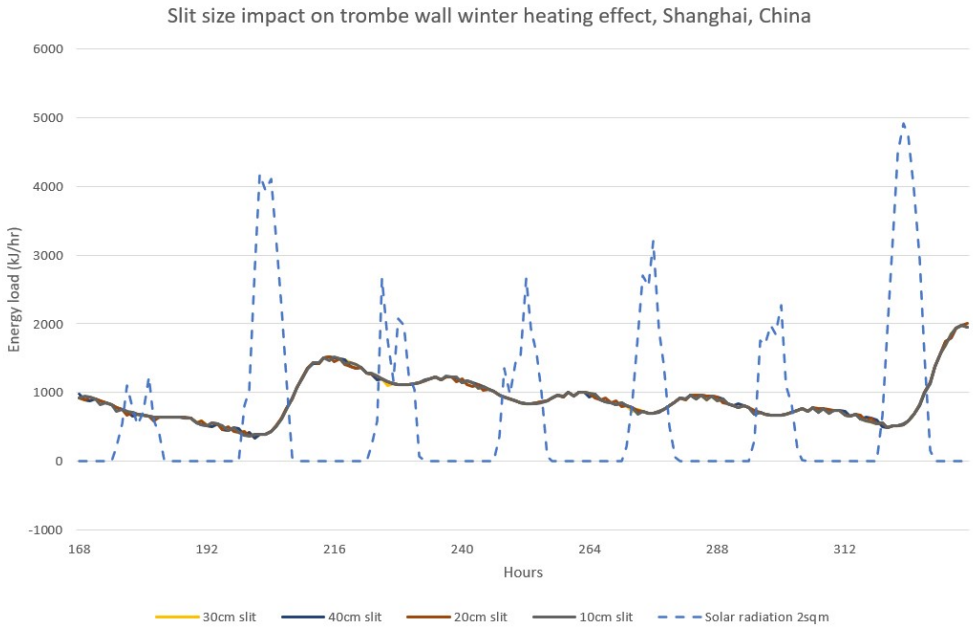

Figure 37: Slit size impact on trombe wall winter heating, Shanghai.

Table 4: Emission savings from each simulated trombe wall locations.

Location	**Gothenburg**	**Reykjavik**	**Shanghai**	**Kashi**
Total energy saved (kWh/year)	1935.35	2181.93	1442.37	2444.76
Total CO2-eq saved (kg/year)	332.88	375.29	363.48	616.08
EPBT (years)	2.42	2.15	2.22	1.31
ERF (10 year lifespan)	4.13	4.65	4.51	7.64

6.6 GHG-emissions

The GHG-emsissions from the wall, and its gains from the reduction of energy use can be found through equations 69 and 70, and through the values in table 3. For the trombe wall of size 2.7x2.0x0.3 metres and a window of the same size, the total life cycle CO_2-eq. emissions are

$$m_{CO2} = (2,200 * 2.7 * 2.0 * 0.3 * 0.15 + 2.7 * 2.0 * 50.4) \text{ kg}, \tag{74}$$

which is 806.76 kg CO2 per trombe wall unit.

The total energy saved from each of the four locations are calculated through addition of the values in table 3. To find each locations EPBT and ERF equation 21 and 20 is used. The results can be read in table 4.

For all locations, there is a high ERF for an assumed 10 year lifespan. As the trombe wall has few movable parts and a sturdy construction, a long lifespan is feasible. The highest ERF is for Kashi, with its high heating gain in the winter and high cooling in the summer. Shanghai has a much lower ERF, as it has a very high unwanted heat gain and lower cooling. Shanghai, Gothenburg and Shanghai all have ERFs between four and five years. The total energy saved in Shanghai is much lower than in the Nordic countries, but with China's high CO2-cost for electricity production, each kWh saved represents a higher amount of CO2 saved.

The EPBT for each location is also low, below two and a half years for all locations, with Kashi being the lowest. Even having a trombe wall with a life expectancy of two years would be beneficial to the environment according to these results.

7 Discussion

In this section, sources of simulation errors and teachings from the results will be discussed.

7.1 Sources of simulation errors

This project presents a good and somewhat validated simulation of the trombe wall component, embedded in a realistic building simulation.

7.1.1 Summer overheating of Kashi and Shanghai

The building model and the size of its heating and cooling equipment is sized for Norwegian climates, and does not have the cooling power needed to keep the building temperatures down in the summer. This is a fairly easy fix in TRNSYS, but the error was caught too late in the project to allow it to be fixed. The result of this is that the cooling loads for these two locations are higher than they should be, and the unwanted heat gains are lower than they should be. Having an interior temperature that is realistic is quite important to the trombe wall performance.

7.1.2 Load diagrams

Using load diagrams to show a change from positive to negative flux does not work to well with how the load diagram is supposed to be read. The hours are usually denoting how many hours the specific part of the system is under the specific load. Thus allowing the user to properly dimension their heating equipment easily. When the heating suddenly turns to cooling, this does not work. It is, however, a very effective way to show the data, and this was deemed the most presentable and readable way to show the data.

7.1.3 Simulation of locations without trombe wall

Simulating the buildings in these locations without the trombe wall would give some insight into how the trombe wall affects the buildings performance. However, the performance by the trombe wall and its effect on the building performance can be somewhat inferred by inspect and understanding of the diagrams. This method is not possible to use for all cases of building heating and cooling, and reference simulations are often needed to gain full insight into the nature of the component.

One major issue with this way of understanding energy gains and heat losses are that the way cooling energy gain is calculated overestimates the value of the cooling created by the ventilation in the slit. When the outside temperature is lower than the interior temperature, cooling through mechanical ventilation is caused by powering on the fans. If the ambient temperature is low enough, the only energy use is by the fans. The fan energy demand is lower than the total cooling that is given to the building, as the exhaust air temperature is higher than the intake temperature. In this project, cooling energy gain was calculated as the difference between the room temperature and the ambient temperature, times the mass flow rate. To more accurately depict cooling gains, the mass flow rate caused and some efficiency factor could be used. Finding this efficiency factor would be important to get the right values using this method.

7.1.4 Winter slit heating

For all of the tested simulations, there was no heating effect gained from the circulation of slit air. This seems unrealistic, although the cause of this is unknown. There could be issues with the controlling unit for the trombe wall, where the conditions for opening the interior vent are too hard to reach, or simply some error in the vent. Another possible error could be that the calculation of the heat transfer from the slit to the room somehow is faulty. The final major reason as to why there are no heating is that there simply are no heating gains from the trombe wall slit in these conditions. This seems to be unreasonable, as the slit reaches quite high temperatures during periods of high solar radiation. In Kashi during the summer period, one would assume that some heating through the slit would happen.

This error was found too late in the project to find and fix the error, so it will need to be understood more in the further work.

7.1.5 Simulation calibration

The calibration and validation of the simulation was performed in a less than optimal setting. Using literature to replicate experiments in order to validate and calibrate the simulation leads to many sources of uncertainty, as previously mentioned. Having an unfamiliar setup that lacks key information can be avoided by performing the experiments, and having deep knowledge and sensoring of the experiment. With monitoring of key temperatures, airflows and radiation values, the realistic and unrealistic parts of the simulation can be found. Performing an experiment in this manner was, as mentioned previously, the initial plan for this project, as it is such an essential part of attaining realistic simulation results. The experiment should also be for both summer and winter conditions, as these lead to very different trombe wall responses.

7.2 Trombe wall locations

The different locations of the trombe wall has of varying degree of use for the trombe wall component. During the cold winters of Reykjavik, transmission losses of moderate degree is caused. In the hot sunny summers of Shanghai and Kashi, high positive heat gain into the room is caused.

These very different locations could have different types of trombe walls implemented, or have different focus areas. The need for shading, is a key example. In Reykjavik, too much solar radiation is very rarely an issue, and shading is not needed. But in Shanghai and Kashi, shading during the summer seems to be very important. The solar radiation levels are very high, in addition to the ambient temperature being higher than the wanted interior temperature for a lot of the summer months. This means that shading the trombe wall, lowering the amount of unwanted heat gain into the building is a simple and cheap way to lower the buildings total energy need. In Gothenburg, the need for shading could sometimes be present, but an unshaded trombe wall seems to be implementable in the city without too much issue. Having shading would decrease the unwanted heat gain, but it would also decrease the cooling load, rendering the gain obsolete.

8 Conclusion

The trombe wall model, and the building model, has been validated to an acceptable degree. Creating a Matlab script from scratch has shown to be a good solution, as the trombe wall model shows similar results as experiments found in literature. More validation of the simulation should be performed, however, as the experiments in the literature has many uncertainties associated with them.

The trombe wall model was simulated successfully in different locations in Northern Europe and China. Each location has their own characteristic climates, that brings their own trombe wall possibilities and challenges. This was researched and understood in depth by full year inspection, and closer inspection of summer and winter performance. Using this methodology to gain insight into the trombe wall performance proved successful. In both Chinese locations, shading of the trombe wall is needed, while in Reykjavik, some way to isolate the wall better should be implemented.

A life cycle analysis was performed, and all locations of the trombe wall proved to be climate friendly components, according to this methodology. The Kashi trombe wall was the most effective, and Gothenburg the least effective. Location determines both the climate and the electricity mix of the energy saved, both major factors in determining total GHG-emissions saved.

This trombe wall analysis gives valuable insight into multiple facets of the trombe wall. Multiple sizes of wall width and slit sizing was performed, both in Shanghai and Gothenburg. The wall width is shown to be a very important parameter, directly influencing the cooling loads and heat gains into the building. The slit, on the other hand, does not determine the performance of the wall in this simulation.

The project has shown promise on the implementation of a trombe wall in various climates, when lowering GHG-emissions are in focus. More research of this component is warranted, as there are several more research areas that needs attention. These are presented in the further work section.

9 Further work

9.1 Slit size investigations

In this simulation scheme, the size of the ventilation slit was found to be of little importance. This could be due to the way the governing equations are setup, and what simplifications that are made to create them. Having a small slit size is not supported in this calculation, neither is very large sizes. Having smaller slits may be of interest, as it will cause a smaller area footprint in the building component, leading to a larger indoor area or smaller exterior footprint. Depending on the building type and location, this could be very beneficial, as many building locations have a very limited ground area to work with. A very narrow slit would start having larger viscous effects and stop having non-interactivity between the glazing and wall, however, so the governing equations needs to be reworked for this to be feasible.

9.2 In-depth life cycle analysis

The life cycle analysis (LCA) in this project was merely superficial, and a more in-depth analysis should be performed. Having a good understanding of the basis for the wall's GHG-emissions is important if the component is to be viewed as an environmentally friendly component. The LCA performed previously in the project is a good indicator for what the trombe wall's emissions are like, but in this modern ZEB-project era more thorough LCAs are needed. The manufacture, installment and end-of-life processes like recycling should be researched deeper to find an even more accurate value for the GHG-emissions of each component.

9.3 Natural ventilation in low infiltration buildings

In this project a low infiltration, Norwegian passive house standard building is used. These buildings have very low infiltration rates, meaning that even with high pressure differences between the interior and exterior, there is little air being infiltrated through the envelope. This effect was mostly negated in the trombe wall airflow calculations for summer ventilation, as the literature sources for these underlying equations are from higher infiltration setups. The result of this could be that the mass air flow through the building in the project is overvalued, as a the flow resistances are higher than estimated. The effects of having natural ventilation in a building like this needs to be researched. A possible solution to this could be to have a varying infiltration rate in the building, that is higher in the summer than in the winter, mimicking the effect of having open summer natural ventilation.

9.4 Implementations of other trombe wall technologies

There are several other trombe wall technologies that are of interest. The insulated Trombe-Michel wall could maybe be of use to prevent summer overheating in Kashi and Shanghai, or prevent winter cooling in Reykjavik. Setting up a Trombe-Michel wall simulation would have the same equation foundation as this simulation, but the heat transfers would merely have a somewhat different placement and order.

The combined technology of PV and trombe wall could be implemented as well, and research into its use and effectiveness could be done. This would allow the component to output electricity at the same time as it heats or cools the building.

Phase change materials (PCM) should also be researched and implemented into a simulation of this type. The theory behind the heat transfer through a PCM wall is quite different from a massive wall, and the simulation would need to be changed a bit. In a PCM wall the conductivity, thermal inertia, heat transfer, emissivity and transmissivity changes with the changes from solid to liquid in the wall. However, implementing this into a simulation of this type is entirely feasible.

9.5 Control strategies

Analysing the effect of using different trombe wall control strategies would be beneficial. As of now, the control strategy for the trombe wall is automatic and assumed motor controlled. As a result of this, an energy consuming motor is introduced into a system with the sole purpose of saving energy and emissions. Therefore, the effects of using user controlled control strategies should be examined. Using a control strategy that is detrimental to the trombe wall efficiency could end up in a net positive gain for the trombe wall system with regards to power consumption and emission.

Nomenclature

Abbreviations

HRU	Heat recovery unit
HVAC	Heating, ventilation and air conditioning
LCA	Life Cycle Analysis
LCC	Life Cycle Cost
ZEB	Zero Emission Building
ZEB*	Zero Energy Building

Greek symbols

α	The absorbtivity of a solid or fluid
β	The volumetric expansion coefficient
ϵ	The emissivity of a solid or fluid
μ	Dynamic viscosity of a fluid
ρ	The density of a solid or fluid
σ	The Stefan-Boltzmann constant
τ	The transmittance of a solid or fluid

Symbols

$\dot{I}$	Radiation flux
$\dot{Q}$	Energy flux, of radiation, convection or conduction
$\dot{V}$	The volumetric flow of a fluid
A	Area
c	Thermal capacity
C_d	The discharge coefficient
C_{cover}	The cloudiness factor
D_h	The hydraulic diameter
f	Body forces working on a fluid
F_{ij}	The view factor from one surface i to a surface j
g	The gravitational constant
Gr	The Grashofs number of a fluid flow
h	Convective heat transfer coefficient
h	Height
k	Thermal conductivity
L	Length
p	The pressure of a fluid

Pr	The Prandtl number of a fluid flow
R	Thermal resistance or Avogadro's constant
Re	The Reynolds number of a fluid flow
T	The temperature of a solid or fluid
t	Time
u, v, w	The velocity vectors of a fluid, in three dimension
x, y, z	Coordinates of the system, with z being vertical

Subscripts

0	Initial conditions
a	Thermal diffusivity
air	Standard composition air
amb	Ambient
atm	Atmosphere
$ceiling$	The interior ceiling
$cond$	Conduction
$conv$	Convection
g	Glazing
$ground$	The exterior or interior ground
i	Instantaneous conditions, or conditions of air entering the lower ventilation opening of the trombe wall
o	Air exiting one of the upper ventilation openings of the trombe wall
rad	Radiation
$room$	The room connected to the trombe wall system
$slit$	The air cavity between the trombe wall glazing and the solid wall
$solar$	Related to solar radiation
tot	Total
$vent$	The upper or lower trombe wall vents
w	The massive trombe wall

References

Book Sources

Agrawal, Basant and G. N. Tiwari (2010). *Building Integrated Photovoltaic Thermal Systems: For Sustainable Developments*. URL: https://academic.microsoft.com/paper/618612826.

Incropera, Frank P. et al. (2013). *Principles of Heat and Mass Transfer*. Wiley. URL: https://academic.microsoft.com/paper/578586814.

Solar Energy Laboratory, University of Wisconsin-Madison (2012). *TRNSYS 17 documentation*.

Articles

Abbassi, Fakhreddine, Narjes Dimassi, and Leila Dehmani (2014). "Energetic study of a Trombe wall system under different Tunisian building configurations". In: *Energy and Buildings* 80, pp. 302–308. ISSN: 0378-7788. DOI: 10.1016/j.enbuild.2014.05.036. URL: http://www.sciencedirect.com/science/article/pii/S037877881400440X.

Akbarzadeh, A., W.W.S. Charters, and D.A. Lesslie (1982). "Thermocirculation characteristics of a Trombe wall passive test cell". In: *Solar Energy* 28.6, pp. 461–468. ISSN: 0038-092X. DOI: https://doi.org/10.1016/0038-092X(82)90317-6. URL: http://www.sciencedirect.com/science/article/pii/0038092X82903176.

Andersen, Karl Terpager (2003). "Theory for natural ventilation by thermal buoyancy in one zone with uniform temperature". In: *Building and Environment* 38.11, pp. 1281–1289. URL: https://academic.microsoft.com/paper/1990227504.

Andresen, Inger et al. (Oct. 2019). "The Norwegian ZEB definition and lessons learnt from nine pilot zero emission building projects". In: *IOP Conference Series: Earth and Environmental Science* 352, p. 012026. DOI: 10.1088/1755-1315/352/1/012026. URL: https://iopscience.iop.org/article/10.1088/1755-1315/352/1/012026.

Anton, Karin and Inge Vestergaard (Oct. 2013). "Norsk passivhusstandard og Passivhauskonzept: en sammenlignende analyse av krav og kriterier". In: DOI: 10.13140/RG.2.1.1673.4808.

Balcomb, J.D. et al. (Jan. 1980). "Passive solar design handbook. Volume two of two volumes: passive solar design analysis". In:

Bansal, N.K., Jyotirmay Mathur, et al. (2005). "Modeling of window-sized solar chimneys for ventilation". In: *Building and Environment* 40.10, pp. 1302–1308. ISSN: 0360-1323. DOI: https://doi.org/10.1016/j.buildenv.2004.10.011. URL: http://www.sciencedirect.com/science/article/pii/S0360132304003245.

Bansal, N.K., Rajesh Mathur, and M.S. Bhandari (1993). "Solar chimney for enhanced stack ventilation". In: *Building and Environment* 28.3, pp. 373–377. ISSN: 0360-1323. DOI: https://doi.org/10.1016/0360-1323(93)90042-2. URL: http://www.sciencedirect.com/science/article/pii/0360132393900422.

Bassiouny, Ramadan and Nader S.A. Koura (2008). "An analytical and numerical study of solar chimney use for room natural ventilation". In: *Energy and Buildings* 40.5, pp. 865–873. ISSN: 0378-7788. DOI: https://doi.org/10.1016/j.enbuild.2007.06.005. URL: http://www.sciencedirect.com/science/article/pii/S0378778807001806.

Burek, S.A.M. and A. Habeb (2007). "Air flow and thermal efficiency characteristics in solar chimneys and Trombe Walls". In: *Energy and Buildings* 39.2, pp. 128–135. ISSN: 0378-7788. DOI: https://doi.org/10.1016/j.enbuild.2006.04.015. URL: http://www.sciencedirect.com/science/article/pii/S0378778806001356.

Chen, B. et al. (2006). "Shading effects on the winter thermal performance of the Trombe wall air gap: An experimental study in Dalian". In: *Renewable Energy* 31.12, pp. 1961–1971. ISSN: 0960-1481. DOI: https://doi.org/10.1016/j.renene.2005.07.014. URL: http://www.sciencedirect.com/science/article/pii/S0960148105002752.

Gan, Guohui (1998). "A parametric study of Trombe walls for passive cooling of buildings". In: *Energy and Buildings* 27.1, pp. 37–43. URL: https://academic.microsoft.com/paper/2024944374.

Hastings, Robert S and Maria Wall (2007). "Sustainable Solar Housing; Volume 1: Strategies and Solutions". In: 1. URL: https://academic.microsoft.com/paper/874386543.

Hernández, Víctor et al. (2006). "Experimental and numerical model of wall like solar heat discharge passive system". In: *Applied Thermal Engineering* 26.17, pp. 2464–2469. ISSN: 1359-4311. DOI: https://doi.org/10.1016/j.applthermaleng.2006.01.027. URL: http://www.sciencedirect.com/science/article/pii/S1359431106001001.

Hirunlabh, J et al. (1999). "Study of natural ventilation of houses by a metallic solar wall under tropical climate". In: *Renewable Energy* 18.1, pp. 109–119. ISSN: 0960-1481. DOI: https://doi.org/10.1016/S0960-1481(98)00783-6. URL: http://www.sciencedirect.com/science/article/pii/S0960148198007836.

K.S. Ong, C.C. Chow (2003). "03/02421 Performance of a solar chimney: Ong, K. S. and Chow, C. C. Solar Energy, 2003, 74, (l), 1–17". In: *Fuel and Energy Abstracts* 44.6, pp. 392–393. ISSN: 0140-6701. DOI: https://doi.org/10.1016/S0140-6701(03)92550-1. URL: http://www.sciencedirect.com/science/article/pii/S0140670103925501.

Koyunbaba, Basak Kundakci and Zerrin Yilmaz (2012). "The comparison of Trombe wall systems with single glass, double glass and PV panels". In: *Renewable Energy* 45, pp. 111–118. ISSN: 0960-1481. DOI: https://doi.org/10.1016/j.renene.2012.02.026. URL: http://www.sciencedirect.com/science/article/pii/S0960148112001656.

Martin, Marlo and Paul Berdahl (1984). "Characteristics of infrared sky radiation in the United States". In: *Solar Energy* 33.3, pp. 321–336. ISSN: 0038-092X. DOI: https://doi.org/10.1016/0038-092X(84)90162-2. URL: http://www.sciencedirect.com/science/article/pii/0038092X84901622.

Mathur, Jyotirmay et al. (2006). "Experimental investigations on solar chimney for room ventilation". In: *Solar Energy* 80.8, pp. 927–935. ISSN: 0038-092X. DOI: https://doi.org/10.1016/j.solener.2005.08.008. URL: http://www.sciencedirect.com/science/article/pii/S0038092X05003014.

Matuska, Tomas and Borivoj Sourek (2006). "Façade solar collectors". In: *Solar Energy* 80.11. European Solar Conference (EuroSun 2004), pp. 1443–1452. ISSN: 0038-092X. DOI: https://doi.org/10.1016/j.solener.2006.04.006. URL: http://www.sciencedirect.com/science/article/pii/S0038092X06001125.

Norge, Standard (2001). "Norsk Standard NS-EN ISO7726:2001". In:

– (2012). "Norsk Standard NS3701:2012". In:

– (2013). "Norsk Standard NS3700:2013". In:

– (2016). "Norsk Standard SN/TS3031:2016". In:

Nwachukwu, Nwosu P. and Wilfred I. Okonkwo (2008). "Effect of an Absorptive Coating on Solar Energy Storage in a Thrombe wall system". In: *Energy and Buildings* 40.3, pp. 371–374. ISSN: 0378-7788. DOI: https://doi.org/10.1016/j.enbuild.2007.03.004. URL: http://www.sciencedirect.com/science/article/pii/S0378778807000989.

Probst, MariaCristina Munari and Christian Roecker (2007). "Towards an improved architectural quality of building integrated solar thermal systems (BIST)". In: *Solar Energy* 81.9. CISBAT 2005, pp. 1104–1116. ISSN: 0038-092X. DOI: https://doi.org/10.1016/j.solener.2007.02.009. URL: http://www.sciencedirect.com/science/article/pii/S0038092X07000576.

Rabani, Mehran, Vali Kalantar, and Mehrdad Rabani (2017). "Heat transfer analysis of a Trombe wall with a projecting channel design". In: *Energy* 134, pp. 943–950. ISSN: 0360-5442. DOI: https://doi.org/10.1016/j.energy.2017.06.066. URL: http://www.sciencedirect.com/science/article/pii/S0360544217310605.

Ram, Sant and H.P. Garg (1985). "Heat flux through a Trombe wall/roof". In: *Applied Energy* 19.1, pp. 61–71. ISSN: 0306-2619. DOI: https://doi.org/10.1016/0306-2619(85)90040-6. URL: http://www.sciencedirect.com/science/article/pii/0306261985900406.

Saadatian, Omidreza et al. (2012). "Trombe walls: A review of opportunities and challenges in research and development". In: *Renewable and Sustainable Energy Reviews* 16.8, pp. 6340–6351. ISSN: 1364-0321. DOI: https://doi.org/10.1016/j.rser.2012.06.032. URL: http://www.sciencedirect.com/science/article/pii/S136403211200425X.

Sartori, Igor, Assunta Napolitano, and Karsten Voss (2012). "Net zero energy buildings: A consistent definition framework". In: *Energy and Buildings* 48, pp. 220–232. ISSN: 0378-7788. DOI: https://doi.org/

10.1016/j.enbuild.2012.01.032. URL: http://www.sciencedirect.com/science/article/pii/S0378778812000497.

Shen, Jibao et al. (2007). "Numerical study on thermal behavior of classical or composite Trombe solar walls". In: *Energy and Buildings* 39.8, pp. 962–974. ISSN: 0378-7788. DOI: https://doi.org/10.1016/j.enbuild.2006.11.003. URL: http://www.sciencedirect.com/science/article/pii/S0378778806002726.

Stazi, Francesca, Alessio Mastrucci, and Costanzo di Perna (2012a). "The behaviour of solar walls in residential buildings with different insulation levels: An experimental and numerical study". In: *Energy and Buildings* 47, pp. 217–229. ISSN: 0378-7788. DOI: https://doi.org/10.1016/j.enbuild.2011.11.039. URL: http://www.sciencedirect.com/science/article/pii/S0378778811005858.

– (2012b). "Trombe wall management in summer conditions: An experimental study". In: *Solar Energy* 86.9, pp. 2839–2851. ISSN: 0038-092X. DOI: https://doi.org/10.1016/j.solener.2012.06.025. URL: http://www.sciencedirect.com/science/article/pii/S0038092X1200237X.

Union, The European (2010). "Directive 2010/31/EU on the energy performance of buildings". In: *Official Journal of the European Union* 153, pp. 13–35. URL: https://www.buildup.eu/sites/default/files/content/EPBD2010_31_EN.pdf.

Weir, G. and T. Muneer (1998). "Energy and environmental impact analysis of double-glazed windows". In: *Energy Conversion and Management* 39.3, pp. 243–256. ISSN: 0196-8904. DOI: https://doi.org/10.1016/S0196-8904(96)00191-4. URL: http://www.sciencedirect.com/science/article/pii/S0196890496001914.

Wilson, Alex (1979). "Thermal storage wall design manual". In:

Zalewski, L., M. Chantant, et al. (1997). "Experimental thermal study of a solar wall of composite type". In: *Energy and Buildings* 25.1, pp. 7–18. ISSN: 0378-7788. DOI: https://doi.org/10.1016/S0378-7788(96)00974-7. URL: http://www.sciencedirect.com/science/article/pii/S0378778896009747.

Zalewski, L., S. Lassue, et al. (2002). "Study of solar walls — validating a simulation model". In: *Building and Environment* 37.1, pp. 109–121. ISSN: 0360-1323. DOI: https://doi.org/10.1016/S0360-1323(00)00072-X. URL: http://www.sciencedirect.com/science/article/pii/S036013230000072X.

Zhou, Yuekuan, Chuck W.F. Yu, and Guoqiang Zhang (2018). "Study on heat-transfer mechanism of wallboards containing active phase change material and parameter optimization with ventilation". In: *Applied Thermal Engineering* 144, pp. 1091–1108. URL: https://academic.microsoft.com/paper/2803001789.

Other

Assosiation, International Energy (2020). *CO2 intensity of energy mix*. URL: https://www.iea.org/regions/.

bygningskvalitet, Direktoratet for (2020). *Byggteknisk forskrift(TEK17)*. Accessed 18.11.19. URL: https://dibk.no/byggereglene/byggteknisk-forskrift-tek17.

Ellis, Peter Graham (2003). *Development and validation of the unvented Trombe wall model in EnergyPlus*.

Engineeringtoolbox.com (2020). *Thermal Conductivity of Selected Materials and Gases*. Accessed 23.11.19. URL: https://www.engineeringtoolbox.com/thermal-conductivity-d_429.html.

EPS-Group, BPF (2020). *Properties of EPS*. URL: http://www.eps.co.uk/applications/properties.html.

Hamre, Liv Mette (2018). *Enhancement of Natural Ventilation in Residential Buildings with Roof Integrated PV/T Components*. URL: http://hdl.handle.net/11250/2575519.

IEA, International Energy Agency (2019). *Energy Efficiency - Buildings*. Accessed 12.11.2019. URL: https://www.iea.org/topics/energyefficiency/buildings/.

Institute, Passive House (2020a). *Passive house - definition*. Accessed 18.11.19. URL: https://passipedia.org/basics/the_passive_house_-_definition.

– (2020b). *Passive house database*. Accessed 18.11.19.

Mitalas, G. P. and J. G. Arseneault (1972). *Fortran IV program to calculate Z-transfer functions for the calculation of transient heat transfer through walls and roofs*. Tech. rep. DOI: https://doi.org/10.4224/20328318. URL: https://nrc-publications.canada.ca/eng/view/fulltext/?id=9a383a07-6830-401d-a3a7-ab15ad077208.

Nilsson, Marte Wigen (2015). *Analysis of the novel solar heating wall installed as building envelop in the Green Energy Laboratory*. URL: http://hdl.handle.net/11250/2374932.

Petroleum, British (2019). *British Petroleum Energy Outlook 2019 - Energy demand by sector*. Accessed 23.11.19. URL: https://www.bp.com/en/global/corporate/energy-economics/energy-outlook/demand-by-sector.html.

Solar, Naked (n.d.). *Solar panel aesthetics*. Accessed 23.11.19. URL: https://nakedsolar.co.uk/solar-pv/solar-panel-aesthetics/.

Statsbygg (2019). *INN, studiested Evenstad. Nybygg*. Accessed 19.11.19. URL: https://www.statsbygg.no/Prosjekter-og-eiendommer/Byggeprosjekter/HiHm-Evenstad-Nybygg/.

Teenou, Raya Yousef (2012). "Energy and CO2 emissions associated with the production of Multi-glazed windows". MA thesis. Mid Sweden University. URL: http://www.diva-portal.org/smash/get/diva2:532125/FULLTEXT01.pdf.

Tesla (2019). *Tesla Solarglass Roof*. Accessed 23.11.19. URL: https://www.tesla.com/solarroof.

Trust, Passivhaus (2019). *Passivhaus Trust - Homepage*. Accessed 18.11.19. URL: http://www.passivhaustrust.org.uk/.

Winnipeg, City of (2011). *WINNIPEG SEWAGE TREATMENT PROGRAM - Appendix 7*. Ed. by Veolia Water. URL: https://www.winnipeg.ca/finance/findata/matmgt/documents/2012/682-2012/682-2012_Appendix_H-WSTP_South_End_Plant_Process_Selection_Report/Appendix%207.pdf.

Zero Emission Buildings, The Research Centre on (n.d.). *ZEB - definitions*. Accessed 19.11.19. URL: https://zeb.no/index.php/en/about-zeb/zeb-definitions.

Appendix A - Trombe wall Matlab scripts

In this appendix, the Matlab script in its entirety is presented.

- Part I - Main Script
- Part II - Function - Glazing temperature profile
- Part III - Function - Wall temperature profile
- Part IV - Function - Air variables
- Part V - Function - Dimensionless numbers
- Part VI - Function - Heat transfer coefficients

```
 %% Trombe wall response to temperatures and initial values.

% The first if statements are checking for what type of calling TRNSYS is
% making to the running Matlab script. Before iterative timestep calculations are
% performed, the script checks to see if this is the last or first call of the
% entire simulation, or the post convergence call for the current timestep.

mFileErrorCode = 50;

%% Last call of simulation
% In the last call of the simulation, occurring after exiting the TRNSYS
% Online Plotter, final kWh values for the current simulation is computed
% and printed to a .txt. file.
% Other applicable hourly values are printed as well.

if ( trnInfo(8) == -1 )
%Calculating simulation summary
E_wr_find = find(history.Q_wr>=0);
E_wr_neg_find = find(history.Q_wr<=0);
E_sr_find = find(history.Q_sr>=0);
E_sr_neg_find = find(history.Q_sr<=0);

%Total values in kWh
E_wr = sum(history.Q_wr(E_wr_find))*dt/kWhJ;                    %kWh, Wall to room↙
positive  energy transfer
E_wr_neg = sum(history.Q_wr(E_wr_neg_find))*dt/kWhJ;    %kWh, Wall to room negative↙
energy transfer
E_sr = sum(history.Q_sr(E_sr_find))*dt/kWhJ;                       %kWh, Slit  to  room↙
positive  energy transfer
E_sr_neg = sum(history.Q_sr(E_sr_neg_find))*dt/kWhJ;       %kWh, Slit  to  room↙
negative energy transfer

% %Values in kWh/day, not used
% simdays = (trnStopTime-trnStartTime)/24; %Number of elapsed days
% E_wr_day = E_wr/simdays;
% E_wr_neg_day = E_wr_neg/simdays;
% E_sr_day = E_sr/simdays;
% E_sr_neg_day = E_sr_neg/simdays;

% Writing to file
time_date = datestr(now);
fileName = 'output_temporary.txt';% + time_date(1:6);

fileID = fopen(fileName, 'w');
fprintf(fileID,'The solid wall heated the room with %f.4 kWh and cooled the room with %↙
f.4 kWh \n', E_wr, E_wr_neg)
fprintf(fileID,'The slit heated the room with %f.4 kWh and cooled the room with %f.4↙
kWh \n\n', E_sr, E_sr_neg)
fprintf(fileID,'Hourly simulation values\n');
fprintf(fileID,'Time[hr] T_o[K] T_room[K] T_amb[K] T_w6[K] I_total[W/m2] Q_sr[W] Q_wr↙
[W]\n')
fprintf(fileID,'%d %d %d %d %d %d %d %d\n', history.time(1:stephr:end), history.T_o(1:↙
stephr:end),history.T_i(1:stephr:end), history.T_amb(1:stephr:end), history.T_w6(1:↙
stephr:end),history.I_total(1:stephr:end),history.Q_sr(1:stephr:end),history.Q_wr(1:↙
stephr:end));
```

```
fclose(fileID);

    mFileErrorCode = 0;
return
end
%% Post convergence call
if (trnInfo(13) == 1)
            mFileErrorCode = 2000;
     %Setting the slit previous temperature for the next calculation.
        T_op = T_o;
        T_gp = T_g;
        T_wp = T_w;
        Tbar_sp = Tbar_s;
        Tbar_savgp = Tbar_savg;
        T_iavgp = T_iavg;
        T_ip = T_i;
    %Writing the history of each component
        history.time(nStep) = nStep*trnTimeStep;
        history.T_o(nStep)   = T_o;
        history.T_g1(nStep)  = T_g(1);
        history.T_g2(nStep) = T_g(2);
        history.T_g3(nStep) = T_g(3);
        history.T_w1(nStep) = T_w(1);
        history.T_w2(nStep) = T_w(2);
        history.T_w3(nStep) = T_w(3);
        history.T_w4(nStep) = T_w(4);
        history.T_w5(nStep) = T_w(5);
        history.T_w6(nStep) = T_w(6);
        history.T_i(nStep)     = T_i;
        history.Tbar_s(nStep)  = Tbar_s;
        history.Q_sr(nStep)     = Q_sr;
        history.Q_wr(nStep)    = Q_wr;
        history.mdot(nStep)   = mdot;
        history.I_total(nStep)    = I_total;
        history.T_amb(nStep) = T_amb;

%        history.Q_cooling      = Q_cooling;
%        history.Q_heating      = Q_heating;

if isPlotting
    isFullHour = mod(nStep*trnTimeStep,1) == 0;
if isFullHour
    % Plotting temperatures every hour
    Time = trnTime-trnStartTime; %Gives the number of hours since simulation start
    plot(Time,T_amb,'Color',[0,0,0.5],'Marker','p')
    plot(Time,T_g(1),'Color',[0,0.4,1],'Marker','x')
    plot(Time,T_g(2),'Color',[0,0.7,0.7],'Marker','x')
    plot(Time,T_g(3),'Color',[0,1,0.4],'Marker','x')
    plot(Time,T_o,'Color',[0,1,0],'Marker','d')
%    plot(Time,Tbar_s,'k-o')
    plot(Time,T_w(1),'Color',[0.5,1,0],'Marker','*')
    plot(Time,T_w(2),'Color',[0.6,0.8,0],'Marker','*')
    plot(Time,T_w(3),'Color',[0.7,0.6,0],'Marker','*')
    plot(Time,T_w(4),'Color',[0.8,0.4,0],'Marker','*')
    plot(Time,T_w(5),'Color',[0.9,0.2,0],'Marker','*')
```

```
    plot(Time,T_w(6),'Color',[1,0,0],'Marker','*')
    plot(Time,T_i,'Color',[1,0,0.7],'Marker','+')
   end
end
       nStep = nStep+1;

        mFileErrorCode = 0;
    return
end

%% First call of the simulation, setting the simulation parameters and initial values
% Static values are calculated only at the first call of the simulation,
% making this if statement extensive.

    mFileErrorCode = 100;

if ( (trnInfo(7) == 0) && (trnTime-trnStartTime < 1e-6) )    % First call of the↙
simulation
%% Constant parameters and misc
C_s = 0.74;          %-, average slit temperature adjustment, from Ong et.al 03
C_d = 0.57;          %-, discharge coefficient, from Akbarzadeh et.al 82
CK = 273.15;          %Celsius to Kelvin conversion
kWhJ = 3.6*10^6;  %kWh to Joules conversion
g =          9.81;               %m/s^2, gravitational acceleration
sigma =      5.6704 * 10^(-8);   %W/(m^2 K^4),Stefan Boltzmann

dt = trnTimeStep*3600; %s, Timestep of the simulation, converted from hr.
h_choice = 2; %Setting the convective heat transfer component, from Shen, Bass, Akbar,↙
Ashrae.
nStep = 1; %This is the first time step
%hrStart = 72; %This can be chosen to allow data aquisition to be delayed, to allow the↙
wall and glazing to reach real-case temperatures.
%nStepStart = hrStart/trnTimeStep; %hrStart converted to number of timesteps before↙
data logging begins.
profile on; %Starts the profiler mode (development tool).
stephr = 1/trnTimeStep; %Calculating the number of timesteps per hour
calc_pause = [stephr/10, stephr/10, stephr/10]; %#steps between [air variables,↙
dimensionless numbers, heat transfer coefficient] calculations, for faster simulation↙
times.

global trnTime trnStopTime trnStartTime
%% Setup variables
% Building simulation
H_w = 2;  L_w = 2.7;      d_w = 0.30;  %m, height, length, width og wall
H_g = H_w;       L_g = L_w;    d_g = 0.008;  %m, height, length and thickness of each↙
glazing
N_g = 3; % number of panes

H_s = H_w;  L_s = L_w;  d_s = 0.3;   %m, height, length and width of slit
H_v = 0.2;         L_v = L_s;    d_v=d_w; %m, height, length and width of vents
A_vo = 1*d_s; A_vi = (H_s-H_w)*1; %From fig 1, in Mathur.

alpha_w = 0.9; %Old value: 0.9; %-, absorptivity
rho_w = 2400; %kg/m3, density %2400 was the original rho
k_w = 1.2;  %W/mK, conductivity %0.8 was the original k
```

```
cp_w = 880; %880; %J/kgK, specific heat capacity, @http://www2.ucdsb.on.↙
ca/tiss/stretton/database/Specific_Heat_Capacity_Table.html

isPlotting = 0;

iswallheatloss = 1;
R_wceiling = 4;
R_wfloor = 4;

%T_floor = monthly average temperature.
%T_ceiling = T_amb
%Use ACH_mathur(mdot,rho_i) to evaluate the ACH.

%% Solid wall parameters
A_w = H_w*L_w; %m^2, area of wall
R_w = 0.05;  eps_w = 0.9;   N_w = 8; %-, reflectivity, emissivity, number of nodes.
%alpha_w = 0.9; %-, absorptivity

a_w = k_w/(rho_w*cp_w); %m^2/s, thermal diffusivity.
dx_w = d_w/(N_w-1) ; %m, length between and of each sentral node in the wall
cp_nw = dx_w*H_w*L_w*cp_w*rho_w ; %J/K, heat capacity of each sentral nodal element
F_ow = a_w*dt/dx_w^2; %-, Fourier number. Eq. 5.80 in PoHaMT.

%% Glazing parameters
A_g = H_g * L_g; %m^2, area of the glazing
d_g = 0.004; %m, thickness of glazing [Weir, 1998]
C_g = 0.85; %Glazing correction factor
d_gair = 0.01; %m, distance between each pane
cp_g = 840; %J/kgK @http://www2.ucdsb.on.↙
ca/tiss/stretton/database/Specific_Heat_Capacity_Table.html
R_g = 0.05;   eps_g = 0.1; %-, reflectivity and emissivity
tau_g = 0.9; alpha_g= 0.1;  %-, transmittance and absorptivity
rho_g = 2500; %kg/m^3, density @https://uk.saint-gobain-building-glass.com/en-↙
gb/architects/physical-properties
k_air = 0.024; %W/mK, NOTE! https://en.wikipedia.org/wiki/Thermal_conductivity
h_glass = k_air*(A_g/d_gair)*C_g; %W/K, thermal conductivity
cp_gn = cp_g * d_g * H_g * L_g*rho_g; %J/K, heat capacity of each glazing

%a_gk = k / (rho_g * cp_g) ; %% Thermal Diffusivity. Actual equation.
%a_gh = (h_glass*A_g) / (d_gair* rho_g * cp_g); %s^-1, note. (misses m^2) thermal diff,↙
modified equation.
%F_og = a_gh*dt/d_gair^2 ; %%note. is m^-2, Fourier number for the glazing. Unsure if↙
this is something i can do


    mFileErrorCode = 140;
%% Slit and vent parameters
A_s = H_s*L_s; %m^2, slit area

A_v = H_v * L_v; %m^2, area of the vents

    mFileErrorCode = 190;

%% Setting initial temperatures [K]
T_op = 293; %Slit outlet temperature
```

```
T_gp = ones(1,3)*T_op; %Glazing initial temperature
T_wp = ones(1,N_w)*(T_op+30);%Wall initial temperature;
Tbar_sp = T_op;
T_o = T_op;
T_g = T_gp;
T_w = T_wp;
Tbar_s = Tbar_sp;
T_amb = 293;
T_i = 293;
T_ip = T_i;
T_iavgp = T_i;
mdot = 0;
Tbar_savgp = Tbar_s;

    mFileErrorCode = 180;
%% Data aquisition
% Initialize history of the variables for plotting at the end of the simulation
nTimeSteps = (trnStopTime-trnStartTime)/trnTimeStep;
history.time = zeros(nTimeSteps,1);
history.T_o    = zeros(nTimeSteps,1);
history.T_i    = zeros(nTimeSteps,1);
history.T_g1      = zeros(nTimeSteps,1);
history.T_g2      = zeros(nTimeSteps,1);
history.T_g3      = zeros(nTimeSteps,1);
history.T_w1      = zeros(nTimeSteps,1);
history.T_w2      = zeros(nTimeSteps,1);
history.T_w3      = zeros(nTimeSteps,1);
history.T_w4      = zeros(nTimeSteps,1);
history.T_w5      = zeros(nTimeSteps,1);
history.T_w6      = zeros(nTimeSteps,1);
history.Q_sr      = zeros(nTimeSteps,1);
history.Q_wr      = zeros(nTimeSteps,1);
history.mdot    = zeros(nTimeSteps,1);
history.I_total    = zeros(nTimeSteps,1);
history.T_amb  = zeros(nTimeSteps,1);
%history.Q_cooling      = zeros(nTimeSteps,1);
%history.Q_heating      = zeros(nTimeSteps,1);
history.Tbar_s      = zeros(nTimeSteps,1);

%% Plotting
if isPlotting
clf
hold on
plot(0,T_amb,'Color',[0,0,0.5],'Marker','p')
plot(0,T_g(1),'Color',[0.2,0.6,1],'Marker','x')
plot(0,T_g(2),'Color',[0.2,0.8,0.8],'Marker','x')
plot(0,T_g(3),'Color',[0.2,1,0.6],'Marker','x')
plot(0,T_o,'Color',[0,1,0],'Marker','d')
plot(0,Tbar_s,'k-o')
plot(0,T_w(1),'Color',[0.5,0.8,0],'Marker','*')
plot(0,T_w(2),'Color',[0.6,0.6,0],'Marker','*')
plot(0,T_w(3),'Color',[0.7,0.5,0],'Marker','*')
plot(0,T_w(4),'Color',[0.8,0.3,0],'Marker','*')
plot(0,T_w(5),'Color',[0.9,0.2,0],'Marker','*')
plot(0,T_w(6),'Color',[1,0,0],'Marker','*')
```

```
plot(0,T_i,'Color',[1,0,0.7],'Marker','+')
title('Instanteneous temperatures in the trombe wall simulation')
xlabel('Hours since simulation start')
ylabel('Temperatures (K)')
legend('T_{amb}','T_g(1)','T_g(2)','T_g(3)','Outlet','Slit','T_w(1)','T_w(2)','T_w↙
(3)','T_w(4)','T_w(5)','T_w(6)','T_{room}')
end
    mFileErrorCode = 170;    % After initialization

tic; %Starts the clock timer, using "toc" outputs the elapsed time of the simulation.

% No 'return' here, calculations will be performed at this call.
end

mFileErrorCode = 160;
%% Setting the inputs

% Input variables from the building simulation
T_i =    trnInputs(1)+CK;       %K, Room temperature, equal to the incoming air to the↙
slit.
T_walls =   trnInputs(2)+CK;       %K, Type 56 average indoor wall temperature
T_floor =   trnInputs(3)+CK;       %K, Floor temperature, for solid wall heat loss.
T_ceiling = trnInputs(4)+CK;       %K, Ceiling temperature, for solid wall heat loss.

Ctrl_trombe = trnInputs(5);     %-, Control mode for trombe wall.
% -1 -> open exterior vent, 0 -> shut vents, 1 -> open interior vent.
T_ground =  trnInputs(6)+CK;        %K, Ground temp, for radiation heat exchange??

% Weather file input variables
I_total =   trnInputs(7)/3.6;      %from kJ/(hr*m^2) to W/m^2, total incident radiation
T_amb =     trnInputs(8)+CK;      %K, ambient dry bulb temperature
T_sky = trnInputs(9)+CK; %K, effective sky temperature
v_wind =    trnInputs(10);      %m/s, wind speed

    mFileErrorCode = 170;
%% Calculation of the glazing radiative heat transfer coefficient through T_sky

%These are only calculated every [calc_pause(1)]th call, for faster simulation
%times.
if mod(trnInfo(8),calc_pause(1))==0 || trnInfo(8)<= 5
h_grad = sigma * eps_g * (T_sky^2 - T_gp(1)^2) * (T_sky - T_gp(1)) ;       %W/Km^2,↙
glazing sky radiation heat loss

h_wind = 5.7 + 3.8*v_wind;      %W/Km^2, glazing exterior wind heat loss coefficient

    mFileErrorCode = 200;

%% Air variables, from Bansai et. al 05, appendix A.
[rho_air, mu_air, k_air, c_air, beta_air, rho_i, mu_i, k_i, beta_i, rho_o] =↙
air_variables(Tbar_sp, T_i, T_op,T_w(1));

end

    mFileErrorCode = 210;
%% Airflow mass and speed
```

```
Tbar_savg = 0.9 * Tbar_savgp + 0.1 * Tbar_sp;
T_iavg =      0.9 * T_iavgp      + 0.1 * T_ip;

if Ctrl_trombe ==0
    mdot = 0;       % If the vents are shut, the trombe wall has no mass flow.
else
    if Tbar_savg >= (T_iavg)
     mdot = 0.9 * mdot + 0.1 * C_d*(rho_o*A_v)*sqrt(g*H_s*(Tbar_savg-T_iavg)/T_iavg); %↙
kg/s, from Mathur et. al 06
    else % this is removed from the above eq.: (1 + (A_vo/A_vi)^2.
    mdot =  0.9 * mdot ; % Assumes reverse airflow device is operational
    end
end

V_s = mdot / ((rho_air+rho_i)/2 * d_s*L_s);   %m^3/s

       mFileErrorCode = 215;

%These are only calculated every [calc_pause(2)]th call, for faster simulation times.

if mod(trnInfo(8),calc_pause(2))==0 || trnInfo(8)<= 5
%% Dimensionless numbers
[Re, Ra, Gr, Pr] = dimensionless_numb(L_w, d_w, rho_air, V_s, mu_air, beta_air, T_gp↙
(3), Tbar_sp, H_w, c_air, k_air, g);

    mFileErrorCode = 220;
%% Convective heat transfer coefficients
h_conv = conv_heat_transf(h_choice, Ra, Gr, Pr, d_s, H_s, k_air, V_s);

%Convective heat transfer coefficient from wall to room
[Re, Ra, Gr, Pr] = dimensionless_numb(L_w, d_w, rho_air, V_s, mu_air, beta_air, T_wp↙
(1), Tbar_sp, H_w, c_air, k_air, g);
h_convwr = conv_heat_transf(h_choice, Ra, Gr, Pr, d_s, H_s, k_air, V_s);

end
    mFileErrorCode = 250;

%% Calculating the heat flows in the system, based on the last call's temperatures.
%The heat flows are positive is the flux is coming from the outside and
%towards the inside. [W]

Q_gamb = h_wind * (T_amb-T_gp(1))*A_g; %Appendix #2
Q_gs = h_conv * (T_gp(3) - Tbar_sp)*A_g; %Appendix #3
Q_wg =  (A_g*sigma*(T_gp(3)^4-T_wp(1)^4))/(1/eps_g*2+1/(eps_w)-1); %Appendix #4
Q_solarg =  I_total * (1-R_g) * (1-tau_g)*A_g; %Appendix #5
Q_sky =  h_grad*(T_sky - T_gp(1))*A_g; %Appendix #6

Q_ws =  h_conv * (Tbar_sp - T_wp(1))*A_w; %Appendix #9
Q_solarw =  I_total * (1-R_g) * tau_g * (1-R_w) * alpha_w*(A_w); %Appendix 10.↙
Reflected sunlight is neglected in further calculations. %%Taken away:: NOTE.*0.9 to↙
have shading effects effect the system.
Q_wr =  A_w*eps_w*sigma*(T_wp(N_w)^4-T_walls^4) + h_convwr * (T_wp(N_w)-T_i)*A_w; %↙
Appendix 11+12.
```

```
Q_ds = mdot * c_air * (T_op - T_i); %Appendix #7 %Change in internal slit energy, from interaction with the room air.


if Ctrl_trombe == 1 %Interior vent
    Q_sr =  mdot * c_air * (T_op - T_i); %Appendix #7
elseif Ctrl_trombe == 0 %Shut vent
    Q_sr = 0;
elseif Ctrl_trombe == -1 %Exterior vent
    Q_sr = mdot * c_air * (T_amb - T_i);
else
    mFileErrorCode = 260;
    return
end

if iswallheatloss
    Tbar_w = mean(T_wp);
    Q_lossw = L_w*d_w* ((Tbar_w - T_floor)/R_wfloor + (Tbar_w - T_ceiling)/R_wceiling); %Appendix 13.
else
    Q_lossw = 0;
end

    mFileErrorCode = 280;
%% Calculating the wall temperature profile
T_w(1:N_w) = wall_temperature(T_wp(1:N_w), F_ow, Q_ws, Q_wg, Q_solarw, Q_lossw, N_w, cp_nw, dt, Q_wr);

     mFileErrorCode = 320;
%% Calculating the glazing temperature profile
T_g = glazing_temp(T_gp, Q_sky, Q_gamb, Q_solarg, Q_gs, Q_wg, N_g, dt, cp_gn, h_glass);

    mFileErrorCode = 350;
%% Calculating the new slit air temperature
% if nStep <= 1000
    Tbar_s = Tbar_sp + (Q_gs-Q_ds-Q_ws)/(d_s*H_s*L_s*rho_air*c_air)*dt; %K, Change in slit air internal energy
% else
%     Tbar_s = Tbar_savgp + (Q_gs-Q_ds-Q_ws)/(d_s*H_s*L_s*rho_air*c_air)*dt; %K, Change in slit air internal energy
% end

    %if mdot <= 100 %Check for airflow above 100 kg/s
%    T_o = Tbar_s;                          %K
%else
T_o =  0.9*T_op + 0.1 * (Tbar_s-C_s*T_i)/(1-C_s); %K, Average temperature of airflow equation, solved for T_o %
%end

% Sometimes the way T_op is calculated from Tbar_s gives bad output values,
% this fixes some of the unrealistic outliers.
if T_o >= (120 + CK)
    T_o = 120+CK ;
elseif T_o <= (10+CK)
    T_o = 10 + CK;
```

```
end

    mFileErrorCode = 360;
%% Setting the output variables
% The output variables are converted back to TRNSYS units.
if mdot == 0 %If there is no mass flow, T_o is not needed
    trnOutputs(1) = 0;
else
    trnOutputs(1) = T_o-CK ;
end

trnOutputs(2) = T_g(1)-CK; %trnOutputs(3) = T_g(2)-CK;
trnOutputs(3) = T_g(3)-CK;

trnOutputs(4) = T_w(1)-CK; %trnOutputs(6) = T_w(2)-CK; trnOutputs(7) = T_w(3)-CK; %↙
trnOutputs(8) = T_w(4)-CK; trnOutputs(9) = T_w(5)-CK;
trnOutputs(5) = T_w(6)-CK;

trnOutputs(6) = Q_sr*3.6; %From W to kJ/hr
trnOutputs(7) = Q_wr*3.6;
trnOutputs(8) = Q_lossw*3.6;
trnOutputs(9) = (Q_gamb+Q_sky+Q_lossw)*3.6; %Total loss in the system
trnOutputs(10) = (Q_solarg+Q_solarw)*3.6; %Total solar gain in the system
trnOutputs(11) = (trnOutputs(6)+trnOutputs(7))/(trnOutputs(10)+0.01); %Efficiency of↙
the system

trnOutputs(12) = mdot*3600; %From kg/s to kg/hr

trnOutputs(13) = Tbar_s -CK;
trnOutputs(14) = T_i - CK;

%% Remaing time estimation
mins_left = toc*((trnStopTime-trnTime)/(trnTime-trnStartTime))/60; %mins_left can be↙
evaluated to give the estimated minutes until simulation completion

%% Error handling at  the end of the current call
% If mFileErrorCode =/= 0 at 'return', the simulation is aborted.
mFileErrorCode = 0;
% mFileErrorCode = mFileErrorCode + 1000 * (mdot < 0); %Reverse flow
% mFileErrorCode = mFileErrorCode + 1001 * (sum(T_g>10^4)+sum(T_w>10^4)); %↙
Unrealistically high temperatures
% mFileErrorCode = mFileErrorCode + 1002 * (sum(T_g<0)+sum(T_w<0)+sum(T_o<0)); % Check↙
for negative Kelvin temperatures
% mFileErrorCode = mFileErrorCode + 1003 * (any([h_conv, h_convwr, h_grad, h_wind,↙
h_glass]>10^3)); %Check for too high heat transfer coefficents
return
```

```
function T_g = glazing_temp(T_gp, Q_sky, Q_gamb, Q_solarg, Q_gs, Q_wg, N_g, dt, cp_gn,↙
h_glass)

if N_g == 3
    T_g(1) = T_gp(1) + (Q_sky + Q_gamb + Q_solarg/N_g +  h_glass*(T_gp(2)-T_gp(1)))↙
*dt/cp_gn;
    T_g(2) = T_gp(2) + (Q_solarg/N_g +                              h_glass*(T_gp(3)↙
+T_gp(1)-2*T_gp(2))) *dt/cp_gn;
    T_g(3) = T_gp(3) + (-Q_gs - Q_wg + Q_solarg/N_g+       h_glass*(T_gp(2)-T_gp(3)))↙
*dt/cp_gn ;

elseif N_g == 2
    T_g(1) = T_gp(1) + (Q_sky + Q_gamb + Q_solarg/N_g + h_glass*(T_gp(2)-T_gp(1)))↙
*dt/cp_gn;
    T_g(2) = T_gp(2) + (-Q_gs - Q_wg + Q_solarg/N_g+h_glass*(T_gp(1)-T_gp(2)))↙
*dt/cp_gn;
    T_g(3) = T_g(2);
elseif N_g == 1
    T_g(1) = T_gp(1) + (Q_sky + Q_gamb + Q_solarg/N_g - Q_gs - Q_wg)*dt/cp_gn;
    T_g(2) = T_g(1);
    T_g(3) = T_g(1);
else
    return
end
```

```
function [T_w] = wall_temperature(T_wp, F_ow, Q_ws, Q_wg, Q_solarw, Q_lossw, N_w,↙
cp_nw, dt, Q_wr)
%% Calculating the wall temperature profile

% Calculating the temperature of the external nodes by assuming instant
% heat transfer to these points. From Page 332 in PoHaMT:
% The edge nodal points are half the size of the sentral ones.
T_w(1) = T_wp(1) + 2*F_ow*(T_wp(2)-T_wp(1)) + (Q_ws + Q_wg + Q_solarw - Q_lossw/N_w) /↙
(cp_nw/2) * dt; %%K

T_w(N_w) = T_wp(N_w) + 2*F_ow*(T_wp(N_w-1)-T_wp(N_w)) + (- Q_wr - Q_lossw/N_w) /↙
(cp_nw/2) * dt ; %Q_wr is negative as a positive Q_wr means heat transfer from wall to↙
room.

%Setting the rest by using Equation 5.81 in PoHaMT.
for i=2:(length(T_w)-1);
    T_w(i) = F_ow * (T_wp(i+1) + T_wp(i-1)) + (1-2*F_ow) * T_wp(i) - Q_lossw*dt/↙
(N_w*cp_nw);
end

end
```

```
function [rho_air, mu_air, k_air, c_air, beta_air, rho_i, mu_i, k_i, beta_i, rho_o] =
air_variables(Tbar_sp1, T_i, T_op,T_w1)

%% Air variables, from Bansai et. al 05, appendix A.
%These are only calculated every [calc_pause(1)]th timestep, for faster simulation
%times.
%if mod(trnInfo(8),calc_pause(1))==0 || trnInfo(8)<= 5
Tbar_sp = (Tbar_sp1 + T_w1)/2;
    %Average air flow properties
    rho_air =   1.1614  - 0.00353   * ( Tbar_sp - 300 );                    %kg/m^3,
density
    mu_air =  ( 1.846   + 0.00472   * ( Tbar_sp - 300 ) ) * 10^(-5);  % kg/ms,dynamic
viscosity
    k_air =     0.0263  + 0.000074  * ( Tbar_sp - 300 );                   %W/mK,
conductivity
    c_air =   ( 1.007   + 0.00004   * ( Tbar_sp - 300 ) ) * 10^3;         %J/kgK,
specific heat capacity
    beta_air = 1/(Tbar_sp);                                                        %
K^-1, thermal expansion coefficient
%    a_air = 0.5;
% NOTE! (Dette er bare en verdi.
%Airflow into the slit
    rho_i =   1.1614  - 0.00353   * ( T_i - 300 );
    mu_i =  ( 1.846   + 0.00472   * ( T_i - 300 ) ) * 10^(-5);
    k_i =     0.0263  + 0.000074  * ( T_i - 300 );
    beta_i = 1/(T_i); %Thermal expansion coefficient
%Airflow out of the slit
    rho_o =   1.1614  - 0.00353   * ( T_op - 300 );

end
```

```
function [Re, Ra, Gr, Pr] = dimensionless_numb(L_w, d_w, rho_air, V_s, mu_air,↙
beta_air, T_gw, Tbar_sp, H_w, c_air, k_air, g)
%% Dimensionless numbers
%Reynolds
D_h = 4 * L_w * d_w / (2*L_w + 2*d_w);
Re = (rho_air * D_h * V_s)/ mu_air;
%Grashofs
Gr = (g * rho_air^3 * beta_air * (abs(T_gw-Tbar_sp)) * H_w^3)/ mu_air^2;
%Prandtl
Pr = c_air * mu_air / k_air;
%Rayleigh
Ra = Gr*Pr;%(g * rho_air * beta_air * (abs(T_gw-Tbar_sp)) * H_w^3)/(mu_air * a_air);

end
```

```
function [h_conv] = conv_heat_transf(h_choice, Ra, Gr, Pr, d_s, H_s, k_air, V_s)

%% Convective heat transfer coefficients [
%These are only calculated every [calc_pause(3)]th timestep, for faster simulation
%times.
%if mod(trnInfo(8),calc_pause(3))==0 || trnInfo(8)<= 5
%Shen et.al 07 [J/m2K]
if h_choice == 1
    if V_s ~= 0
             Nu_shen = 0.107*Gr^(1/3);
    else
            Nu_shen_temp = max(0.288*(d_s*Ra/H_s)^0.25,0.039*Ra^0.33);
            Nu_shen = max(1 , Nu_shen_temp);
    end
    h_conv = Nu_shen * k_air / H_s;
elseif h_choice == 2
    %Rabani et.al 17, Bassiouny et.al 08
    Nu_bass = 0.68 + (0.67*Ra^0.25)/(1+(0.492/Pr)^(9/16))^(4/9);
    h_conv = Nu_bass * k_air / H_s;
elseif h_choice == 3
    % Akbarzadeh et.al 82
    h_conv = 5.68 * 4.1 * V_s;
        mFileErrorCode = 230;
elseif h_choice == 4
    %Shen et.al 07, ASHRAE
    if Gr >= 10^4 && Gr < 10^8
            Nu_ashrae = 0.516*Ra^0.25;
    elseif Gr >= 10^8 && Gr < 10^12
            Nu_ashrae = 0.117*Ra^(1/3);
    else %Uses Nu_bass for exception handling and prints stuff to somewhere.
            Nu_ashrae = 0.68 + (0.67*Ra^0.25)/(1+(0.492/(Ra/Gr))^(9/16))^(4/9);
            mFileErrorCode = 240;
        %print('Tried to use h_conv_ashrae when 10^4 > Gr > 10^12')
    h_conv = Nu_ashrae * k_air / H_s;
    end
end
```